SYNTHESIS AND CHARACTERIZATION OF NOVEL SENSITIZERS FOR DYE SENSITIZED SOLAR CELLS

A THESIS

SUBMITTED TO DEPARTMENT OF CHEMISTRY
AND THE INSTITUTE OF ENGINEERING AND SCIENCES
OF BİLKENT UNIVERSITY
IN PARTIAL FULFILLMENT OF THE REQUIREMENTS

FOR THE DEGREE OF

MASTER OF SCIENCE

By
SAFACAN KÖLEMEN

July 2010

I certify that I have read this thesis and that in my opinion it is fully adequate, in scope and in quality, as a thesis of the degree of Master of Science.

…….

Prof. Dr. Engin U. Akkaya (Principal Advisor)

I certify that I have read this thesis and that in my opinion it is fully adequate, in scope and in quality, as a thesis of the degree of Master of Science.

…….

Prof. Dr. Özdemir Doğan

I certify that I have read this thesis and that in my opinion it is fully adequate, in scope and in quality, as a thesis of the degree of Master of Science.

…….

Assist. Prof. Dr. Dönüş Tuncel

I certify that I have read this thesis and that in my opinion it is fully adequate, in scope and in quality, as a thesis of the degree of Master of Science.

…….

Assist. Prof. Dr. Emrah Özensoy

I certify that I have read this thesis and that in my opinion it is fully adequate, in scope and in quality, as a thesis of the degree of Master of Science.

…….

Assist. Prof. Dr. Neslihan Şaki

Approved for the Institute of Engineering and Science:

…….

Prof. Dr. Levent Onural

Director of the Institute of Engineering and Science

ABSTRACT

SYNTHESIS AND CHARACTERIZATION OF NOVEL SENSITIZERS FOR DYE SENSITIZED SOLAR CELLS

Safacan Kölemen

M.S. in Department of Chemistry
Supervisor: Prof. Dr. Engin U. Akkaya
July, 2010

Increasing concerns about the global warming and energy demand force scientists to find out new source of energy supply. Among possible energy sources, solar cells are promising candidates. Production costs unfortunately restrict the usage of these cells. Cheaper and environment friendly dye sensitized solar cells (DSSCs) appear to be successful alternatives to more widely used traditional semiconductor based designs. However, most people would agree that, there is still room for improvement for a few components of a typical DSSC. This is perhaps more apparent for the electrolyte, and the sensitizer dye component itself.

In this study, we targeted novel Boradiazaindacene (Bodipy) sensitizers which were studied in two types of DSSCs; liquid electrolyte based (Gratzel type) and solid state DSSC. Six different sensitizers were synthesized and characterized. Effects of design and electrolyte type on solar light to electricity conversion efficiency were investigated.

We have demonstrated that Bodipy dyes, through rational design, yield promising new materials in Gratzel type dye sensitized solar cells. Their applicability in solid state electrolyte regime offers additional opportunities for practical applications. Bodipy sensitizers hold significant promise as they can be derivatized as desired and the absorption peaks can be moved along the visible and near IR region.

Keywords: Boradiazaindacene (Bodipy), dye sensitized solar cell, sensitizers, solid state electrolyte, liquid electrolyte

ÖZET

BOYAR MADDE UYARIMLI GÜNEŞ PİLLERİ İÇİN YENİ DUYARLAŞTIRICILARIN SENTEZİ VE KARAKTERİZASYONU

Safacan Kölemen

Yüksek Lisans, Kimya Bölümü
Tez Yöneticisi: Prof. Dr. Engin U. Akkaya
Temmuz, 2010

Artan küresel ısınma, çevre kirliliği ve enerji kaynaklarının gereken talebi karşılayamayacak duruma gelmesi, bilim camiasını yeni enerji kaynakları bulmaya zorlamaktadır. Olası yeni kaynaklar arasından güneş pilleri umut verici bir alternatif olarak görülmektedir. Ancak pahalı üretim süreci klasik güneş pillerinin yaygın bir şekilde kullanımını engellemektedir. Bu nedenle, günümüzde ucuz ve çevre dostu boyar madde uyarımlı güneş pilleri silisyum temelli klasik güneş pillerinin yerini almaya başlamıştır. Hiç kuşku yok ki bu yeni teknolojide geliştirilmesi gereken çok nokta vardır. Bunlardan en önemlileri duyarlaştırıcı ve elektrolit kısımlarıdır.

Bu çalışmada, yeni Boradiazaindasen (Bodipy) bazlı duyarlaştırıcılar tasarlanmış, sentezlenmiş ve karakterize edilmiştir. Bu boyalar sıvı elektrolit ve katı hal elektrolit içeren boyar madde uyarımlı güneş pillerinde kullanılmıştır. Boya tasarımının ve elektrolit tipinin güneş ışığının elektriğe çevrim verimine olan etkisi gözlemlenmiştir. Sonuç olarak görülmüştür ki Bodipy boyaları uygun bir şekilde tasarlandıklarında, sıvı elektrolitli güneş pillerinde kullanılmak üzere umut veren duyarlaştırıcılardır. Ayrıca katı hal elektrolitli sistemlerde gösterdikleri performans ile de pratik uygulamalar için yeni bir alternatif olarak görülmektedir. Bodipy boyar maddeleri istenilen şekilde tasarlanıp, güneş ışığını yakın kızıl ötesi bölgede de soğurarak etkili bir duyarlaştırıcı olması mümkündür.

Anahtar Kelimeler: Bodipy, boyar madde uyarımlı güneş pilleri, sensitizörler, katı hal elektrolit, sıvı elektrolit

Dedicated to my father and mother

ACKNOWLEDGEMENT

I would like to express my gratitude to my supervisor Prof. Dr. Engin U. Akkaya for his guidance, support, patience and for teaching us how to become a good scientist. I will never forget his support throughout my life.

I would like to thank Yusuf Çakmak, Yiğit Altay and Gökhan Barın for their partnership in this research. I owe a special thank to Dr. Ö. Altan Bozdemir for his support, friendship and guidance to improve my skills in the field of supramolecular chemistry.

I want to thank our group members Ruslan Guliyev, Bilal Kılıç, Sündüs Erbaş Çakmak, Tuğba Özdemir, Onur Büyükçakır, Sencer Selçuk, Ziya Köstereli, Merve Türkşanlı, Eser İden, Dr. Serdar Atılgan, Fazlı Sözmen, Nisa Yeşilgül, Şeyma Öztürk, Fatma Pir, Gizem Çeltek, Seda Demirel, Tuğçe Durgut, F. Tuba Yaşar, Ahmet Bekdemir, Muhammed Büyüktemiz, Gökhan Gülten, Hande Boyacı and rest of the SCL (Supramolecular Chemistry Laboratory) members for valuable friendships, wonderful collaborations, and great ambiance in the laboratory. They are very precious for me. It was wonderful to work with them.

I would like to express my special thanks to Dr. Şule Ertan-Ela and Prof. Dr. Michael Gratzel for their generous help for calculating photovoltaic parameters of DSSCs.

I would like to thank Göksu Seda Şentürk, Beril Baykal for their valuable friendship.

Finally, I want to express my gratitude to Ece Aytan and my family for their love, support, and understanding. I owe them a lot.

LIST OF ABBREVIATIONS

PV: Photovoltaic

DSSC: Dye sensitized solar cell

FTO: Fluorine doped tin oxide

CTO: Conductive and transparent oxide

HTM: Hole transport material

Spiro-OMeTAD: 2,2,7,7-tetrakis(*N*,*N*di-*p*-methoxyphenyl-amine)9,9-spirobifluorene

IPCE: Incident photon to current efficiency

LHE: Light harvesting efficiency

DFT: Density functional theory

BODIPY: Boradiazaindacene

TLC: Thin layer chromatography

NMR: Nuclear magnetic resonance

CHENO: 3a,7a-dihydroxy-5b-cholic acid

CV: Cyclic voltammetry

DMF: Dimethylformamide

THF: Tetrahydrofuran

DDQ: Dichlorodicyanoquinone

TABLE OF CONTENTS

LIST OF FIGURES

LIST OF TABLES

CHAPTER 1

INTRODUCTION

1.1. Energy Sources

Energy is admittedly one of the primary necessities for daily life and it is indispensable. According to the latest data, humans all around the world consume 13 terawatts (13 trillion watts) of power.[1] Moreover, by 2050 additional 30 terawatts will be needed as a result of increasing population, growing industry and technology.[1] This tremendous need for energy is satisfied mostly from fossil fuels and nuclear energy (78% of the energy request) which release carbon dioxide and strengthen the greenhouse effect that triggers the global warming. Economical aspects are also troublesome, since they are not renewable, as the consumption rate increases, production and cost increase accordingly. Additionally, fossil fuels reserve will not adequately fulfill the requirements of humans in coming years. There are also other minor non-fossil energy sources such as biomass, hydro and geothermal sources, but the production of energy is expensive and the outcome is not sufficient. Generation of electricity from fossil fuels (coal, oil, and natural gases), nuclear energy and some other minor sources and the consumption rates are shown in figure 1.[2] Almost one third of energy is suitable to generate electricity. Only 10% of the produced electricity can be used and unfortunately 20% percent is lost during conversion. The remaining is mostly consumed by industry and household activities.[2]

Energy concerns force scientists and industry to find out new, clean, cheap and renewable energy sources. The most notable and promising type of renewable energy source is solar cells where direct conversion of sunlight to electricity takes place.

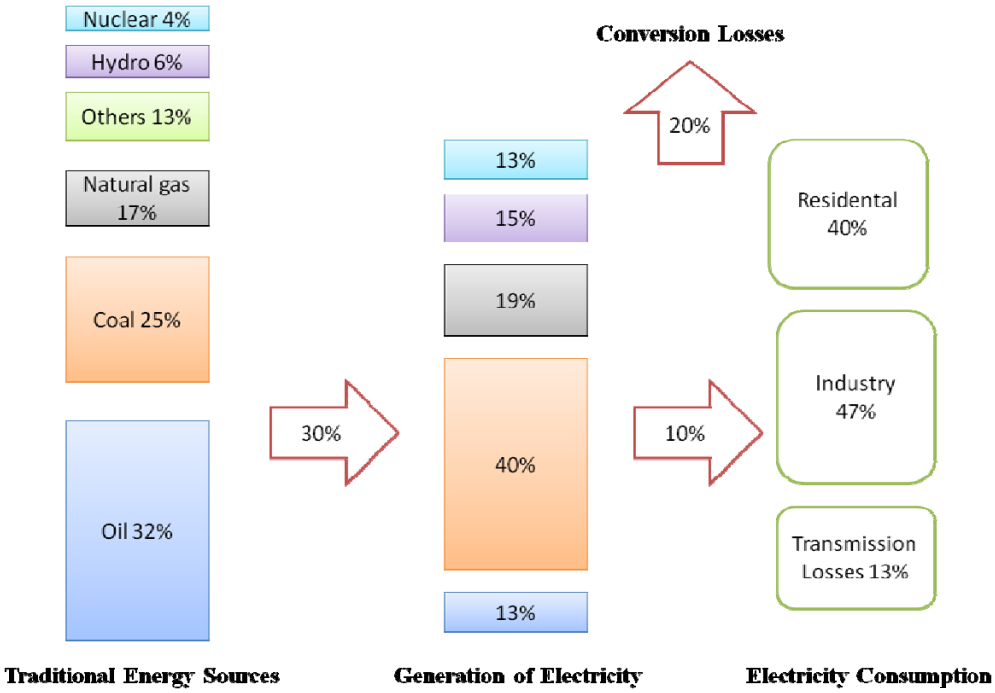

Figure 1. Generation of electricity and consumption rates of common energy sources[2]

1.2. Dye Sensitized Solar Cells

All conversion processes of solar radiation to electricity can be collected under the title of photovoltaics (PV). In fact, molecular photovoltaic is not a new idea. More than 100 years ago, after the discovery of photography, scientists have been dealing with PVs.[3] One of the practical applications of photovoltaic technology is solar cells. Photovoltaic solar energy is significant since it does not use fuels and only benefits from the sun.

Sun is the most powerful and practically endless energy source, such that, earth surface acquire in one hour much more energy from sun than people need in one year.[4] So that, if it will be possible to cover 0.1% of the earth surface with solar cells that have 10% conversion efficiency, present needs will be satisfied.[4] It is important to use this generous energy source. At the present time, crystalline

or amorphous silicon based solar cells are commercially available and being widely used. 94% of manufactured solar cells are silicon based.[4] Furthermore, silicon solar cell manufacturing is growing by approximately 40% in each year.[5] These inorganic solid state materials have conversion efficiencies ranging from 15% to 29% depending on the semiconductor construction.[2] Despite high efficiency, silicon based solar cells involve high purity silicon and expensive manufacturing processes which increases the cost. On the other hand, **dye sensitized solar cells (DSSC)** where dye is used in the replacement of silicon have received considerable attention after the invention of Michael Gratzel in 1991.[6] This promising type of DSSC offers high overall conversion efficiency, design flexibilities, lower costs, and easier fabrication processes. There are two main types of DSSCs which are known as Gratzel type (traditional DSSC) with liquid electrolyte and solid state DSSCs with hole transport material.

Cell type	**Efficency (%)**		**Research needs**
	cell	**module**	
crystalline silicon	24	10-15	higher production yield
multicrystalline solid	18	9-12	manufacturing cost
amorphous silicon	13	7	lowering cost, product stability
$CuInSe_2$	19	12	finding replacement for Indium
DSSC-liquid electrolyte	10-11	7	improve efficiency and stability
DSSC-solid state	4-5	--	improve efficiency and stability

Table 1. Efficiency comparison of well-known solar cells[2]

In table 1, overall conversion efficiencies and drawbacks of some common solar cells are shown. The notable problem with silicon based solar cells is cost, for dye sensitized solar cells efficiency is still primary research topic. With high efficiency indium solar cells, indium itself is a challenge. In order to replace solar cells with conventional fossil fuels intense investigation is still needed.

1.2.1. Traditional "Gratzel Type" DSSCs

Traditional Gratzel type dye sensitized solar cells contains two electrodes which are photo-anode and photoinert counter electrode (cathode). These two electrodes sandwiches a liquid electrolyte. This electrolyte ensures charge recombination and electrical conductivity. Typical electrolytes in DSSCs are ionic solutions which contain free ions. In most of the traditional DSSC, redox couples are used in a solution as a liquid electrolyte.[7-13] The common redox couple is iodide/triiode (I^-/I_3^-),[6] redox couples with other halogens (Br^-/Br_3^-) are also exist but the examples are very rare.[14]

In order to construct the device, five main materials were used (figure 1). The first one is the fluorine doped tin oxide (FTO) which is also classified as conductive and transparent oxide (CTO). Second material is a nanocrystalline titanium oxide (TiO_2) thin film as a semiconductor. TiO_2 is widely used because of its low price, ease of production, no toxicity and optical excellence in the visible range.[15] Third component is a dye sensitizer. Fourth one is an electrolyte in other words, a redox couple. Fifth and the last material is a platinum coated glass substrate which works as a counter electrode. On the side of photo-anode, there exists dye as a sensitizer adsorbed on TiO_2 and FTO that is covered by TiO_2 – dye complex. Outermost layer is the FTO. The thickness of semiconductor is around 7-10 μm.

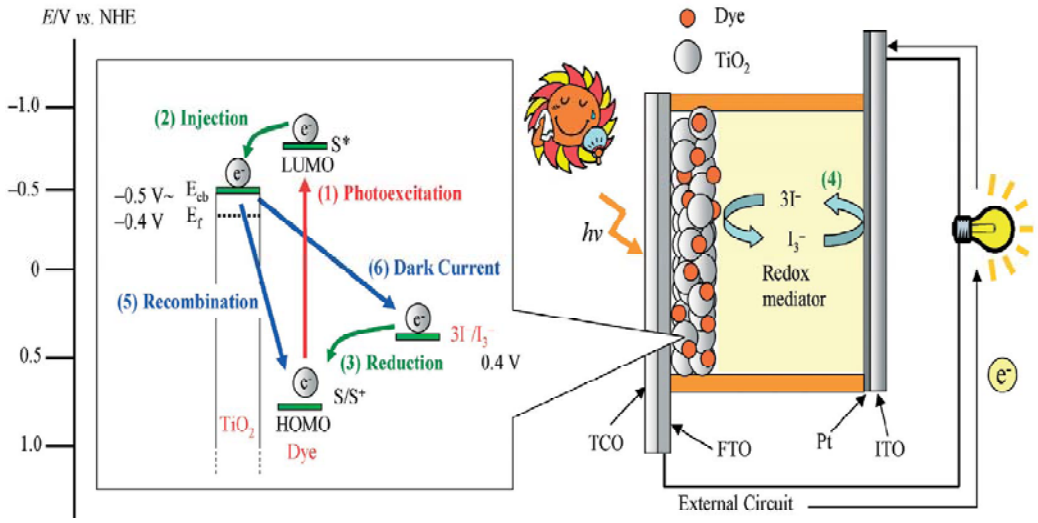

Figure 2. Components of the Gratzel type DSSC and its working scheme[21]. Copyright Wiley-VCH Verlag GmbH & Co. KGaA. Reproduced with permission.

1.2.1.1. Operational Principle

In dye sensitized solar cells, the current generation steps[6,16-20] include following processes; Initially, a sensitizer dye adsorbed on TiO_2 absorbs sun light. Photoexcited dye transfers an electron to the TiO_2 conduction band. During this photoinduced electron transfer charge separation takes place. The oxidized dye is reduced by the redox mediator. I^- ions donate an electron to perform reduction. This step is named as dye regeneration and it is a very significant step in order to have continuous electron transfer to TiO_2. The electron which is injected to semiconductor moves across the circuit and reaches to counter electrode (cathode). I^- ion that is needed for reduction of the dye is regenerated at the cathode by the reduction of I_3^-, the other component of the redox mediator. Two electrons which are needed for reduction of I_3^- are the electrons that come from the external circuit. Each step in this cyclic should be ordered. Below, it is shown that the equations that take place in electron flow cycle.[2]

$$Dye + h\nu \rightarrow Dye^* \quad (1)$$

$$Dye^* \rightarrow Dye^+ + e^- \text{ (on semiconductor)} \quad (2)$$

$$2Dye^+ + 3I^- \rightarrow 2Dye + I_3^- \quad (3)$$

$$I_3^- + 2e^- \text{ (from circuit)} \rightarrow 3I^- \quad (4)$$

$$Dye^+ + e^- \text{ (on semiconductor)} \rightarrow Dye \quad (5)$$

$$I_3^- + 2e^- \rightarrow 3I^- \quad (6)$$

As in all devices, there are some imperfections in DSSCs. These faults are caused by possible undesirable pathways in electron flow. After the injection of electrons to conduction band of TiO_2, electrons can combine either with oxidized dye (recombination, equation 5) or oxidized redox couple (equation 6, dark current) rather than continuing through external circuit. These pathways directly diminish the photovoltaic performance. This means that, there is a great competition between equation 3 and equations 5, 6. In order to avoid dark current and recombination, reduction of dye to its original state (equation 3) should be kinetically more favorable than dark current and recombination steps.

The idea behind the operational principle of dye sensitized solar cell was based on 1960s when it was understood that photoexcited dye can inject electron to titanium oxide conduction band and also a dye which is chemisorbed on semiconductor work better.[22]

1.2.2. Solid State DSSCs

Liquid electrolyte based DSSCs have leakage and solvent evaporation problems which restrict the practical and commercial usage of these cells.[23] To overcome the disadvantages of liquid electrolyte, solid state DSSCs were introduced. The major difference between liquid electrolyte based and solid state DSSCs is the replacement of (I^-/I_3^-) redox couple with solid state hole-transport

material (HTM).[24,25] Organic compounds[26] and p-type semi conductors[27] were used in this regard. Solid state DSSC mainly consists of a fluorine doped tin oxide (FTO), blocking TiO_2 layer, semiconductor (mesoporous TiO_2),[28] sensitizer dye which is chemisorbed on semiconductor, hole transport material and gold counter electrode.

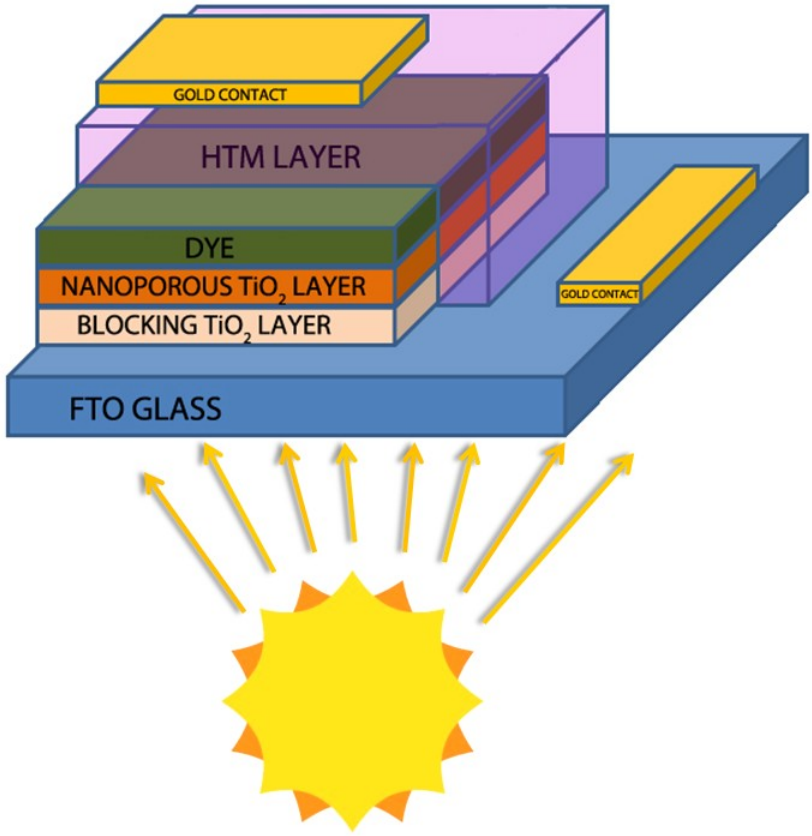

Figure 2. Components of solid-state dye sensitized solar cell

The role of the blocking TiO_2 is to avoid short circuit by hindering the contact between the fluorine-doped tin oxide and the hole-transport material. HTM is needed for regenerating the sensitizer dye. Its HOMO and LUMO energy levels must be compatible with the HOMO of the dye and conduction band of the semiconductor to have effective electron flow. Moreover, HTM should be transparent and amorphous (no crystallization). Crystallization causes pore filling and reduce the carrier mobility.[17] Most widely used HTM is 2,2,7,7-

tetrakis(*N*,*N*di-*p*-methoxyphenyl-amine)9,9-spirobifluorene (spiro-OMeTAD) (figure 3).[17,29-33] It is preferred because of its amorphous structure and good solubility. The structure of spiro-OMeTAD (**1**) contains tetrahedral carbon centre that links two aromatic moieties (figure 3). This centre prevents crystallization and increases the glass forming properties.

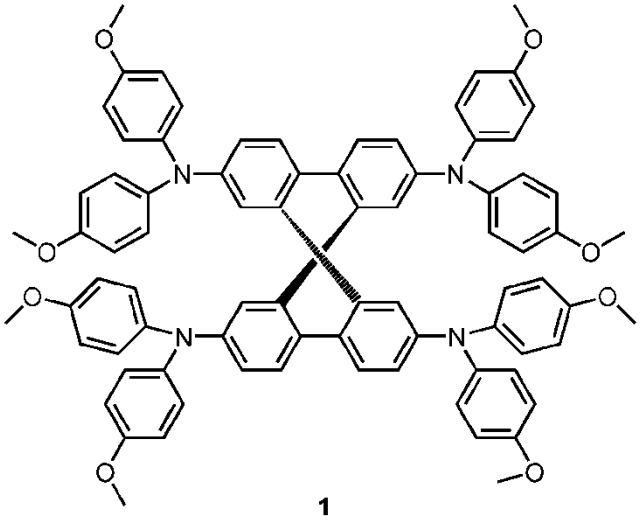

1

Figure 3. Molecular structure of spiro-OMeTAD

Solid state DSSC is solvent-free alternative of dye sensitized solar cells. It accommodates practical usage and removes some disadvantages of traditional DSSCs but solar light to electricity conversion efficiency is lower than traditional DSSCs.[34,35] This reduced efficiency is due to two problems. First, the thickness of solid state DSSC is around 4-5 μm. This thickness restricts the loading of dye, which causes less absorption of solar light.[36] Furthermore, electron diffusion length in HTM based DSSC is shorter than liquid electrolyte based DSSC.[32,37-41]

1.2.2.1. Working Principle

Working principle of solid state dye sensitized solar cell[16,42-25] is similar to traditional DSSCs (figure 4). Following the absorption of light, electron transfer occurs from excited dye to conduction band of the semiconductor. The dye is reduced back by electron transfer from hole-transport material, in other words, hole transport from dye to HTM. The electron passing through the TiO_2 and the hole travelling on HTM are transported by electronic conduction to the gold electrode. HTM is regenerated at counter electrode and circuit is completed (figure 4). As in the liquid electrolyte based DSSC, there is a possibility for electrons which are injected to TiO_2 recombine with oxidized dye (recombination). Thus, there is a competition between recombination and hole transfer to HTM. Hole transfer should proceed faster than recombination in order to produce electricity efficiently.

Excitation of dye takes place in femtosecond range,[46,47] hole transfer range is around 0.3-1 ns,[48] in solid state DSSC, on the other hand, electron injection from redox mediator to excited dye in liquid electrolyte based DSSC takes place in 10 microseconds.

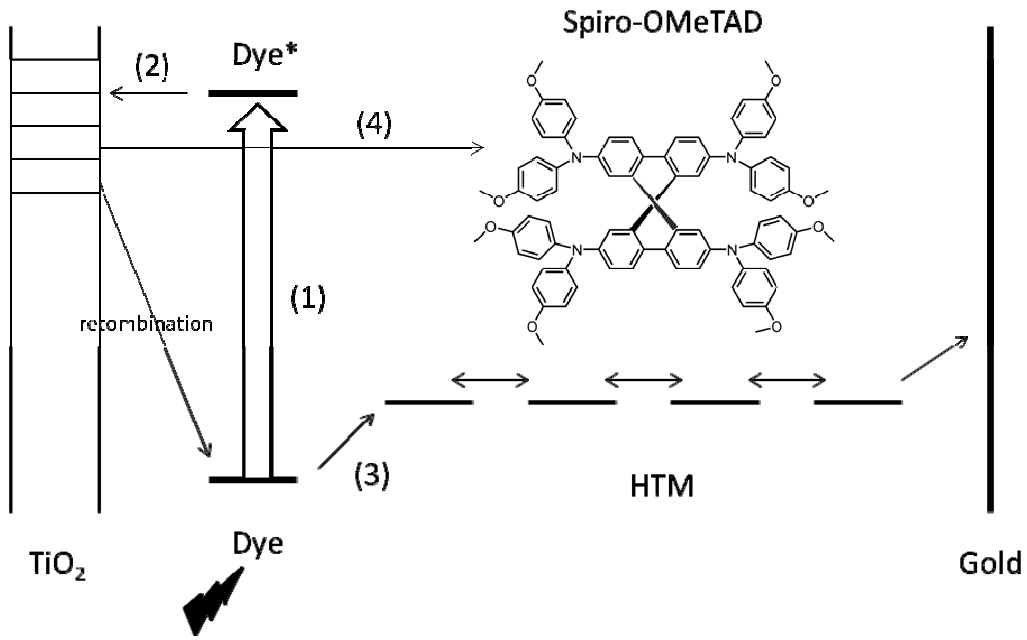

Figure 4. Components of the solid state DSSC and its working scheme

1.2.3. Photovoltaic Parameters

Photovoltaic parameters[6,21] show the performance of the DSSCs and more significantly these parameters help to check the quality of the sensitizer dye design. There are six different parameters to characterize DSSCs performance under AM 1.5 solar light (1 sun): open circuit voltage (V_{oc}), short circuit current density (J_{sc}), fill factor (*ff*), incident photon to current conversion efficiency (IPCE), photocurrent/voltage curve (*J/V* curve), and solar energy to electricity conversion yield (η).

Open circuit voltage (V_{oc})[21] is defined as the electrical potential difference between anode and cathode when the circuit is open (no current). The maximum value of V_{oc} is around 0.8 to 0.9. This value represents the energy gap between the semiconductor and electrolyte or HTM. Energy level of conduction band of semiconductor in DSSCs equals to -0.4 V vs NHE and redox potential is 0.4 V vs. NHE. It is not possible to have maximum V_{oc} since recombination and dark current pathways are always contributing to electron flow in DSSCs. As the

conduction band energy shifts toward vacuum level (negative shift), the V_{oc} increases and effects efficiency in a positive manner.

Short circuit current density[15,21] is the measured photocurrent when a DSSC under light is short circuited. This means that the maximum current of the device since there will be no electrical impendence on the way of electron flow. In order to have high J_{sc} values, all parts of the device which contribute to the electron cycle (current) should function efficiently. Dye, for instance should have intense light absorption and good electron injection efficiencies to TiO_2. Also redox reactions should proceed perfectly on HTM or redox couple. Again as in the case of V_{oc}, high J_{sc} increases the efficiency of DSSC.

Incident photon to current conversion efficiency (IPCE) is the ratio of electrons in external circuit to number of initial photons. The formula of IPCE is given below (equation 7).

$$\text{IPCE} = 1240\ (\text{eV nm})\, J_{ph}\ (\text{mA cm}^{-2}) / \lambda\ (\text{nm})\, I\ (\text{mW cm}^{-2}) \qquad (7)$$

J_{ph} is the short circuit current, I is the light intensity. IPCE is important because it relates the photovoltaic performance to the wavelength (λ). Moreover, light absorption and electron transfer from conduction band to external circuit directly affect the IPCE curve.

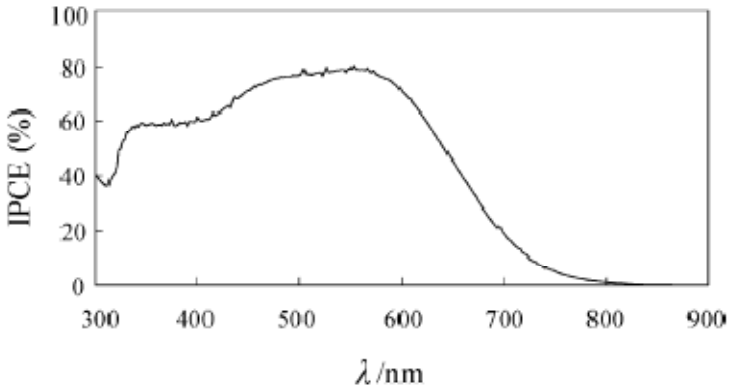

Figure 5. An example of IPCE curve which is obtained by a Ruthenium dye[6]

Another way to express IPCE is to use light harvesting efficiency of photons at specific wavelength (equation 8)[49], quantum yield of electron injection to TiO_2 (equation 9) and the collection efficiency of electron at the FTO glass.

$$\text{LHE}(\lambda) = 1 - 10^{-\alpha d} \tag{8}$$

$$\text{IPCE}(\lambda) = \text{LHE}(\lambda)\Phi_{\text{inj}}\Phi_{\text{coll}} \tag{9}$$

LHE(λ) is the light harvesting efficiency, Φ_{inj} is quantum yield of electron injection and Φ_{coll} represents the quantum yield of the electrons at the FTO glass. Therefore IPCE is directly related with the absorption of light and electron transfer processes.

Photocurrent/Voltage curve which is known as *J/V* curve summarize the photovoltaic performance of the DSSC. One example for Photocurrent/Voltage curve is given in figure 6.

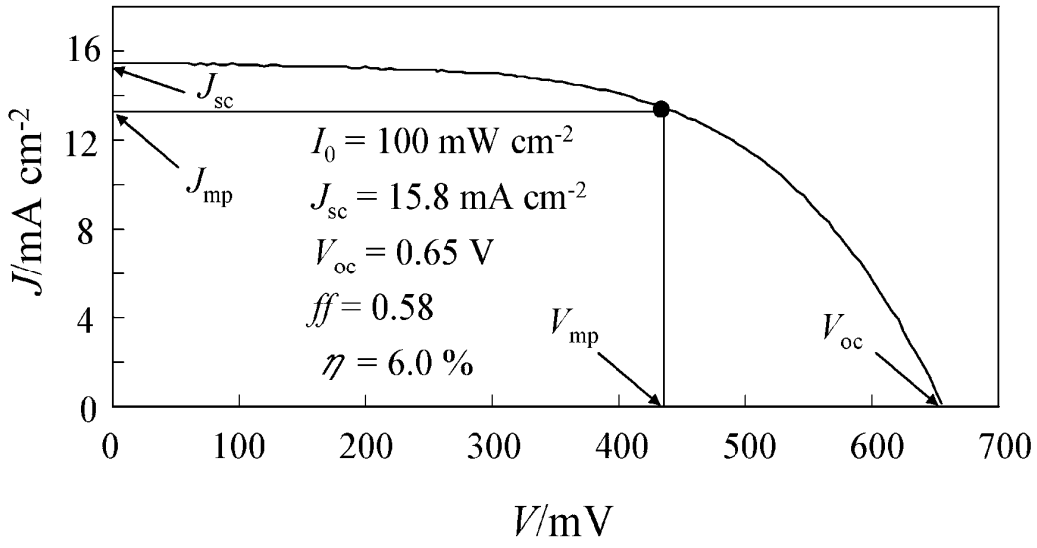

Figure 6. *J/V* curve[21]

J/V curve gives the maximum voltage and current. Furthermore, the point identified on the curve is the maximum power point which means the highest value obtained by multiplication of current and voltage. These current (J_{mp}) and voltage (V_{mp}) that yield maximum power play an important role in efficiency calculation and can be called as the actual power which is received from DSSC.

Fill factor is another significant photovoltaic parameter that gives the ratio between maximum power and the theoretical power values (equation 10).[21]

$$ff = (J_{mp}V_{mp})/(J_{sc}V_{oc}) \quad (10)$$

Last and the most important parameter is solar energy to electricity conversion yield (η) (equation 11).[21] It is defined as the multiplication of fill factor (*ff*) with the ratio of theoretical output power to incident sunlight power per unit area (I_0) which is assumed to be 100 (mW/cm^2).

$$\eta = J_{sc}\ (\text{mA cm}^{-2})\ V_{oc}\ (\text{V})\ \text{ff} / I\text{o}\ (\text{mW cm}^{-2}) \quad (11)$$

Overall conversion efficiency is affected by all parameters described above and each step in electron flow. Well-designed dye and cell construction are needed in order to improve η values.

1.2.4. Molecular Design of Dyes

A dye sensitized solar cell is a multidisciplinary concept where collaborations between different fields of science are needed. Physicists for instance mostly deal with building new devices with effective materials and try to explain the photophysical processes. On the other hand, engineers are trying to manufacture the DSSC devices by applying novel strategies. Chemists focus on designing and synthesizing effective sensitizers. Dye design is one of the limiting steps in achieving high yield DSSC.

Many investigations were performed in order to improve sensitizers.[50-53] In light of these studies, there are some essential points which should be considered while designing a sensitizer.[54-59] An organic dye should have a high molar extinction coefficient over a wide range of solar spectrum in order to have high light harvesting efficiency. Also sensitizer must have an anchoring group which provides chemisorption of dye onto TiO_2 surface. These groups are mostly (-COOH, -CNCOOH, $-SO_3H$, -OH). Carboxylic acid and cyanoacetic acid moieties are widely used because carboxy group binds to TiO_2 by making ester linkage which is very strong and yields good electron connection. Moreover, lowest unoccupied molecular orbital (LUMO) energy of the dye has to be more negative (higher) than the energy level of the conduction band of the semiconductor to conquer electron injection from excited dye to TiO_2. In order to reduce the excited dye, highest occupied molecular orbital (HOMO) energy of the dye must be more positive (lower) than the energy level of redox couple (I^-/I_3^-) (figure 7).

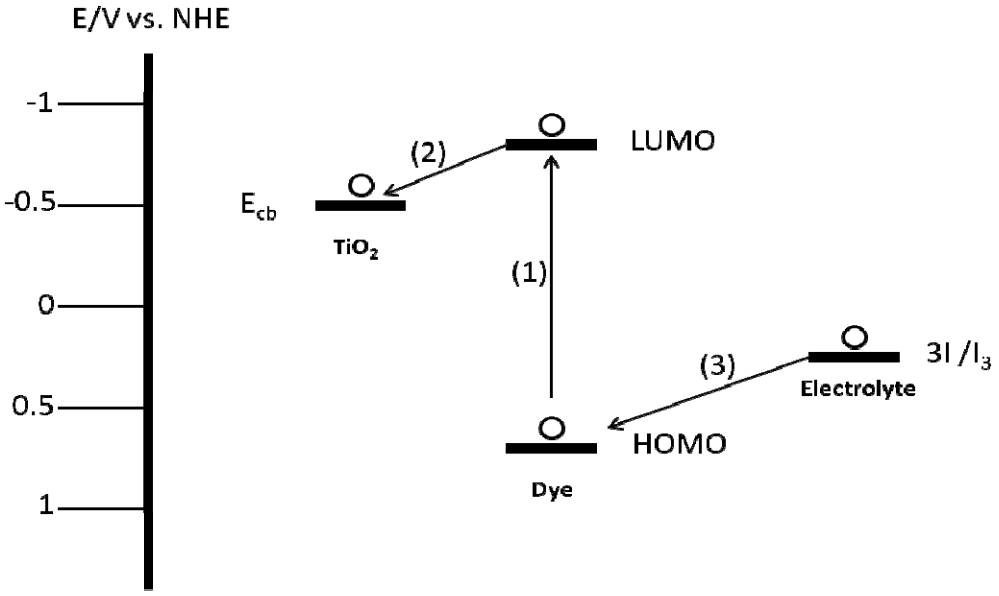

Figure 7. Energy levels representation of DSSC parts and electron transfer pathways

Requirements given above are realized by introducing electron donating and electron withdrawing (acceptor) groups to the dye. Most popular donor groups are shown in figure 8.

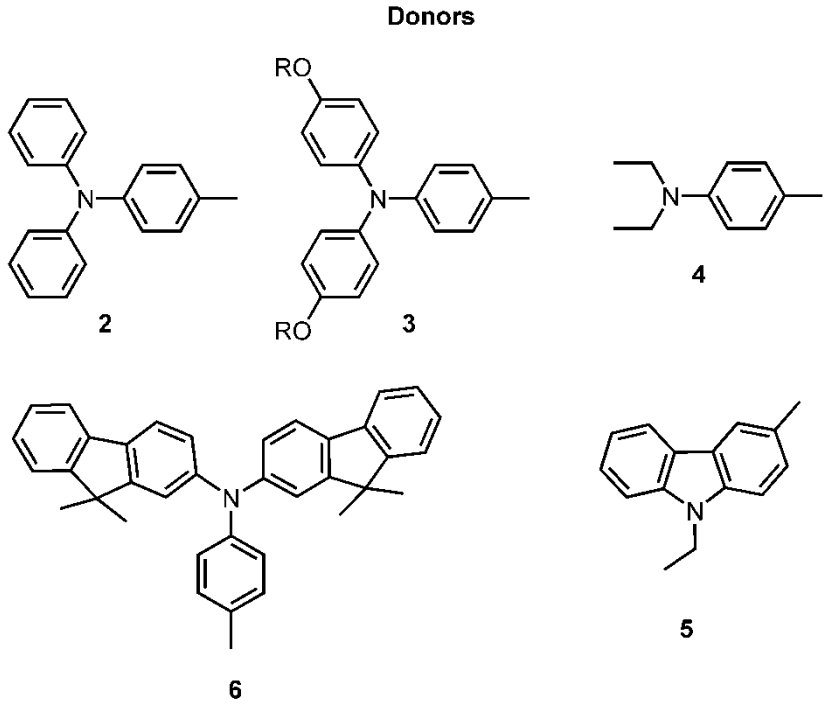

Figure 8. Common donor moieties

In most of the sensitizers, accepting and anchoring groups are similar. Common acceptors and conjugated linkers are listed in figure 9. Sensitizers which consist of donor and acceptor groups that are linked together with conjugated linkers show broad and intense absorption properties.[60] Beside photophysical properties, it is also important to direct electron transfer toward acceptor moiety where dye is adsorbed on TiO_2. In donor-acceptor system, HOMOs of the dye are delocalized on the donor part, on the other hand, upon excitation LUMOs are delocalized on acceptor and anchor groups, and thus the photoinduced electron transfer occurs via HOMO to LUMO transition. The charge separation between donor and acceptor groups in photoexcited dye results effective electron injection to TiO_2 conduction band through anchoring moiety. Since the positive charge resulting after electron transfer to TiO_2 is localized on HOMO or donor part, recombination between injected electron and oxidized dye is suppressed. Introducing good withdrawing and donating groups also decrease the energy gap between the HOMO and LUMO levels of dye which resulting in red shift of

absorption spectrum. Absorbing at longer wavelengths is important since solar radiation is intense at these wavelengths.

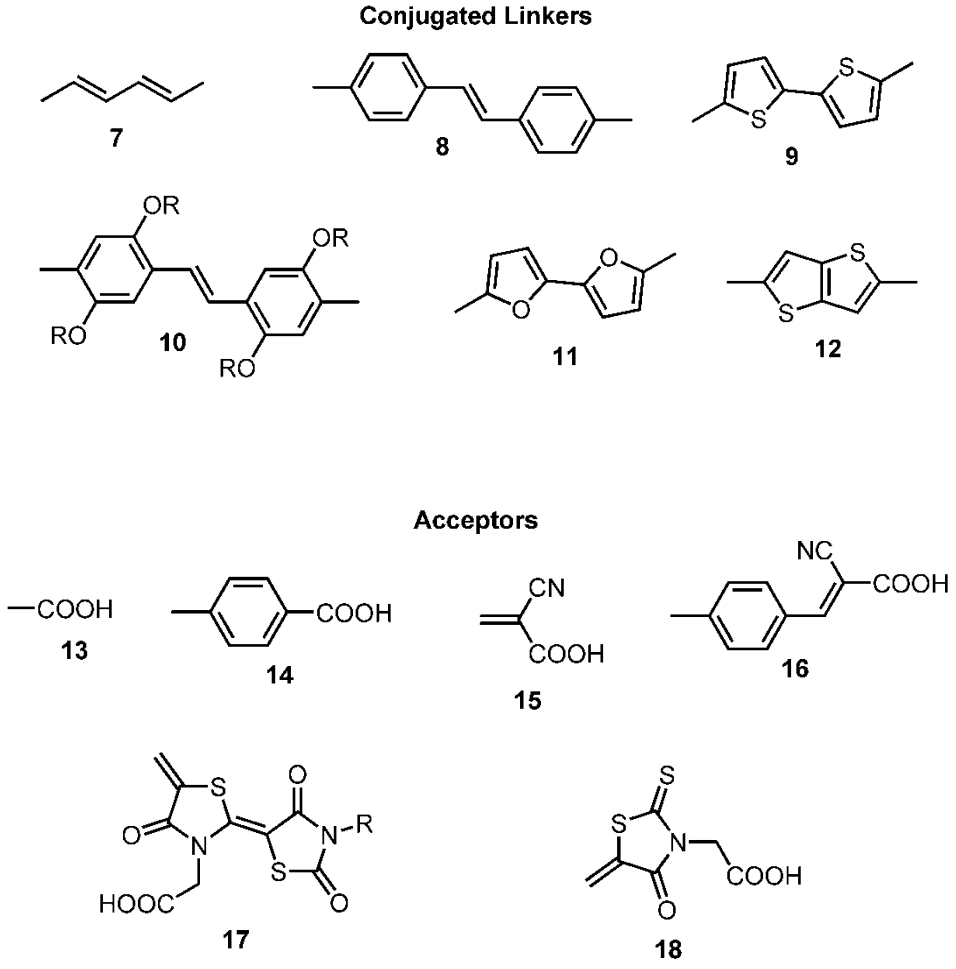

Figure 9. Most widely used linkers and acceptors in DSSC

Another general concept that should be avoided is the π-stacked aggregation which is generally occurs with thicker films.[42] Dye aggregation on TiO_2 directly diminishes the conversion efficiency. It causes intermolecular electron transfer between dyes and restricts the electron transfer to semiconductor. In order to solve this problem, bulky and sterically hindered groups such as long alkyl chains or aromatic compounds are introduced.

A sensitizer should be chemically stable when it is excited and it should complete at least 10^8 redox turnovers under constant sun light. This means, in order to call a DSSC stable, it has to work at least 20 years.[61]

To sum up, for perfect dye design, one should combine photophysical and electrochemical properties with molecular structure of dye.

1.2.5. Photosensitizers

After the first synthesis of ruthenium complexes in 1991 by Gratzel and coworkers, metal based sensitizers were widely studied. Today metal-free organic dyes are quite popular and start to replace ruthenium dyes. Thus it is possible to examine photosensitzers in two topics; metal based (ruthenium complexes) and metal-free (organic donor - acceptor) dyes.

1.2.5.1. Metal Based Photosensitizers (Ruthenium dyes)

Ruthenium complexes were the initial candidates for dye sensitized solar cells. Overall conversion efficiencies (η) have been reported up to 11% with this class of dyes in liquid electrolyte based DSSC. Ruthenium (II)-polypyridyl complexes which are known as N3,[49,62] (**19**) N719[62-64] (**20**), Z907[65-67] (**21**) and black dye[68,69] (**22**) are shown in figure 10.

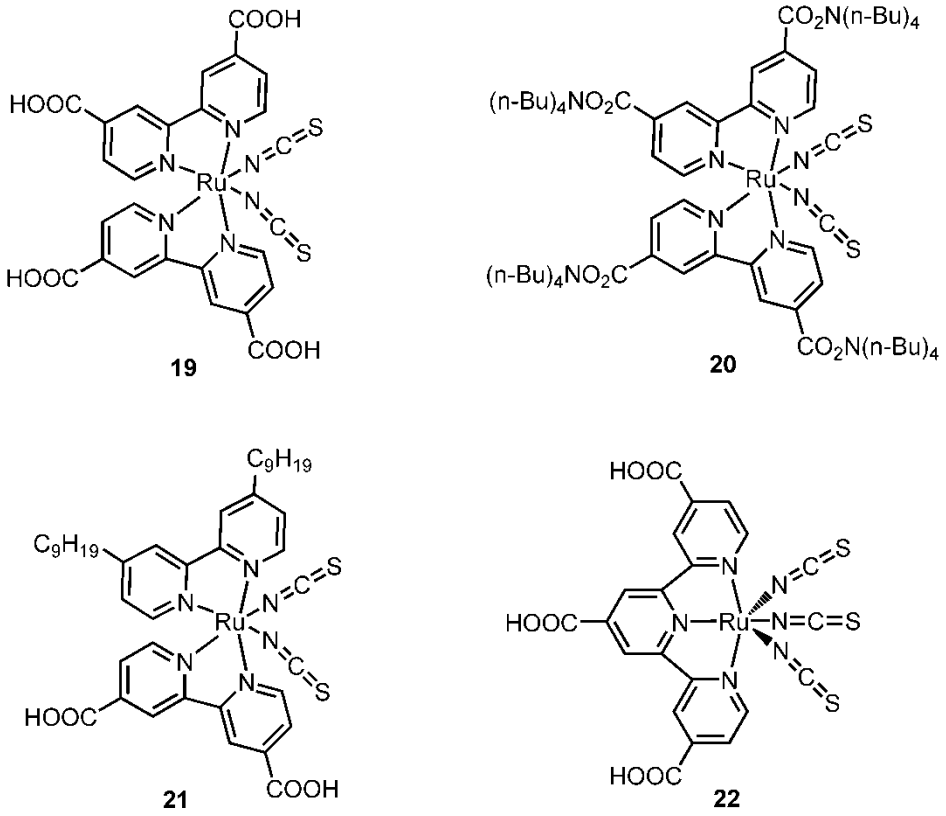

Figure 10. Common ruthenium dyes with 11% overall conversion efficiencies

In all of these dyes, anchoring and the electron withdrawing group is carboxylic acid or deprotonated form of the carboxylate moiety. Compound **21** has long alkyl chains which suppresses the aggregate formation on TiO_2. It is important to note that ruthenium sensitizers consist of at least two anchoring groups so binding with semiconductor is stronger which yields good electron transfer. High performance of ruthenium dyes arise from their intense and wide range of absorption at visible region, effective electron transfer property and high stability at excited state.

In order to increase the charge separation and obtain good efficiencies at Near-IR region, triphenyl amine groups were incorporated to the ruthenium dyes (compound **23**). This group has dual contribution; it is expected to increase the electron donation and extension of the conjugation. Extended conjugation causes absorption at longer wavelengths and higher molar extinction coefficient. The solar light to electricity conversion efficiency was calculated as 6.1% in

traditional DSSC.[70] The main point in this work was to obtain high IPCE values at longer wavelengths.

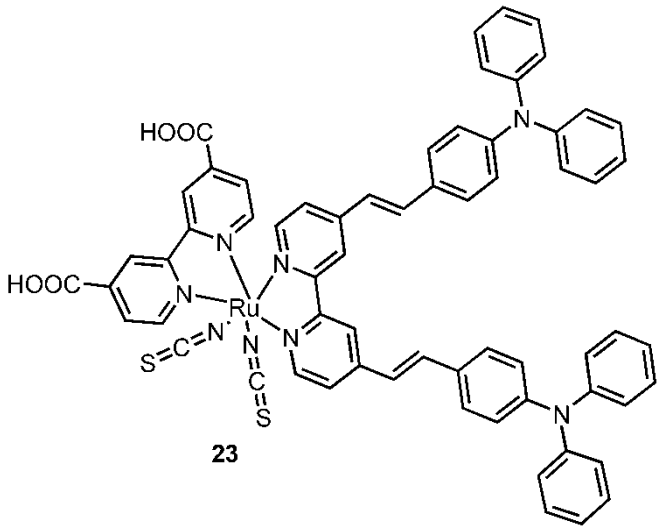

23

Figure 11. Ruthenium dye with electron donor moiety

There are also studies with ruthenium dyes in solid state dye sensitized solar cells. Compounds **19** and **20** were tested with HTM and efficiencies were around 2.5%.[71] An improved efficiency was achieved with these dyes by using silver complex of the sensitizers. Silver complex dramatically increased the open-circuit voltage to yield efficiency of 3.2%.[72] Another class of ruthenium dyes with relatively higher efficiencies in solid state devices is shown in figure 12. Compound **24** and **25** contains triethylene oxide methyl ether group. With the help of this moiety, charge recombination and aggregation are suppressed and efficiency is increased (4.5-5%).[73-75] These are some of the highest efficiencies obtained with solid state DSSC.

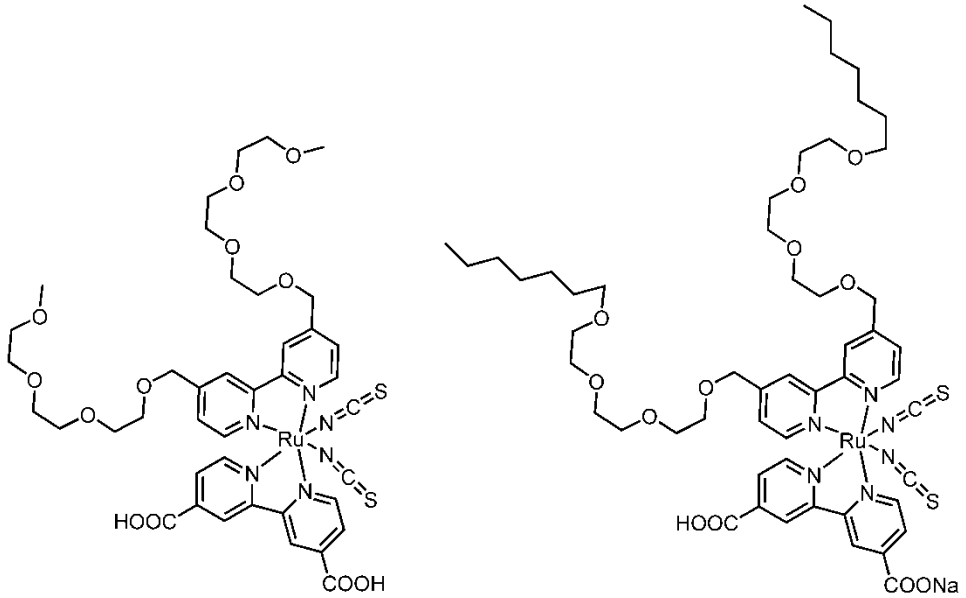

24 25

Figure 12. Ruthenium dyes as a sensitizer in solid state DSSC

Ruthenium dyes hold the record for efficiencies in both traditional and solid state DSSCs however, the expensive raw material, difficult purification steps, low absorbance at longer wavelengths and low extinction coefficients favor metal free organic dyes as a sensitizer.

1.2.5.2. Metal-Free Organic Dyes

In recent years, metal-free organic dyes start to replace ruthenium based DSSC. These organic dyes have many advantages such as high molar absorption coefficients, low cost, wide variety of modification, no concerns about resource limitations, ease of synthetic route and purification, absorption at longer wavelengths.

First trials with organic dyes in liquid based DSSCs were done by Hara et al.[76] and Yanagida and coworkers.[53] They introduced oligoenes with dialkylaminophenyl groups as the donor and cyanoacrylic acid moiety as the

acceptor (compound **26**). Compound **26** has 5.9% conversion efficiency. Later coumarines were used as donor groups (compound **27**, **28**).[77,78] The open circuit voltage and efficiencies were increased due to the strong donation ability of coumarines. Moreover, addition of bithiophene units as linker broadened the absorption spectrum of the compound on TiO_2. Extended conjugation which causes wide absorption at visible range in compound **28** further increased the conversion efficiency up to 8.2%.

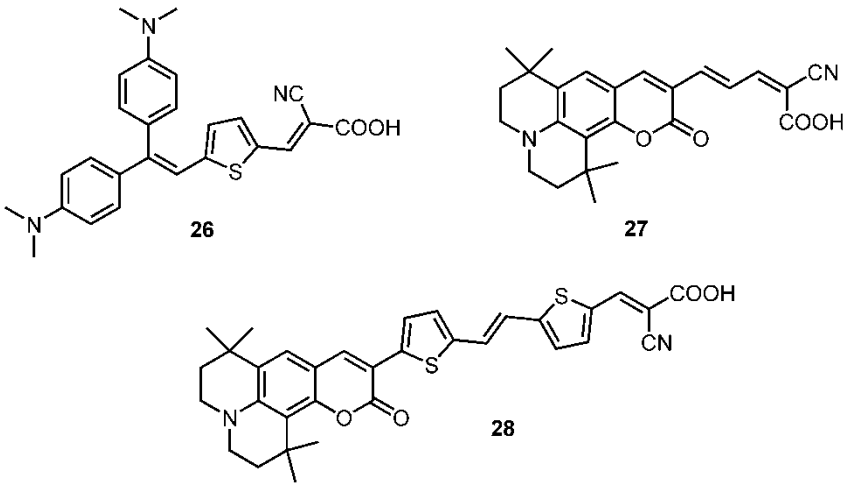

Figure 13. Coumarine and oligoen based sensitizers

Carbazole dyes[79,80] with quaterthiophene and cyanoacrylic acid group showed high performance in liquid electrolyte based DSSCs. The efficiency of compound **29** was calculated as 8.3% (J_{sc} = 15.22 mAcm^{-2}, V_{oc}= 0.73 V, *ff* = 0.75). This high overall efficiency can be attributed to a long electron lifetime. Long alkyl chains in compounds **29** improve efficiency by suppressing the aggregate formation on semiconductor. Another example with hydrophobic long alky chains is the study of Ko, and Gratzel. Introducing bulky difluorenylphenylamine to the core of oligothiophene (compound **30**)[81] prevents aggregation of dyes on semiconductor and decreases charge recombination. Bulky long alkyl chains prohibit hydrophilic I_3^- ions to move through TiO_2. So that electron leakage from redox mediator can be avoided.

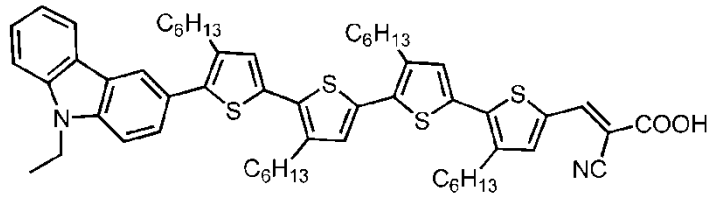

29

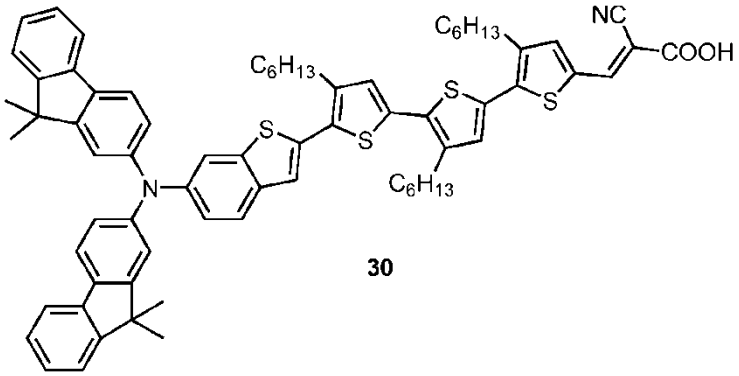

30

Figure 14. Sensitizers with long alkyl chains

Cyanoacrylic group is one of the primary choices as an acceptor and anchor. Another alternative for this successful moiety is the carboxylic acid group. Three selected examples of sensitizers incorporated with carboxylic acid moiety are given in figure 15. Compound **31**[82] that contains rhodanine-3-acetic acid as the anchoring group as well as diethylaniline as the donor showed overall efficiency around 3.9%. Another example with similar anchoring group, compound **32**, which is the derivative of phenothiazine chromophore, scan almost all visible region with absorption maxima at 452 nm and 481 nm, but efficiency is just 1.9%.[83] Low photocurrent generation of compound **32** is explained by DFT (density functional theory) calculations. These studies showed that HOMO of the dye is localized on the donor moiety as expected but the LUMO is mostly located on chromophore rather than contributing to anchoring group. This situation led ineffective electron transfer to the semiconductor when dye is excited. On the other hand a similar dye with cyanoacrylic acid moiety where LUMO is totally localized on anchoring group showed 5.5% efficiency.[83] It seems that carboxy group is inefficient as an anchor but one of the most efficient metal-free organic dyes was obtained by using indoline dye and carboxylic acid (compound **33**)[84]

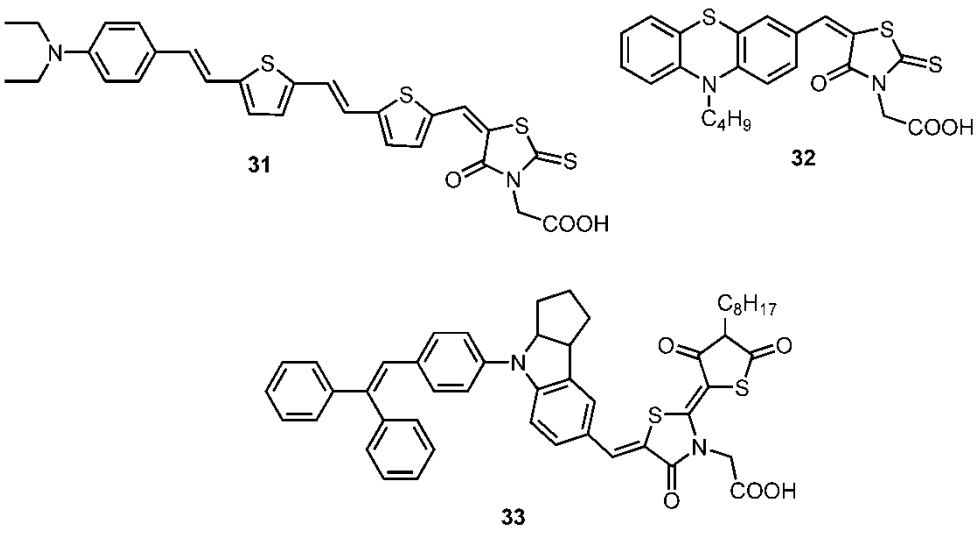

Figure 15. Organic sensitizer with carboxylic acid moiety as an anchor

In solid state DSSCs, however the overall conversion efficiency is typically lower than the liquid counterpart, many organic dyes were studied. Some of the examples are given in figure 16. Compound **34**[29] contains triarylamine groups as donors and gave efficiencies about 2.8% to 3%. When the donor or acceptor groups change, it mostly does not affect too much the efficiency. Nazeeruddin and co-workers introduced perylene dye (compound **35**)[30] with conversion efficiency 1.8%. This design uses spiro-MeOTAD as a hole conductor. The other well known example is blue squarylium dye (compound **36**) with efficiency of 1.5% in solid state DSSC.[85] In solid state based devices, effect of the dye is less, on the other hand, the most important thing is the hole transfer yield.

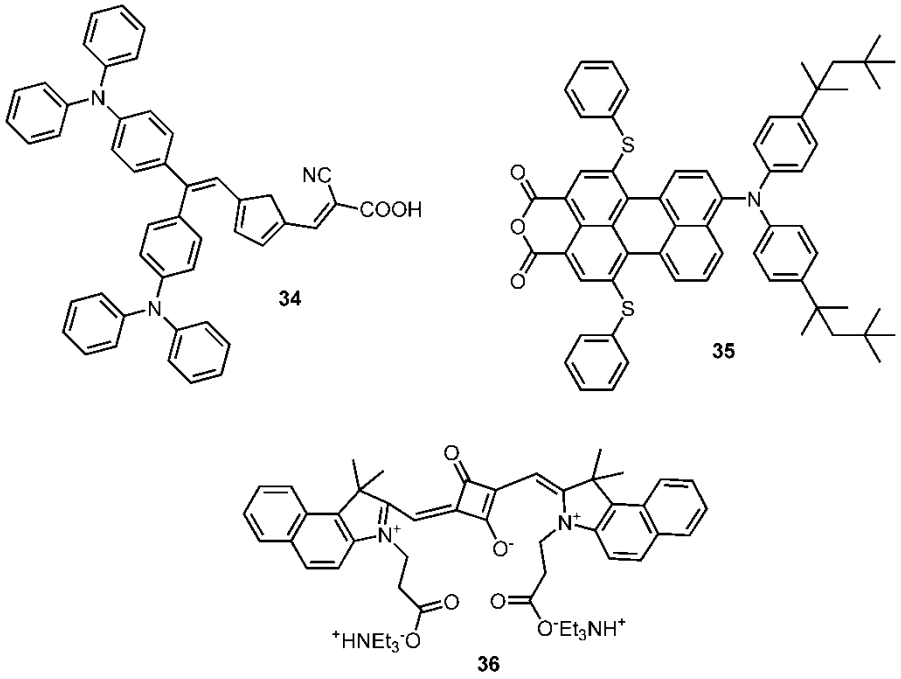

Figure 16. Sensitizers for solid state DSSCs

It is possible to give more examples to sensitizers. There are many studies on both dye and device construction. Recent achievements were reviewed mainly in three articles.[15,21,34]

1.2.6. BODIPY Dyes

Boradiazaindacene (BODIPY) dyes were first discovered in 1968 by Kreuzer and Treibs.[86] After their initial synthesis, they are used in biological imaging (DNA, protein labelling).[87-89] Recently, many research groups all around the world are investigating BODIPY chemistry and its applications. BODIPY's several properties make it unique such as; high molar extinction coefficients, large fluorescence quantum yields, intense absorption at higher wavelengths, ease of synthesis, purification and modification. Moreover, good solubility in organic solvents and chemical stability are additional useful advantages of this class of dye. Due to the photophysical and chemical

properties of BODIPY dyes, there are many applications areas of these dyes. Energy transfer cassettes,[90] photodynamic therapy,[91] fluorescent ion sensing,[92,93] molecular logic gates[94] and light harvesting systems[95] are major examples for these applications.

BODIPY based dyes are also possible candidates for DSSC as a photosensitizer. In literature there are few examples. A contribution that shows current generation with BODIPYs was reported by Vobecka et al (compound **37**).[96] They did not apply their dye to DSSC device so no conversion efficiency was shown.

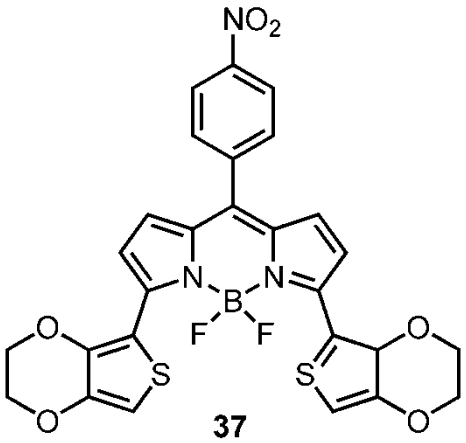

37

Figure 17. Generation of current with BODIPY dye

First contribution which includes photovoltaic parameters was made by Fukuzimi et al.[97] The solar light to electricity conversion efficiencies are around 0.1%.

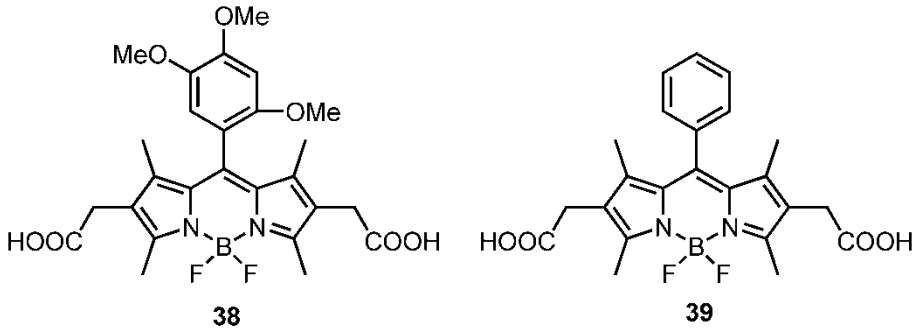

Figure 18. First report of BODIPY dyes in DSSCs

One of the BODIPY derivative integrated to DSSC is compound **40**. In this work, Akkaya et al. synthesized a sensitizer which has high IPCE values at longer wavelengths showing conversion efficiency around 1.6%.[98]

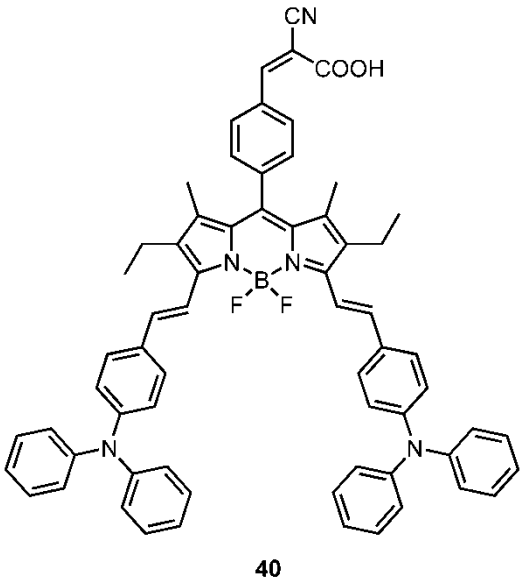

Figure 19. Akkaya Group's sensitizer

Another example where BODIPYs were used as a sensitizers is Ziessel's study (compounds **41**, **42** and **43**).[99] In this article Ziessel and coworkers modified BODIPY core with suitable groups to minimize aggregation induced losses. In solid state DSSCs, Ziessel et al. obtained conversion efficiencies 1.17% and

1.34% with BODIPY dyes (compound **44**).[100] Design strategies for BODIPY sensitizers will be discussed in following chapters.

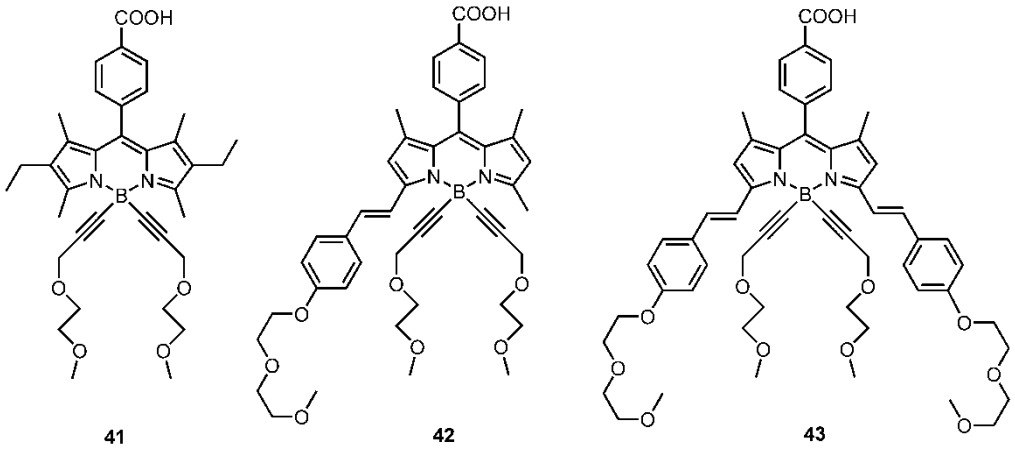

Figure 20. BODIPY derivatives in liquid electrolyte solar cell

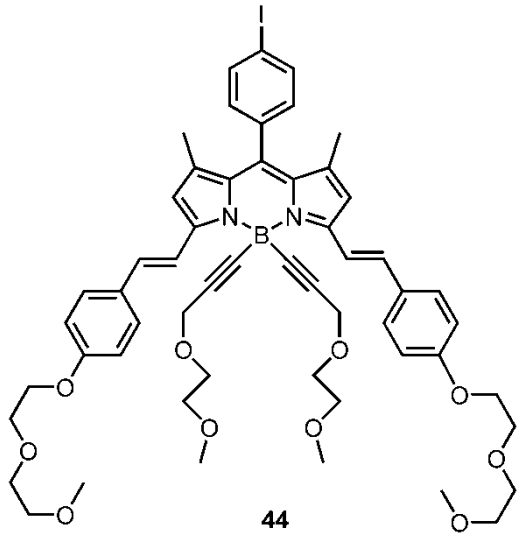

Figure 21. Bodipy as a sensitizer in solid state DSSC

CHAPTER 2

EXPERIMENTAL

2.1. General

All chemicals and solvents obtained from Sigma-Aldrich were used without further purification. Reactions were monitored by thin layer chromatography using Merck TLC Silica gel 60 F_{254}. Chromatography on silica gel was performed over Merck Silica gel 60 (particle size: 0.040-0.063 mm, 230-400 mesh ASTM).

^{1}H NMR and ^{13}C NMR spectra were recorded at room temperature on Bruker DPX-400 (operating at 400 MHz for ^{1}H NMR and 100 MHz for ^{13}C NMR) in $CDCl_3$ or DMSO-d_6 with tetramethylsilane (TMS) as internal standard. Coupling constants (*J values*) are given in Hz and chemical shifts are reported in parts per million (ppm). Splitting patterns are designated as s (singlet), d (doublet), t (triplet), q (quartet), m (multiplet), and p (pentet).

Absorption spectra in solution were acquired using a Varian Cary-100 spectrophotometer. Mass spectra were recorded on Agilent Technologies 6530 Accurate-Mass Q-TOF LC/MS. Spectrophotometric grade solvents were used for spectroscopy experiments. Cyclic voltammetry measurements, absorption spectra on TiO_2 and calculation of photovoltaic parameters for sensitizers in solid state DSSC were done at the Institute of Solar Energy, Ege University, Bornova, Izmir, Turkey. Absorption spectra on TiO_2 and calculation of photovoltaic parameters for sensitizers in liquid electrolyte based DSSC were acquired at Laboratory of Photonics and Interfaces, EPFL SB ISIC LPI Lausanne Switzerland.

2.2. Syntheses

BODIPY based dyes were synthesized as potential sensitizers for both solid state and liquid based DSSCs. Compounds **50**[101], **52**[102] and **59**[103] were synthesized according to literature.

2.2.1. Synthesis of Compound 47

To a stirred argon degassed solution of 400 mL CH_2Cl_2, 2-methyl pyrrole (**46**) (12.3 mmol, 1.0 g) and 4-carboxybenzaldehyde (**45**) (6.0 mmol, 0.9 g) were added. This process was followed by addition of 1-2 drops of TFA. The reaction mixture was stirred under N_2 for 1 day at r.t. After addition of DDQ (6.0 mmol, 1.36 g) to the reaction mixture, stirring was continued for 30 min. Then Et_3N (5 mL) and $BF_3.OEt_2$ (5 mL) were introduced. 100 mL of water was added into the reaction mixture and then extracted into the $CHCl_3$ (3 x 100 mL). Na_2SO_4 was used as a drying agent. The organic layer was concentrated *in vacuo* and the crude product was purified by column chromatography packed with silica gel using ($CHCl_3$: MeOH 95:5) as the eluant. Red solid (1.25 g, 30%).

^{1}H NMR (400 MHz, $CDCl_3$): δ_H 8.25 (2H, d, *J* = 7.6 Hz, Ar*H*), 7.65 (2H, d, *J* = 7.7 Hz, Ar*H*), 6.70 (2H, s, Ar*H*), 6.30 (2H, d, *J* = 3.4 Hz, Ar*H*), 2.70 (6H, s, CH_3).

^{13}C NMR (100 MHz, $CDCl_3$): δ_C 170.5, 158.5, 140.9, 139.4, 134.5, 130.6, 130.5, 130.2, 130.0, 119.9, 15.0 ppm.

MS (TOF- ESI): m/z: : Calcd: 340.1195 $[M-H]^+$, Found: 340.1130 $[M-H]^+$, Δ=19.1 ppm.

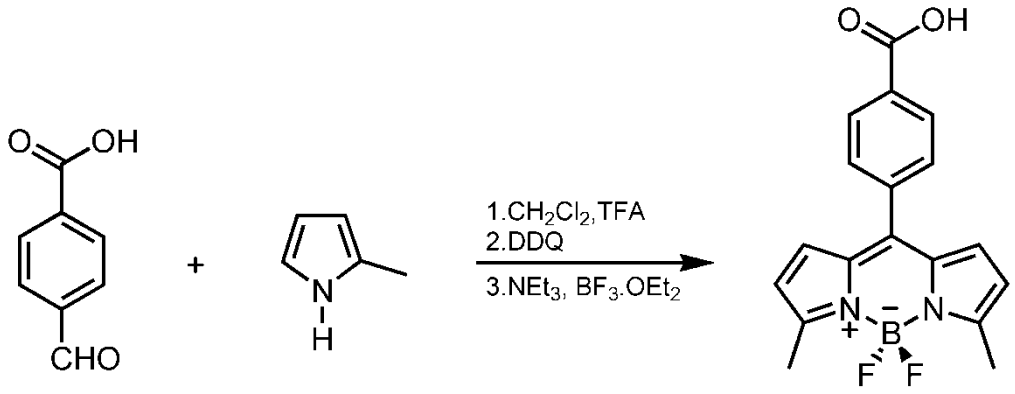

45 **46** **47**

Figure 22. Synthesis of Compound **47**

2.2.2. Synthesis of Compound 49

47 (0.88 mmol, 0.30 g) and N,N-diphenylaminobenzaldehyde (**48**) (3.53 mmol, 0.96 g) were dissolved in 50 mL benzene. To this solution, piperidine (0.3 mL) and acetic acid (0.3 mL) was added. The mixture was heated under reflux in round bottom flask equipped with a Dean Stark trap for 4 hours. The reaction was finished by cooling it to room temperature. Solvent was concentrated *in vacuo*. 100 mL of water was added and then mixture extracted into the $CHCl_3$ (3 x 100 mL). Organic phase dried over Na_2SO_4, evaporated and the crude product was purified by column chromatography packed with silica gel using ($CHCl_3$: MeOH 93:7) as the eluant. Black waxy solid (0.15 mg, 20%).

^{1}H NMR (400 MHz, DMSO-d_6): δ_H 8.31 (1H, s, COO*H*), 8.10 (2H, d, *J* = 8.3 Hz, Ar*H*), 7.72 (2H, d, *J* = 8.2 Hz, Ar*H*), 7.62 (2H, d, *J* = 16.2 Hz, C*H*), 7.51 (4H, d, *J* = 8.7 Hz, Ar*H*), 7.44 (2H, d, *J* = 16.2 Hz, C*H*), 7.38-7.32 (8H, m, Ar*H*), 7.23 (2H, d, *J* = 4.6 Hz, Ar*H*), 7.15-7.05 (12H, m, Ar*H*), 6.95 (4H, d, *J* = 8.5 Hz, Ar*H*), 6.85 (2H, d, *J* = 4.6 Hz, Ar*H*).

^{13}C NMR (100 MHz, DMSO-d_6): δ_C 185.7, 154.9, 149.1, 146.8, 141.5, 137.7, 136.7, 135.6, 130.9, 130.2, 129.9, 129.8, 129.1, 125.5, 124.6, 121.9, 117.8, 116.8, 116.5 ppm.

MS (TOF- ESI): m/z: Calcd: 850.3291 $[M-H]^+$, Found: 850.3271 $[M-H]^+$, Δ=2.3 ppm.

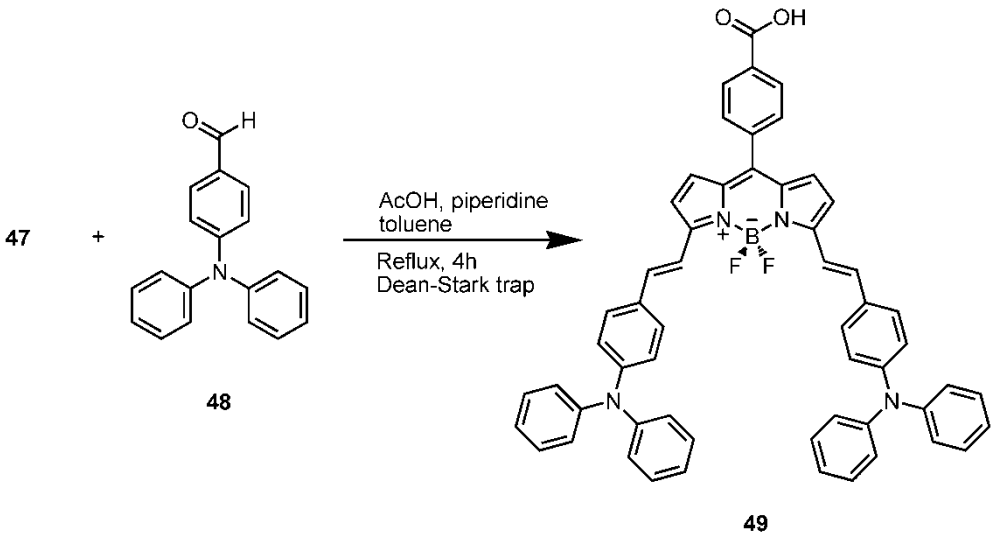

Figure 23. Synthesis of Compound **49**

2.2.3. Synthesis of Compound 51

47 (0.88 mmol, 0.30 g) and N,N-di(4-methoxyphenyl)aminobenzaldehyde (**50**) (3.53 mmol, 1.18 g) were dissolved in 50 mL benzene. To this solution, piperidine (0.3 mL) and acetic acid (0.3 mL) was added. The mixture was heated under reflux in round bottom flask equipped with a Dean Stark trap for 4 hours. The reaction was finished by cooling it to room temperature. Solvent was concentrated *in vacuo*. 100 mL of water was added and then mixture extracted into the $CHCl_3$ (3 x 100 mL). Organic phase dried over Na_2SO_4, evaporated and the crude product was purified by column chromatography packed with silica gel using ($CHCl_3$: MeOH 93:7) as the eluant. Black waxy solid (0.17 g, 20%).

^{1}H NMR (400 MHz, DMSO-d_6): δ_H 8.25 (1H, s, COO*H*), 8.05 (2H, d, *J* = 8.3 Hz, Ar*H*), 7.64 (2H, d, *J* = 8.2 Hz, Ar*H*), 7.52 (2H, d, *J* = 17.2 Hz, C*H*), 7.38 (4H, d, *J* = 8.7 Hz, Ar*H*), 7.32 (2H, d, *J* = 15.2 Hz, C*H*), 7.15 (2H, d, *J* = 4.6 Hz,

Ar*H*), 7.10-7.05 (8H, m, Ar*H*), 6.95-6.85 (12H, m, Ar*H*), 6.78 (2H, d, *J* = 4.6 Hz, Ar*H*), 6.72 (4H, d, *J* = 8.5 Hz, Ar*H*), 3.71 (12H, s, OCH_3).

^{13}C NMR (100 MHz, DMSO-d_6): δ_C 167.5, 156.9, 154.9, 150.2, 139.5, 138.2, 137.8, 135.4, 132.6, 131.0, 129.9, 129.8, 129.6, 129.3, 129.1, 128.0, 127.7, 120.2, 118.4, 117.6, 115.5, 55.7 ppm.

MS (TOF- ESI): m/z: : Calcd: 970.3713, Found: 970.3692, Δ=2.2 ppm.

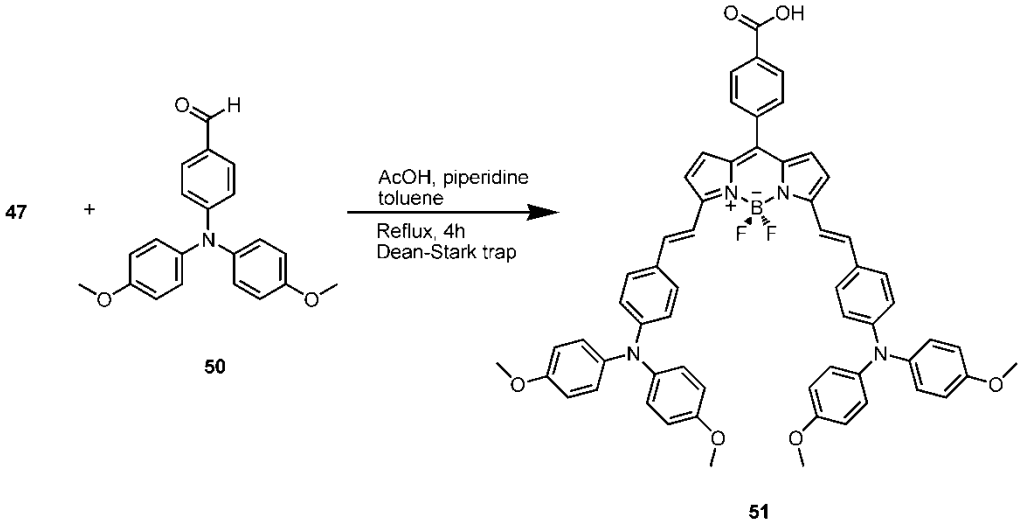

Figure 24. Synthesis of Compound **51**

2.2.4. Synthesis of Compound 53

47 (0.44 mmol, 0.15 g) and 3,4,5-Tris(octadecyloxy)benzaldehyde (**52**) (1.32 mmol, 1.26 g) were dissolved in 50 mL benzene. To this solution, piperidine (0.3 mL) and acetic acid (0.3 mL) was added. The mixture was heated under reflux in round bottom flask equipped with a Dean Stark trap for 4 hours. The reaction was finished by cooling it to room temperature. Solvent was concentrated *in vacuo*. 100 mL of water was added and then mixture extracted into the $CHCl_3$ (3 x 100 mL). Organic phase dried over Na_2SO_4, evaporated and the crude product was purified by column chromatography packed with silica gel using ($CHCl_3$: MeOH 95:5) as the eluant. Dark green solid (0.24 g, 25%).

^{1}H NMR (400 MHz, $CDCl_3$): δ_H 8.28 (2H, d, *J* = 7.8 Hz, Ar*H*), 7.65 (2H, d, *J* = 8.1 Hz, Ar*H*), 7.60 (2H, d, *J* = 15.8 Hz, C*H*), 7.30 (2H, d, *J* = 16.4 Hz, C*H*), 6.95 (2H, d, *J* = 4.6 Hz, Ar*H*), 6.85 (4H, s, Ar*H*), 6.75 (2H, d, *J* = 4.3 Hz, Ar*H*), 4.15-4.01 (12H, m, OCH_2), 1.85-1.72 (12H, m, CH_2), 1.69-1.21 (180H, m, CH_2), 1.05-0.85 (18H, m, CH_3).

^{13}C NMR (100 MHz, DMSO-d_6): δ_C 155.3, 153.4, 140.0, 139.3, 137.8, 137.0, 135.9, 131.6, 130.5, 130.0, 129.1, 118.1, 116.7, 106.6, 73.6, 69.3, 31.9, 30.4, 29.8, 29.7, 29.5, 29.4, 26.2, 26.1, 22.7, 14.1 ppm.

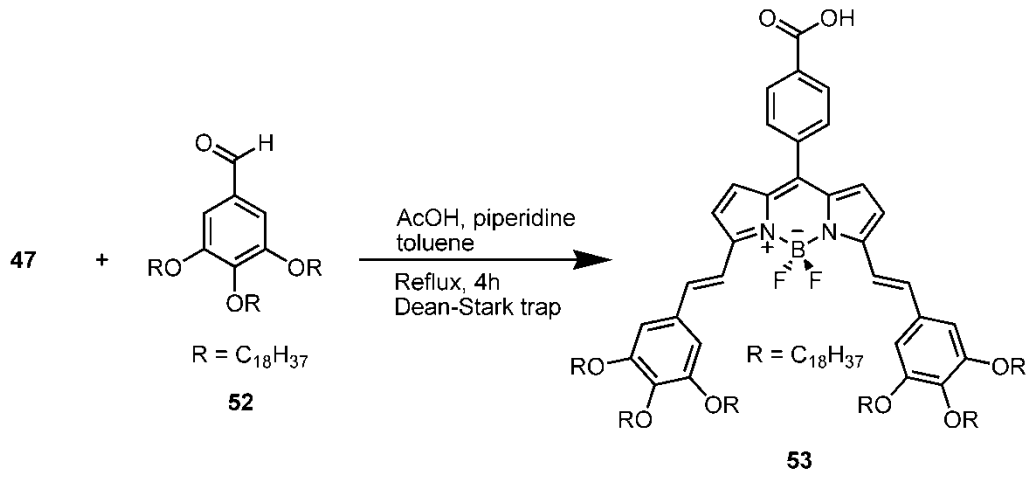

Figure 25. Synthesis of Compound **53**

2.2.5. Synthesis of Compound 54

Iodic acid (0.88 mmol, 0.16 g) dissolved in 2 mL of water. Iodic acid solution was added to mixture of **47** (0.44 mmol, 0.15 g) and iodine (1.10 mmol, 0.28 g). The reaction mixture was stirred at 60^{o}C and was monitored by TLC ($CHCl_3$: MeOH 93:7). When all the starting material had been consumed, saturated $Na_2S_2O_3$ solution in water was added and the product was extracted into chloroform. Solvent was concentrated *in vacuo*. Red waxy solid (0.26 g, 100%).

^{1}H NMR (400 MHz, DMSO-d_6): δ_H 8.15 (2H, d, J = 8.2 Hz, Ar*H*), 7.65 (2H, d, J = 8.2 Hz, Ar*H*), 7.15 (2H, s, Ar*H*), 2.50 (6H, s, CH_3).

^{13}C NMR (100 MHz, DMSO-d_6): δ_C 167.2, 160.2, 159.0, 140.4, 137.2, 136.8, 134.9, 133.1, 131.1, 130.0, 15.8 ppm.

MS (TOF- ESI): m/z: : Calcd: 591.9128 $[M-H]^+$, Found: 591.9031 $[M-H]^+$, Δ=16.4 ppm.

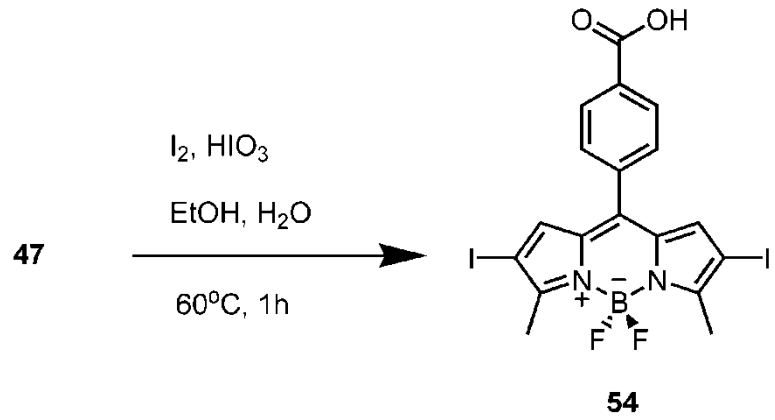

Figure 26. Synthesis of Compound **54**

2.2.6. Synthesis of Compound 55

54 (0.18 mmol, 0.11 g) and N,N-diphenylaminobenzaldehyde (**48**) (0.55 mmol, 0.15 g) were dissolved in 50 mL benzene. To this solution, piperidine (0.3 mL) and acetic acid (0.3 mL) was added. The mixture was heated under reflux in round bottom flask equipped with a Dean Stark trap for 4 hours. The reaction was finished by cooling it to room temperature. Solvent was concentrated *in vacuo*. 100 mL of water was added and then mixture extracted into the $CHCl_3$ (3 x 100 mL). Organic phase dried over Na_2SO_4, evaporated and

the crude product was purified by column chromatography packed with silica gel using ($CHCl_3$: MeOH 93:7) as the eluant. Black solid (0.05g, 25%).

^{1}H NMR (400 MHz, DMSO-d_6): δ_H 8.20 (1H, s, COO*H*), 8.05 (2H, d, *J* = 7.9 Hz, Ar*H*), 8.00 (2H, d, *J* = 16.6 Hz, C*H*), 7.60 (2H, d, *J* = 8.2 Hz, Ar*H*), 7.41 (4H, d, *J* = 8.6 Hz, Ar*H*), 7.35 (2H, d, *J* = 16.4 Hz, C*H*), 7.30-7.21 (8H, m, Ar*H*), 7.09-6.97 (14H, m, Ar*H*), 6.85 (4H, d, *J* = 8.5 Ar*H*).

^{13}C NMR (100 MHz, DMSO-d_6): δ_C 164.8, 162.5, 161.1, 155.7, 151.7, 149.6, 147.9, 146.8, 142.7, 139.3, 136.8, 132.7, 132.1, 130.2, 129.9, 129.3, 125.7, 125.6, 124.8, 121.9 ppm.

MS (TOF- ESI): m/z: : Calcd: 1102.1223 $[M-H]^+$, Found: 1102.1184 $[M-H]^+$, Δ=3.5 ppm.

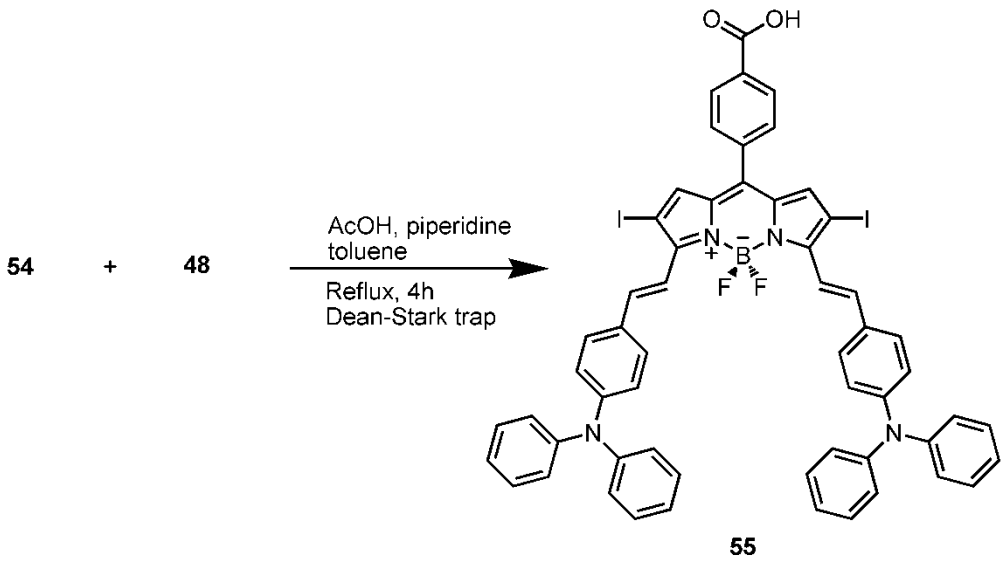

Figure 27. Synthesis of Compound **55**

2.2.7. Synthesis of Compound 58

To a stirred argon degassed solution of 400 mL CH_2Cl_2, 2,4-dimethyl pyrrole (**57**) (15.8 mmol, 1.5 g) and 3,5-bis(decyloxy)phenylbenzaldehyde (**56**) (7.17 mmol, 3.0 g) were added. This process was followed by addition of 1-2 drops of TFA. The reaction mixture was stirred under N_2 for 1 day at r.t. After addition of DDQ (7.17 mmol, 1.63 g) to the reaction mixture, stirring was continued for 30 min. Then Et_3N (5 mL) and $BF_3.OEt_2$ (5 mL) were introduced. 100 mL of water was added into the reaction mixture and then extracted into the $CHCl_3$ (3 x 100 mL). Na_2SO_4 was used as a drying agent. The organic layer was concentrated *in vacuo* and the crude product was purified by column chromatography packed with silica gel using ($CHCl_3$: Hexanes 2:1) as the eluant. Red solid (1.38 g, 30%).

^{1}H NMR (400 MHz, $CDCl_3$): δ_H 6.45 (s, 1H, Ar*H*), 6.35 (s, 2H, Ar*H*), 5.90 (s, 2H, Ar*H*), 3.85 (t, 4H, *J* = 6.56 Hz, OCH_2), 2.47 (s, 6H, CH_3), 1.70 (m, 4H, CH_2), 1.49 (s, 6H, CH_3), 1.35 (m, 4H, CH_2), 1.20 (s, 24H, CH_2), 0.80 (t, 6H, *J* = 6.5 Hz, C*H*3).

^{13}C NMR (100 MHz, $CDCl_3$): δ_C 161.2, 155.4, 143.2, 136.4, 131.2, 121.0, 106.4, 102.3, 68.4, 31.9, 29.6, 29.5, 29.3, 29.2, 26.0, 22.7, 14.6, 14.2, 14.0 ppm.

MS (TOF- ESI): m/z: : Calcd: 636.4638 $[M-H]^+$, Found: 636.4564 $[M-H]^+$, Δ=11.6 ppm.

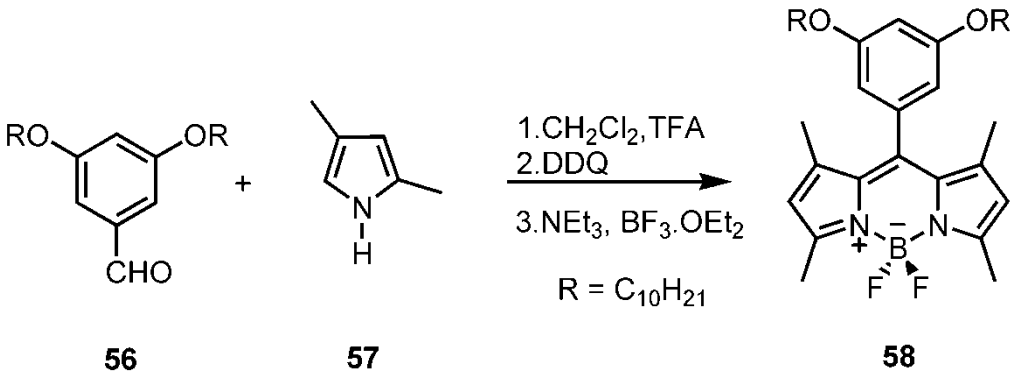

56 **57** **58**

Figure 28. Synthesis of compound **58**

2.2.8. Synthesis of Compound 61

59 (0.10 g, 0.14 mmol) was dissolved in 10 mL freshly distilled THF and 5 mL $(i\text{-}Pr)_2NH$. Then the reaction was purged with argon until all the chemicals were added. After 15 minutes $Pd(PPh_3)_2Cl_2$ (4.71 mg, 0.0067 mmol) and CuI (2.13 mg, 0.0112 mmol) were added to the reaction mixture. Then 4-ethynyl benzoic acid (**60**) (0.04 g, 0.27 mmol) was added after 10 minutes. The reaction was proceeded for 12 hours at 60°C. The reaction mixture was evaporated under reduced pressure and the compound was purified over silica gel using ($CHCl_3$: MeOH 95:5). Red solid (76.44 mg, 70%).

^{1}H NMR (400 MHz, $CDCl_3$): δ_H 8.05 (2H, d, *J* = 8.2 Hz, Ar*H*), 7.55 (2H, d, *J* = 8.2 Hz, Ar*H*), 6.60 (1H, d, *J*=2.1 Hz, Ar*H*), 6.41 (2H, d, *J* = 2.2 Hz, Ar*H*), 6.05 (1H, s, Ar*H*), 3.97 (4H, t, *J* = 6.6 Hz, OCH_2), 2.72 (3H, s, CH_3), 2.60 (3H, s, CH_3), 1.75 (4H, p, *J* = 5.6 Hz CH_2), 1.71 (3H, s, CH_2), 1.62 (3H, s, CH_3), 1.45 (4H, m, CH_2), 1.40-1.18 (24H, m, CH_2), 0.88 (6H, t, *J* = 6.7 Hz, CH_3).

^{13}C NMR (100 MHz, $CDCl_3$): δ_C 171.2, 161.4, 158.4, 156.3, 145.4, 142.9, 142.3, 137.1, 136.0, 132.5, 131.1, 130.2, 129.4, 128.0, 122.3, 114.2, 106.2, 102.5, 95.3, 86.2, 68.5, 31.9, 29.5, 29.4, 29.3, 29.1, 26.0, 22.7, 14.5, 14.1, 13.1 ppm.

MS (TOF- ESI): m/z: : Calcd: 780.4849 $[M-H]^+$, Found: 780.4807 $[M-H]^+$, Δ=5.4 ppm.

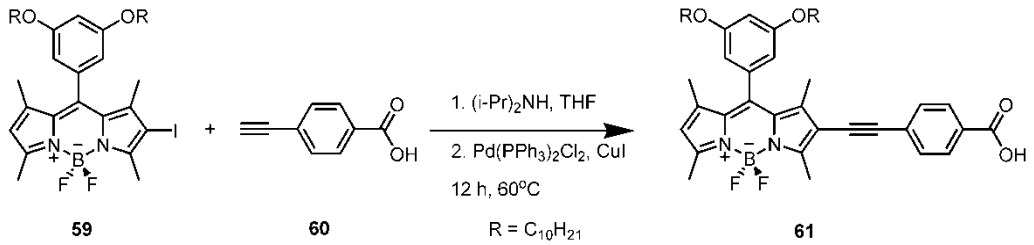

Figure 29. Synthesis of Compound **61**

2.2.9. Synthesis of Compound 62

61 (0.13 mmol, 0.10 g) and N,N-diphenylaminobenzaldehyde (**48**) (0.51 mmol, 0.14 g) were dissolved in 50 mL benzene. To this solution, piperidine (0.3 mL) and acetic acid (0.3 mL) was added. The mixture was heated under reflux in round bottom flask equipped with a Dean Stark trap for 4 hours. The reaction was finished by cooling it to room temperature. Solvent was concentrated *in vacuo*. 100 mL of water was added and then mixture extracted into the $CHCl_3$ (3 x 100 mL). Organic phase dried over Na_2SO_4, evaporated and the crude product was purified by column chromatography packed with silica gel using ($CHCl_3$: MeOH 93:7) as the eluant. Dark-green solid. (58.76 mg, 35%).

^{1}H NMR (400 MHz, $CDCl_3$): δ_H 8.29 (1H, d, *J* = 16.1 Hz, C*H*), 8.07 (2H, d, *J* = 7.4 Hz, Ar*H*), 7.72 (1H, d, *J* = 16.1 Hz, C*H*), 7.63 (1H, d, *J* = 16.1 Hz, C*H*), 7.58-7.47 (7H, m, Ar*H*-C*H*), 7.35-7.21 (8H, m, Ar*H*), 7.20-7.02 (16H, m, Ar*H*), 6.67 (1H, s, Ar*H*), 6.62-6.55 (1H, br s, Ar*H*), 6.52-6.46 (2H, br s, Ar*H*), 4.05-3.80 (4H, br s, OCH_2), 1.85-167 (4H, m, CH_2), 1.61 (3H, s, CH_3), 1.58 (3H, s, CH_3), 1.52-1.41 (4H, m, CH_2), 1.38-1.15 (24H, m, CH_2), 0.95-0.80 (6H, m, CH_3).

^{13}C NMR (100 MHz, $CDCl_3$): δ_C 161.2, 149.1, 148.7, 147.3, 147.0, 137.9, 137.0, 136.5, 134.4, 130.9, 130.7, 130.3, 129.8, 129.4, 128.9, 128.5, 125.2,

125.0, 123.8, 123.5, 122.7, 122.2, 106.9, 102.4, 96.8, 68.5, 31.9, 29.6, 29.5, 29.4, 29.3, 29.2, 26.0, 22.7, 14.7, 14.1, 12.9 ppm.

MS (TOF- ESI): m/z: : Calcd: 1290.6945 $[M-H]^+$, Found: 1290.6899 $[M-H]^+$, Δ=3.6 ppm.

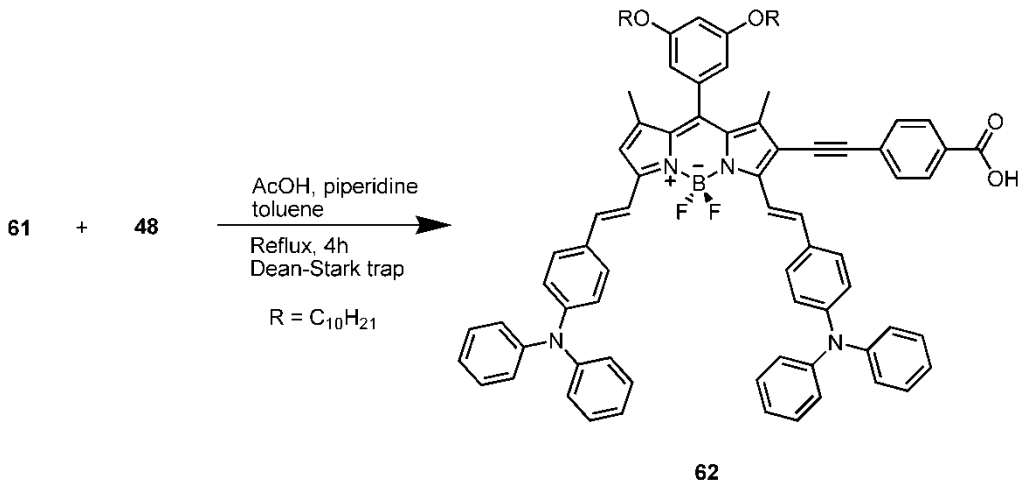

Figure 30. Synthesis of Compound **62**

2.2.10. Synthesis of Compound 63

A mixture of DMF (6 mL) and $POCl_3$ (6 mL) was stirred under argon for 5 min in the ice bath. After warming solution up to room temperature, it was stirred for additional 30 min. **58** (0.50 mmol, 158.0 mg) in 60 mL dichloroethane was added to the solution and temperature raised to 50^0C. After stirring for 2 h, the mixture was cooled to room temperature and then poured in to iced cooled saturated aqueous solution of $NaHCO_3$ (150 mL). Then reaction mixture was stirred for 30 min after warming solution to room temperature. After 30 min. the mixture was washed with H_2O (2x100 mL). The product was extracted into the dichloromethane. Organic phase dried over Na_2SO_4. Reddish-brown solid was obtained (157.0 mg, 89%).

^{1}H NMR (400 MHz, $CDCl_3$, 300K): δ_H 10.02 (1H, s; C*H*O), 6.58 (1H, t; *J*=2.61 Hz, Ar*H*), 6.41 (2H, d; *J*=2.20 Hz, Ar*H*), 6.15 (1H, s; Ar*H*), 3.92 (4H, t; *J*=6.60 Hz, OCH_2), 2.81 (3H, s; CH_3), 2.60 (3H, s; CH_3), 1.85 (3H, s; CH_3), 1.75 (4H, m; CH_2), 1.42 (4H, m; CH_2), 1.40-1.15 (24H, m; CH_2), 0.85 (6H, t; *J*=6.68 Hz, CH_3).

^{13}C NMR (100 MHz, $CDCl_3$): δ_C 185.8, 161.4, 156.4, 147.3, 143.5, 142.9, 135.5, 133.8, 130.8, 129.5, 128.8, 126.3, 123.8, 106.1, 102.5, 68.5, 31.9, 29.5, 29.3, 29.1, 26.0, 22.7, 15.0, 14.7, 14.1, 13.0, 11.5 ppm.

MS (TOF- ESI): m/z: : Calcd: 664.4587 $[M-H]^+$, Found: 664.4503 $[M-H]^+$, Δ=12.7 ppm.

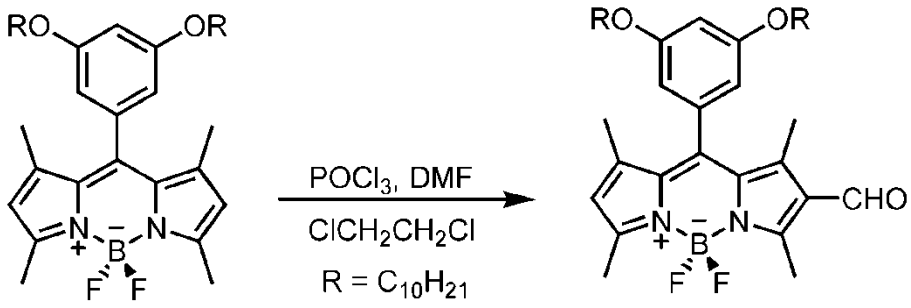

Figure 31. Synthesis of Compound **63**

2.2.11. Synthesis of Compound 64

63 (0.12 mmol, 83.0 mg) and cyanoacetic acid (0.49 mmol, 42.3 mg) were dissolved in toluene. One drop of piperidine and catalytic amount of acetic acid were added to the mixture under argon atmosphere. The reaction mixture was refluxed and stirred under argon for 3 h. Then mixture washed with water (2x50 mL). Organic phase dried over Na_2SO_4 and solvent was evaporated and

the residue was purified by silica gel column chromatography using ($CHCl_3$: MeOH 90:10) as the eluant. Red solid was obtained (50.0 mg, 57%).

^{1}H NMR (400 MHz, $CDCl_3$): δ_H 8.18 (1H, s; C*H*), 6.55 (1H, s; Ar*H*), 6.41 (2H, d; *J* = 1.9 Hz, Ar*H*), 6.08 (1H, s; Ar*H*), 3.91 (4H, t; *J* = 6.5 Hz OCH_2), 2.57 (6H, s; CH_3), 1.80-1.68 (4H, m; CH_2), 1.63 (3H, s; CH_3), 1.59 (3H, s; CH_3), 1.48-1.37 (4H, m; CH_2), 1.45-1.18 (24H, m; CH_2), 0.86 (6H, t; *J* = 6.8 Hz CH_3).

^{13}C NMR (100 MHz, $CDCl_3$): δ_C 161.4, 153.7, 142.8, 140.6, 135.6, 133.4, 130.8, 123.9, 123.3, 106.1, 102.6, 68.5, 31.9, 29.6, 29.4, 29.3, 29.1, 25.9, 14.6, 14.1 ppm.

MS (TOF- ESI): m/z: : Calcd: 731.4645 $[M-H]^+$, Found: 731.4585 $[M-H]^+$, Δ=8.2 ppm.

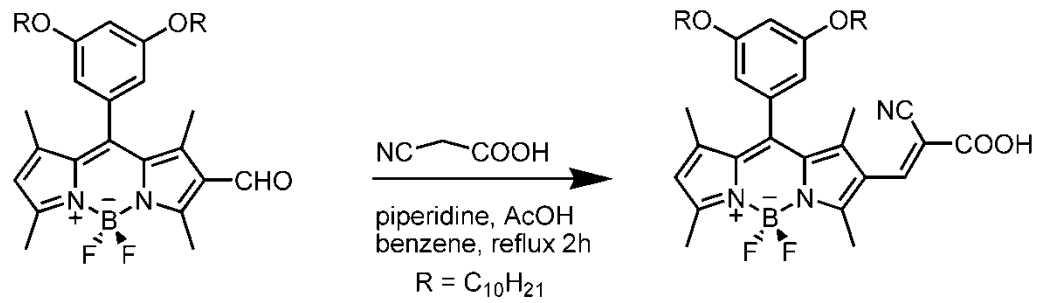

63 **64**

Figure 32. Synthesis of Compound **64**

2.2.12. Synthesis of Compound 65

64 (0.12 mmol, 90.0 mg) and N,N-diphenylaminobenzaldehyde (**48**) (0.37 mmol, 100.9 mg) were dissolved in 50 mL benzene. To this solution, piperidine (0.3 mL) and acetic acid (0.3 mL) was added. The mixture was heated under reflux in round bottom flask equipped with a Dean Stark trap for 4 hours. The reaction was finished by cooling it to room temperature. Solvent was

concentrated *in vacuo*. 100 mL of water was added and then mixture extracted into the $CHCl_3$ (3 x 100 mL). Organic phase dried over Na_2SO_4, evaporated and the crude product was purified by column chromatography packed with silica gel using ($CHCl_3$: MeOH 93:7) as the eluant. Green solid was obtained (52.20 mg, 35%).

^{1}H NMR (400 MHz, $CDCl_3$): δ_H 8.24 (1H, s; C*H*), 7.61-7.52 (1H, m; C*H*), 7.47 (2H, d; *J* = 8.0 Hz, Ar*H*), 7.33-7.24 (6H, m; Ar*H*), 7.21-7.08 (12H, m; Ar*H*), 7.04-6.93 (8H, m; Ar*H*), 6.90-6.69 (4H, m; Ar*H*), 6.62 (1H, s; Ar*H*), 6.46 (2H, s; Ar*H*), 3.92-3.61 (4H, m; OCH_2), 1.89-1.54 (4H, m; CH_2), 1.52-1.49 (4H, m; CH_2), 1.48-1.12 (30H, m; CH_2, CH_3), 0.91-0.74 (6H, m; CH_3).

^{13}C NMR (100 MHz, $CDCl_3$): δ_C 161.1, 148.5, 147.1, 147.0, 139.0, 136.4, 132.7, 129.4, 129.3, 128.9, 128.6, 125.4, 125.1, 124.8, 123.7, 123.3, 122.6, 122.3, 117.0, 106.8, 68.4, 31.9, 29.6, 29.5, 29.4, 29.3, 29.2, 26.0, 22.7, 14.7, 14.5, 14.1 ppm.

MS (TOF- ESI): m/z: : Calcd: 1241.6741 $[M-H]^+$, Found: 1241.6790 $[M-H]^+$, Δ=3.9 ppm.

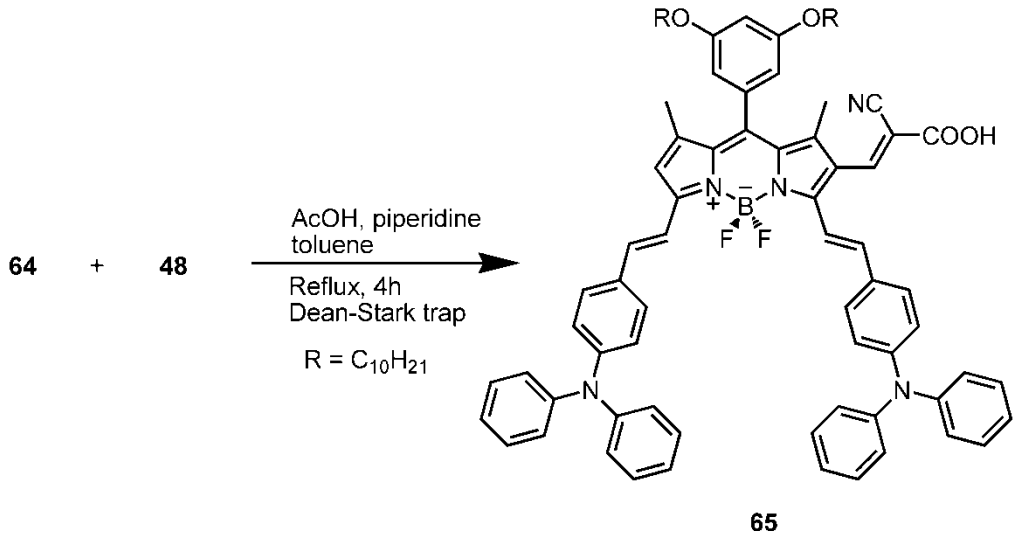

Figure 33. Synthesis of Compound **65**

CHAPTER 3

RESULTS and DISCUSSION

3.1. General Perspective

Dye sensitized solar cells with their high solar light to electricity conversion efficiencies are primary alternatives for conventional energy sources. As described in the introductory part, all around the world, there are many research groups and industrial companies which are investigating ways to improve design of dyes and devices. In fact, there are number of factors affecting the efficiency, molecular design of the dye is clearly the significant one. The common procedure is to build up dyes that consist of donor-spacer-acceptor structure. With this model, acceptable efficiencies were achieved but there are still some problems remain challenging such as obtaining dyes with high efficiencies at longer wavelengths (Near-IR), or with high molar extinction coefficients in the entire visible spectrum. For instance, ruthenium dyes while holding the record for efficiency, the spectral response at Near-IR region is not sufficient.

In this study, we proposed six different BODIPY based sensitizers with different anchoring and donating moieties that absorb sunlight effectively especially at longer wavelengths.

3.2. Novel BODIPY Sensitizers

BODIPY dyes with their unique chemical and photophysical properties are remarkable candidates as a sensitizer in dye sensitized solar cells. BODIPY

derivatives have strong extinction coefficient in the visible and near-IR region of the spectrum (70 000 – 100 000 M^{-1} cm^{-1}), excited state lifetimes of this class of dyes are long enough to achieve electron transfer to the semiconductor. Furthermore, good solubility in organic solvents and ease of purification procedures result in facile synthetic pathways. More importantly, by applying simple modifications, it is possible to shift absorption maxima of the dye to longer wavelengths. Also electron donating, accepting and anchoring groups can be located on the BODIPY core with well known reactions. Figure 34 represents possible modification sides of the BODIPY.

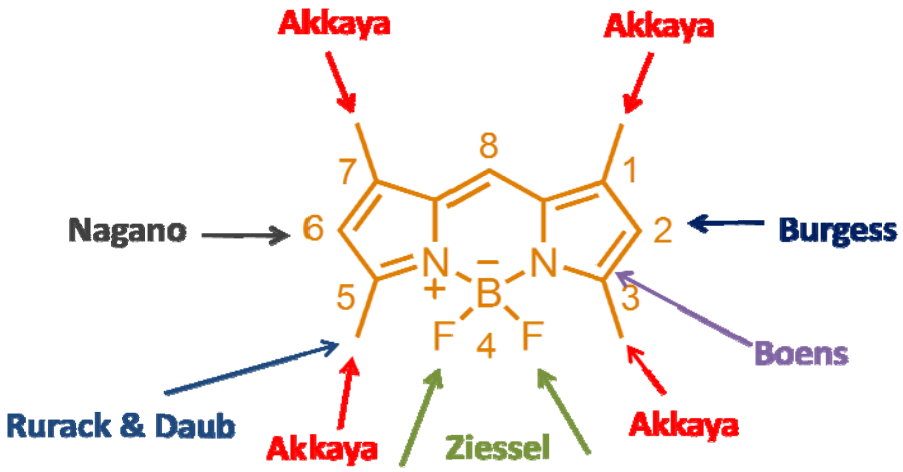

Figure 34. Possible modification sides of BODIPY core

Position 8 which is also named as *meso* position can be modified during the traditional BODIPY synthesis by choosing appropriate aldehyde. Positions 1, 3, 5 and 7 can be functionalized through Knoevenagel condensation reactions. Acidic nature of these methyl groups causes this condensation reaction to occur easily. 2 and 6 positions are favorable for coupling reactions following electrophilic iodination or bromination of these sides. With the help of these reactions, core was modified in order to obtain effective sensitizers. Targeted dyes are shown in figure 35. Effect of different anchoring (acceptor) and donating groups at different positions of the BODIPY core to solar light to electricity efficiency was observed with these target sensitizers.

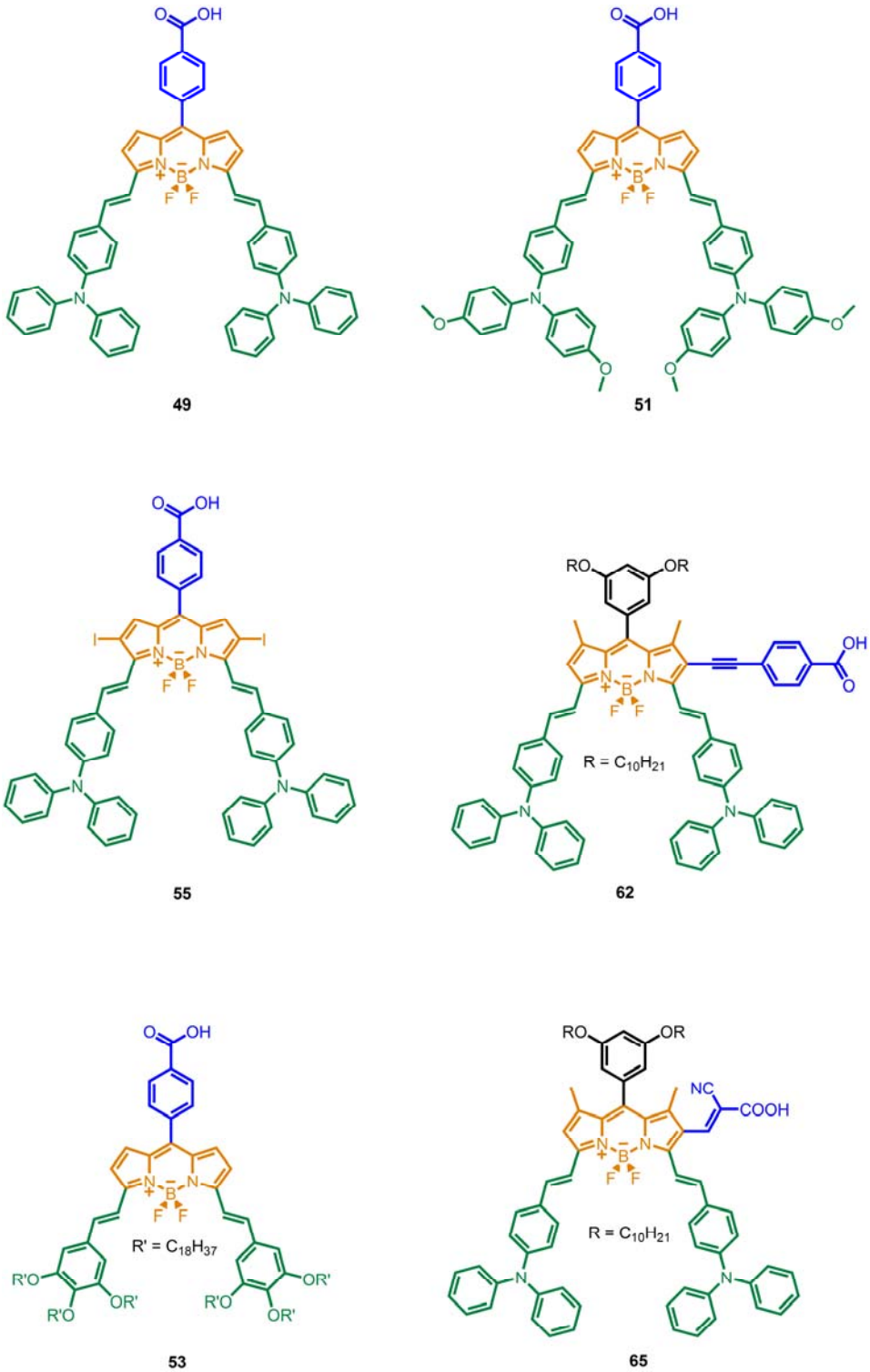

Figure 35. Target Sensitizers

3.2.1. Bodipy Sensitizers in Gratzel Type DSSC

3.2.1.1. Design and Photophysical and Photovoltaic Characterization of Compounds 49, 51, 53 and 55

Compound **49** was our first design among the targeted sensitizers. In order to obtain this dye, initially 8-Carboxyphenyl-Bodipy (compound **47**) was synthesized from appropriate procedures. By this synthesis, Bodipy core was equipped with carboxylic acid moiety which is an anchor and electron acceptor. Carboxylic acid was preferred as an anchoring group due to two reasons; first, carboxylic acid makes an ester linkage with TiO_2 that strengthen the chemisorption of dye onto semiconductor and second, incorporation of carboxylic acid to the Bodipy core is synthetically an easier process. Afterwards, diphenylaminophenyl donor moiety was placed with Knoevenagel condensation reaction. This moiety works as an electron pump and also restricts the aggregation of the dye on the semiconductor surface with its large, non-planar phenyl groups. Moreover, addition of diphenylaminophenyl extends the conjugation that diminishes the HOMO-LUMO gap of the dye and shifts the absorption maxima of the Bodipy to longer wavelengths. Without any modification, the absorption maximum of the Bodipy core is around 500 nm. In a sensitizer, excitation moves an electron from HOMO to LUMO of the dye. For effective photoinduced charge transfer there should be full conjugation between donor groups (where HOMO of the dye localized) and anchoring groups (where LUMO of the dye lies). Thus, it is important to note that methyl groups at 1 and 7 positions on the Bodipy core were removed in order to have full conjugation between the two terminals of the dye. In the presence of those methyl groups phenyl moiety at the *meso* position is almost perpendicular to the Bodipy core that restricts the conjugation, but in the case of compound **49**, the dihedral angle between phenyl and the core is around 30^0.

Compound **51** was synthesized secondly. The Bodipy core and the anchoring group are same as the former compound **49**. The only change was in the donating moiety. We placed additional electron donor *p*-methoxy groups on

the diphenylaminophenyl moiety looking for enhanced electron donation and efficient excited state charge transfer.

The major difference in compound **53** is again the donating part. We performed the Knoevenagel condensation reaction with 3,4,5-Tris(octadecyloxy)benzaldehyde. 3,4,5-Tris(octadecyloxy) group has dual role. While donating electron to the dye, it also minimizes the aggregation induced loses by long alkyl chains. Also these long alkyl chains increase the solubility of the sensitizer in organic solvents which helps a lot in synthetic pathway and purification steps.

On the other hand in compound **55**, we used same donating moiety with compound **49** but placed iodine to the positions 2 and 6 by heating Bodipy in ethanol with iodic acid and iodine. Addition of heavy halogens changes the relaxation pathway of the excited dye. Due to the iodines, intersystem crossing takes place and the electron is transferred from singlet excited state to triplet excited and comes back to singlet ground state. Relaxation of electron from triplet excited state to singlet ground state is known as phosphoresence. Phosphoresence is longer process than the emission where relaxation occurs from singlet excited state to singlet ground state. So the aim was to increase excited state life time of the electron to achieve good electron transfer to semiconductor by forcing intersystem crossing.

The UV-vis spectra of compounds **49**, **51**, **53** and **55** are given in figure 36. The absorption maxima of the dyes are 723, 748, 668 and 761 nm respectively corresponding to $S_0 \rightarrow S_1$ transition. At these wavelengths calculated molar extinction coefficients are 60.000 M^{-1} cm^{-1} for compound **49**, 66,000 M^{-1} cm^{-1} for compound **51**, 74,000 and 68,000 M^{-1} cm^{-1} for **53** and **55.** (figure 37).

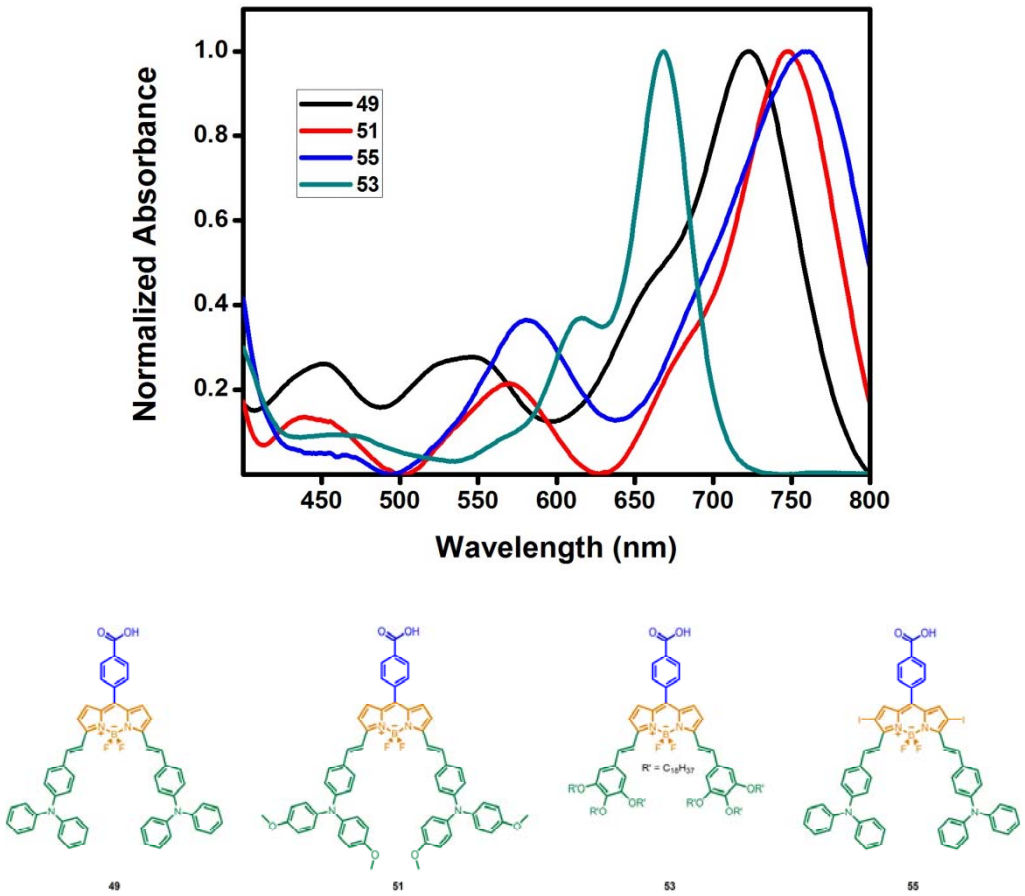

Figure 36. Absorption spectra of compounds **49, 51, 53** and **55** in $CHCl_3$

The red-shift observed with compound **51** can be explained by addition of methoxy groups to the donor moiety that further extends the conjugation. Compound **55** has absorption maximum at 761 nm which is the result of addition of electron withdrawing (relatively to hydrogen) group that stabilizes the LUMO which decreases the HOMO-LUMO gap and shifts absorption maximum to longer wavelengths. It is also seen in figure 36 that all compounds have good molar extinction coefficients throughout the entire spectrum with compound **53** showing highest extinction coefficient value. High molar extinction coefficient (Table 2) of **55** relative to **49** can be explained as a broadened absorption peak of **55** at longer wavelengths. It is important to note that with all of these sensitizers, it is possible to absorb in the visible and Near-IR region of the spectrum. This wide absorption feature cannot be observed in most of the ruthenium and organic dye sensitizers. Having high molar extinction coefficients reduces the

film thickness on semiconductor in solar cell device and increases the open circuit voltage (V_{oc}) and solar light to electricity conversion efficiency (η) in many cases.

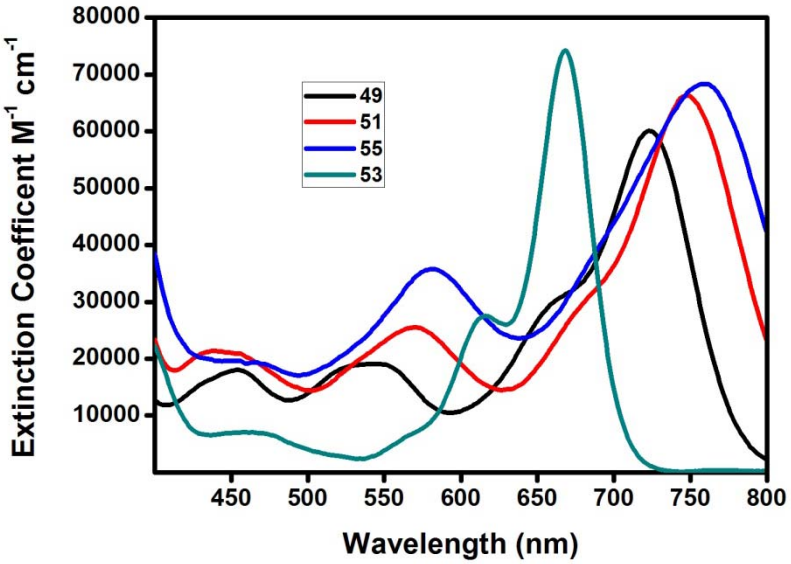

Figure 37. Molar extinction coefficient vs. wavelength plot for compounds **49, 51, 53** and **55**

DYE	λ_{max} (nm)	Є (M^{-1} cm^{-1})
49	724	60.000
51	748	66.000
53	668	74.000
55	761	68.000

Table 2. Photophysical parameters of compounds **49, 51, 53** and **55**

Incident photon to current efficiencies (IPCEs) and current vs. voltage plots of the Gratzel type solar cells based on these four dyes is given in figure 38 and 39. IPCE of compound **49** exceeds over the range from 400 nm to 900 nm with showing its maximum value (25%) around 800 nm. This IPCE value is the record for Bodipy based sensitizers. Although compound **51** with *p*-methoxy substituted donor moiety absorbs at longer wavelengths with high molar

extinction coefficient, IPCE and overall efficiency are lower than the compound **49**, suggesting that increasing the electron donation of the dye did not affect overall efficiency. Compound **49** gave an open circuit voltage (V_{oc}) of 472 mV, a short-circuit photocurrent density (J_{sc}) of 5.95 mA/cm^2, and a fill factor (*ff*) of 0.67, corresponding to overall conversion efficiency (η) of 1.88 %. On the other hand, compound **51** gave an open circuit voltage (V_{oc}) of 456 mV, a short-circuit photocurrent density (J_{sc}) of 4.52 mA/cm^2, and a fill factor (*ff*) of 0.63, that yield 1.32 % overall efficiency. These two similar Near-IR absorbing dyes have similar and high values of V_{oc}, which confirm the effective absorption of light by these two sensitizers on TiO_2. The major difference is in the J_{sc} values. Relatively lower overall efficiency of compound **51** is due to its low current density. This means that in DSSC constructed with compound **51**, electron transfer processes are not effective as in the case of compound **49**. Compound **53** has similar photovoltaic parameters with compound **49** (Table 3). In fact, electron donation from 3,4,5-Tris(octadecyloxy) group is less than the diphenylamino phenyl moiety, suppressed aggregate formation on TiO_2 with the help of long alkyl chains made compound **53** as effective as compound **49** with overall efficiency 1.81% . Furthermore, incorporating long alkyl chain increases the solubility of the dye that simplifies the loading of the sensitizer on semiconductor.

Dye	J_{sc} (mA*cm^{-2})	V_{oc} (mV)	*FF*	efficiency
49	5.949	471.85	0.668	1.88
51	4.52	456.01	0.633	1.32
55	1.052	353.03	0.614	0.23
53	5.447	465.63	0.709	1.81

Table 3. Photovoltaic parameters of compounds **49, 51, 53** and **55.** Dipping: 4 hrs in 0.1 mM THF, TiO_2: 7+4, Electrolyte: A6986.

Compound **55** with two iodine atoms showed very low IPCE values. An open circuit voltage (V_{oc}) is 353 mV, a short-circuit photocurrent density (J_{sc}) is 1.05 mA/cm^2, and a fill factor (*ff*) is 0.614. With these photovoltaic parameters,

calculated overall solar light to electricity conversion efficiency is only 0.23%. The notable thing is again the low short-circuit photocurrent density (J_{sc}). Compound **55** absorbs light, but electron transfer parts seem to be missing. Iodine atoms hold electron density on Bodipy core so injection of electron to TiO_2 via anchoring group could not proceed. Moreover, having different pathways for relaxation of the excited dye diminished the electron transfer from the LUMO of the dye to conduction band of the semiconductor. It was understood that alternative relaxation ways for excited electron should be avoided and excited electron must be directed towards TiO_2.

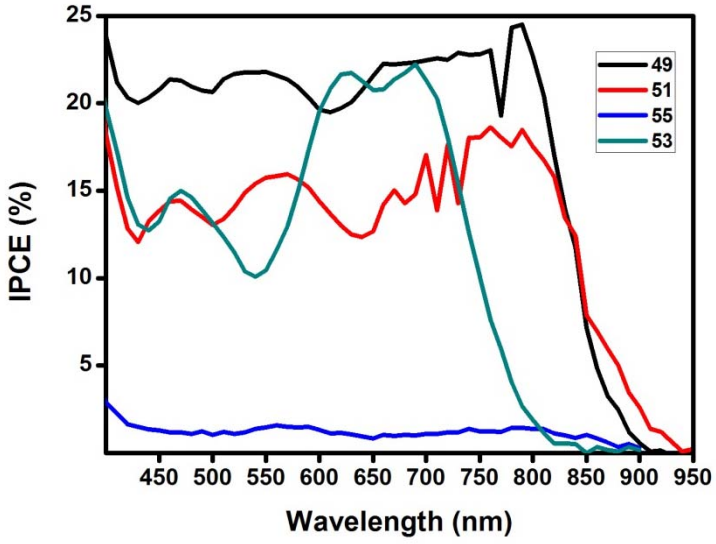

Figure 38. IPCE of compounds **49, 51, 53** and **55**

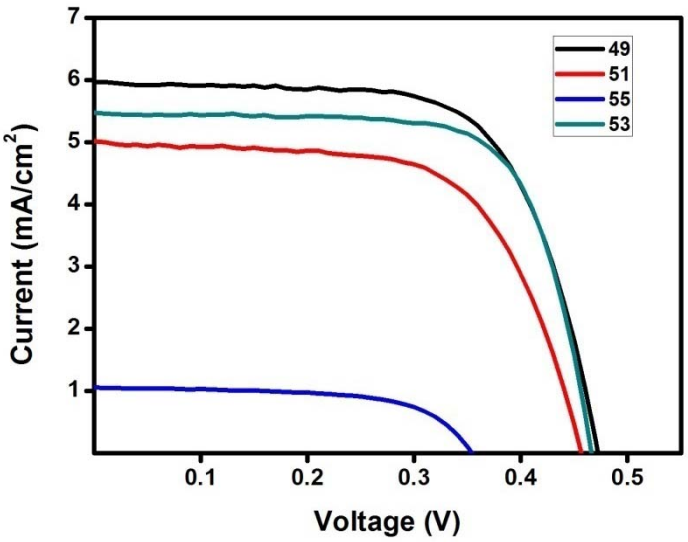

Figure 39. Current vs. Voltage graph of compounds **49, 51, 53** and **55**

In order to improve solar light to electricity efficiency of our most effective sensitizer (compound **49**), our collaborators in EPFL, Switzerland modified the semiconductor. 3a,7a-dihydroxy-5b-cholic acid (cheno) was mixed with the sensitizer while preparing the dye solution just before the chemisorption takes place on to semiconductor. Cheno with its carboxylic acid moiety adsorbed on TiO_2 like the sensitizer and stays perpendicular to the semiconductor surface where it forms a layer between the sensitizer molecules. With this modification aggregate formation on semiconductor was diminished. New photovoltaic parameters of compound **49** are shown in table 4.

Dye	J_{sc} (mA*cm^{-2})	V_{oc} (mV)	*FF*	efficiency
49	9.174	430.61	0.621	2.46

Table 4. Photovoltaic performance of compound **49**. Dipping: 24 hrs in CB/EtOH (1:1) + 2 mM cheno, TiO_2: 8+5+$TiCl_4$, Electrolyte: Z1040

DSSC with cheno additive gave 9.174 mA/cm^2 short circuit photocurrent density (J_{sc}), corresponding overall efficiency of 2.46%. In the initial case where no modification was performed, J_{sc} was 5.949 mA/cm^2. This high value of J_{sc} was the result of suppressed aggregation of sensitizers on TiO_2. Aggregation

control increased electron transfer from excited dye to conduction band of TiO_2. Comparison of IPCE and current values of the compound **49** with cheno and without cheno are given in figure 40. Overall efficiency was increased to 2.46% as a consequence of addition of cheno. Thus, it is also possible to treat other sensitizers with same additive and improve their efficiencies. In this work, cheno was only added to compound **49**.

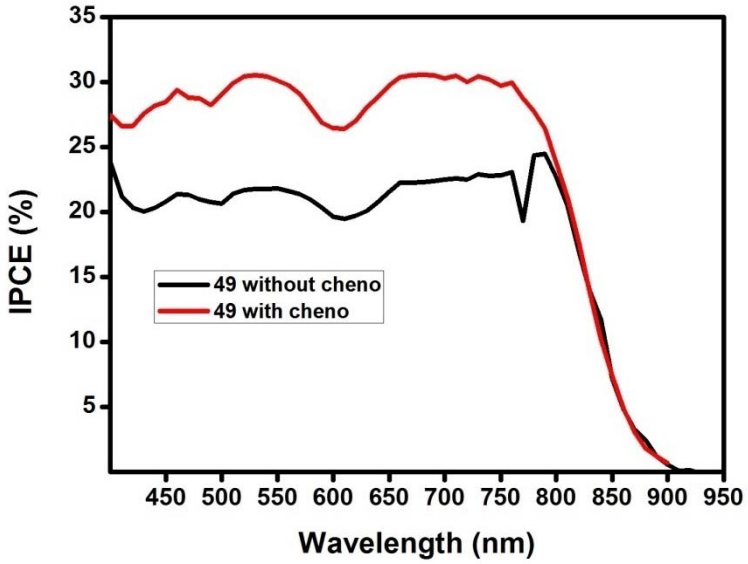

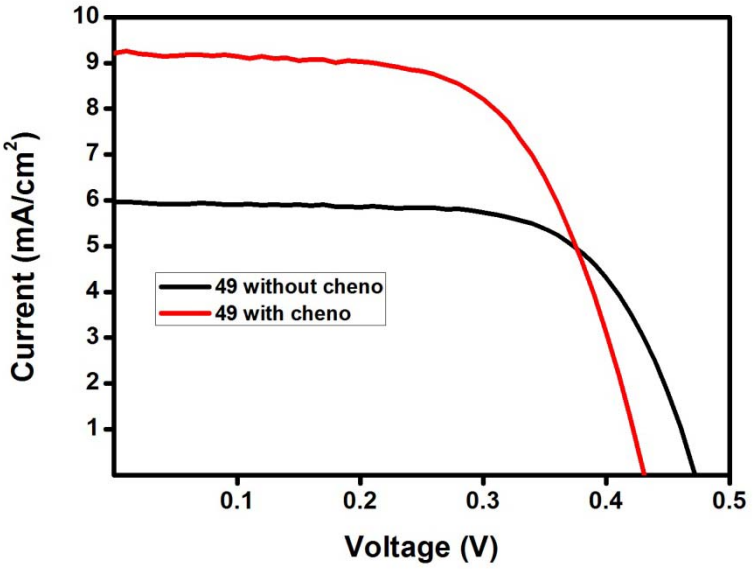

Figure 40. IPCE and current vs. voltage graphs of compound **49**. Red: Dipping: 24 hrs in CB/EtOH (1:1) + 2 mM cheno, TiO_2: 8+5+$TiCl_4$, Electrolyte: Z1040. Black: Dipping: 4 hrs in 0.1 mM THF, TiO_2: 7+4, Electrolyte: A6986

3.2.1.2. Design and Photophysical and Photovoltaic Characterization of Compounds 62 and 65

All compounds discussed above contain the same anchoring group at the comparable positions. In compounds **62** and **65** we changed the position of the anchoring group and substituted it with a different group (compound **65**). As a donor group we chose diphenylamino phenyl moiety after investigating its high performance. In both of the dyes long alkyl chains were incorporated at *meso* position again in order to avoid aggregate formation and to increase the solubility of sensitizers. Compound **62** involved mono iodination intermediate step. After iodination, coupling reaction was performed to attach carboxylic acid moiety at position 2 on Bodipy core. Donor groups were inserted with Knoevenagel condensation reaction as in the case of previous sensitizers.

Compound **65** was synthesized according to relatively new procedure. This new synthetic pathway involves selective formylation of Bodipy core only at positions 2 or 6. Then cyano acetic acid moiety was replaced by formyl

group. Finally donor groups were incorporated. These two new designs gave us chance to discuss the effect of anchor position and type on efficiency.

The UV-Vis spectra of compounds **62** and **65** are given in figure 41. Absorption maxima are 707 nm (ϵ = 71.000) and 695nm (ϵ = 79.000) respectively. Like other dyes, extended conjugation causes these sensitizers to absorb at longer wavelengths with high molar extinction coefficients.

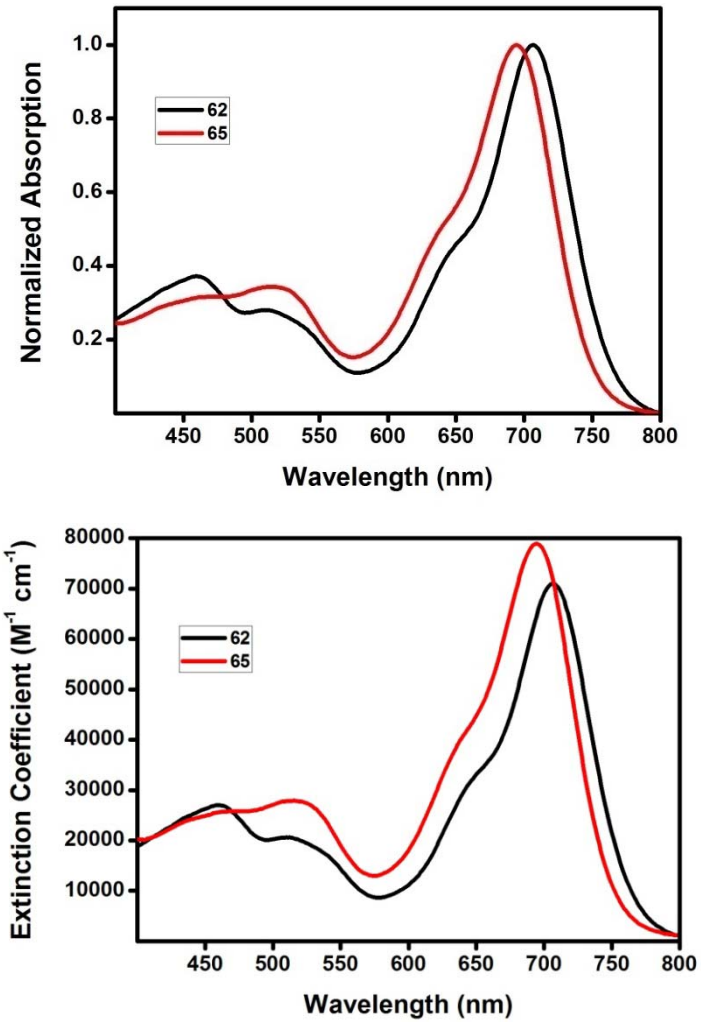

Figure 41. The UV-vis and extinction coefficient vs. wavelength spectra of compounds **62** and **65**

DYE	λ_{max} (nm)	Є (M^{-1} cm^{-1})
62	707	71.000
65	695	79.000

Table 5. Photophysical parameters of compounds **62** and **65**

Incident photon to current efficiencies and current vs. voltage graphs of compounds **62** and **65** are shown in figure 42. IPCE of compound **62** exceeds 18% over the visible and 13% over Near-IR region. An open circuit voltage (V_{oc}) is 524 mV, a short-circuit photocurrent density (J_{sc}) is 3.74 mA/cm^2, and a fill factor (*ff*) is 0.707. With these photovoltaic parameters, calculated overall solar light to electricity conversion efficiency is 1.40%. Compound **65** has lower IPCE values. Compound **65** gave an open circuit voltage (V_{oc}) of 427 mV, a short-circuit photocurrent density (J_{sc}) of 2.55 mA/cm^2, and a fill factor (*ff*) of 0.693, corresponding to overall conversion efficiency (η) of 0.75 %.

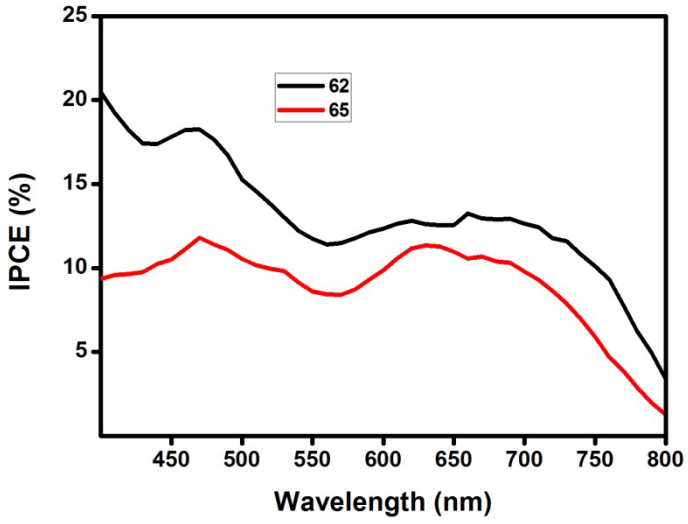

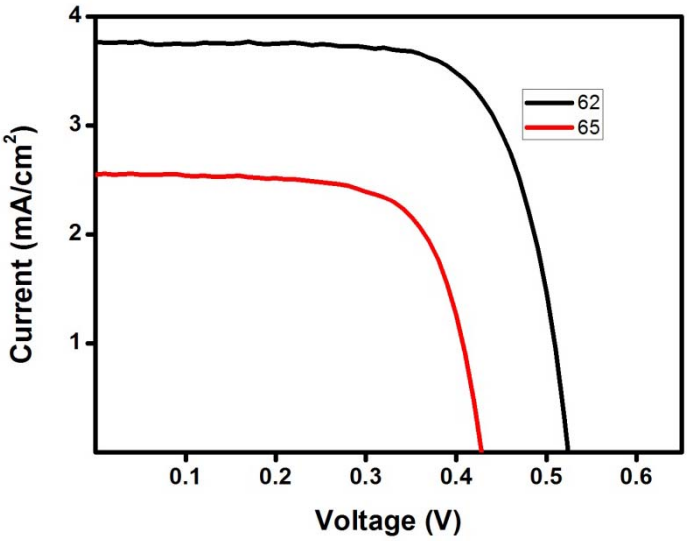

Figure 42. IPCE and current vs. voltage graphs of compounds **62** and **65**

Dye	J_{sc} (mA*cm^{-2})	V_{oc} (mV)	*FF*	efficiency
49	**9.174**	**430.61**	**0.621**	**2.46**
51	**4.52**	**456.01**	**0.633**	**1.32**
55	**1.052**	**353.03**	**0.614**	**0.23**
53	**5.447**	**465.63**	**0.709**	**1.81**
62	**3.742**	**523.86**	**0.707**	**1.40**
65	**2.55**	**427.52**	**0.693**	**0.75**

Table 6. Photovoltaic parameters for all sensitizers

It was understood and supported by the density functional theory calculations (figure 43) that there is a great tendency for Bodipy dyes to delocalize charge density onto *meso*-carbon. Sensitizers **62** and **65** have anchor groups on different position, forcing electron flow to an alternate position, apparently reducing the efficiency of charge injection. Compounds **49** and **51** were chosen as representative examples in DFT in order to observe electron density localization when sensitizers with anchoring groups at *meso* position are excited. It was seen that electron density on anchor of compounds **49** and **51** at LUMO is larger than the compound **65**. Since charge transfer occurs from excited state of the dye to conduction band of the TiO_2 is more efficient.

Sensitizers with anchoring group on the *meso* position are more effective in most case than the dyes with anchoring groups on positions 2 or 6.

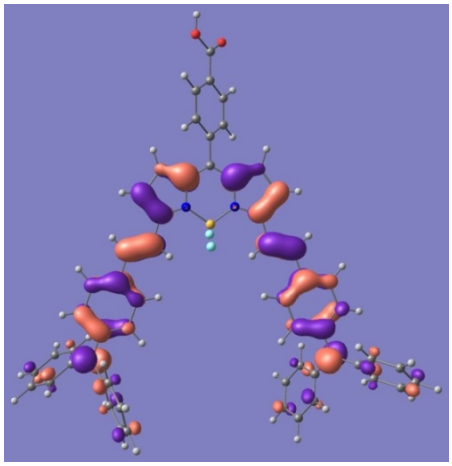

49 (HOMO)

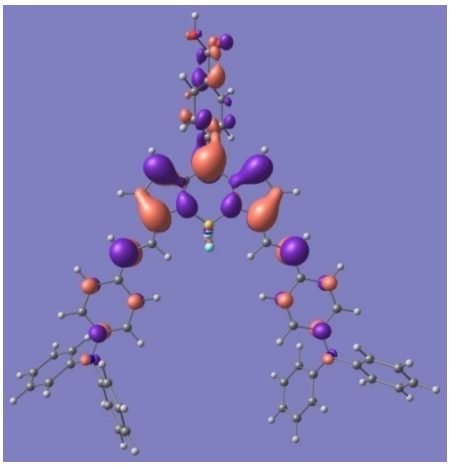

49 (LUMO)

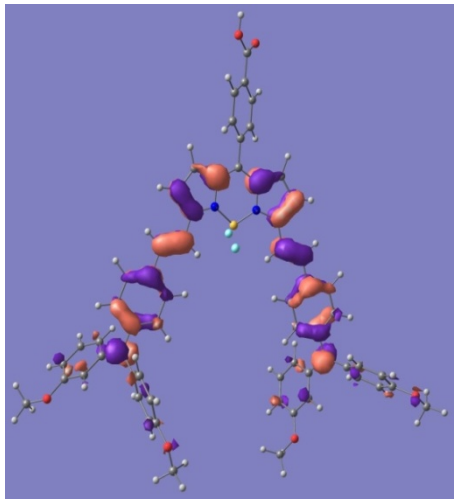

51 (HOMO)

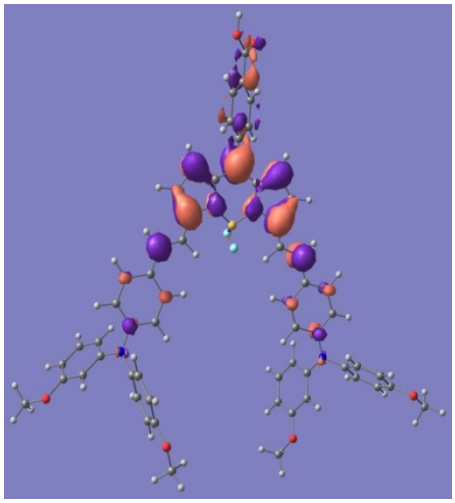

51 (LUMO)

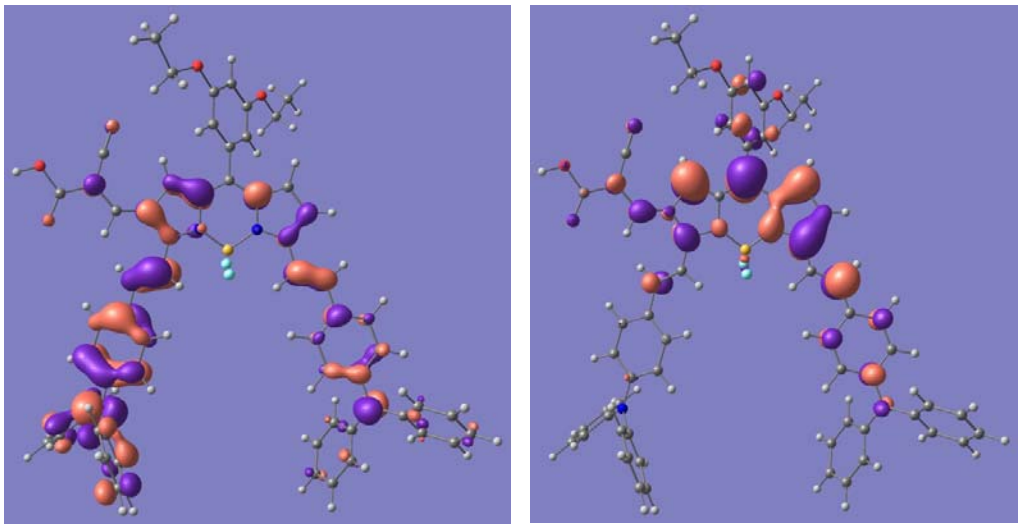

65 (HOMO) **65** (LUMO)

Figure 43. Optimized structures and representation of HOMO-LUMO calculated by DFT using the B3LYP functional and the 6-31G basis set for compounds **49**, **51** and **65**

3.2.2. Bodipy Sensitizers in Solid-State DSSCs

Compounds **51** and **65** were also applied in solid state dye sensitized solar cell with spiro-OMeTAD as a hole transport material. Incident photon to current conversion plots were obtained under standard conditions (AM 1.5G, 100 $mWcm^{-2}$) (figure 45). The UV-Vis spectra of compounds **51** and **65** in solution were given in figure 35 and 40. In figure 44, absorption spectra of the sensitizers adsorbed on nanocrystalline TiO_2 were shown. On absorption over titania, peaks are significantly broadened, suggesting aggregation of the sensitizers in the adsorbed film. Modifications in dye design could not totally suppress the π-π stacking induced aggregation.

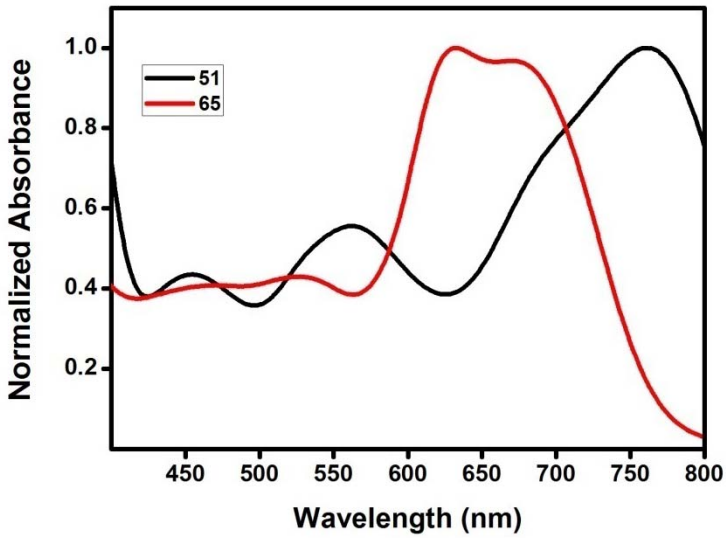

Figure 44. Absorption spectra of the sensitizers **51** and **65** adsorbed on nanocrystalline TiO_2.

The photovoltaic parameters show that the sensitizer **65** has the highest efficiency. It is important to note that dye **51** showed IPCE beyond 800 nm. For sensitizer **65**, IPCE values are below 1 % in the 450-850 nm region. Solid state DSSCs have generally low IPCE values relatively to traditional type DSSCs due to the shorter electron diffusion length in HTM. Furthermore, thickness of the semiconductor in solid state DSSC restricts the loading of dye, which causes less absorption of solar light that diminishes the overall conversion efficiency.

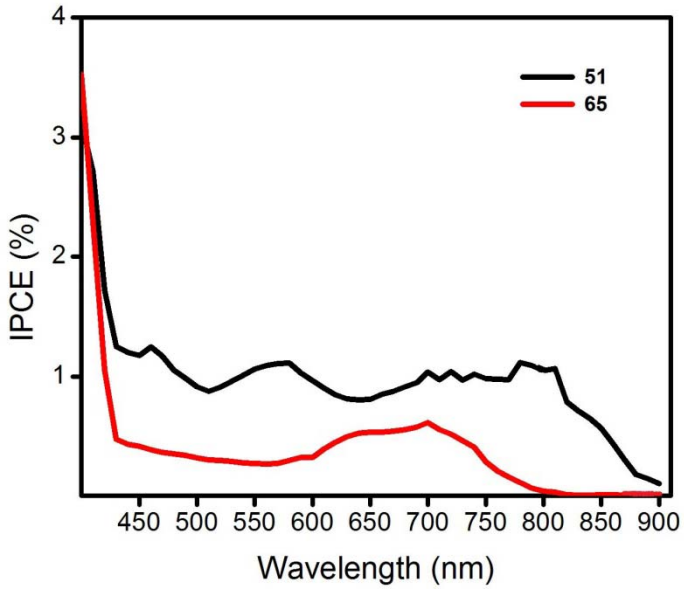

Dye	Jsc (mA*cm^{-2})	Voc (mV)	FF	efficiency
51	1.61	635	27.56 (%)	**0.28**
65	1.49	585	37.90 (%)	**0.33**

Figure 45. IPCE graph and photovoltaic performances of compounds **51** and **65** in solid state DSSC

What is also remarkable is the near flat response of these sensitizers in the visible wavelengths. Actually, the response is one that could be expected from a black dye. Figure 45 lists some cell parameters for the solid state DSSCs prepared using these sensitizers. Compound **51** gave an open circuit voltage (V_{oc}) of 635 mV, a short-circuit photocurrent density (J_{sc}) of 1.61 mA/cm^2, and a fill factor (*ff*) of 0.27, corresponding to overall conversion efficiency (η) of 0.28 %. On the other hand, compound **65** gave an open circuit voltage (V_{oc}) of 585 mV, a short-circuit photocurrent density (J_{sc}) of 1.49 mA/cm^2, and a fill factor (*ff*) of 0.38, that yield 0.33 % overall efficiency.

The sensitizers **51** and **65** were further characterized by cyclic voltammetry. It is clear that the LUMO energies of the sensitizers are appropriate for efficient electron injection to TiO_2. Also, electron transfer from HTM to oxidized dye is energetically favorable (figure 47). BODIPY derivatives showed both reversible reduction and oxidation potential.

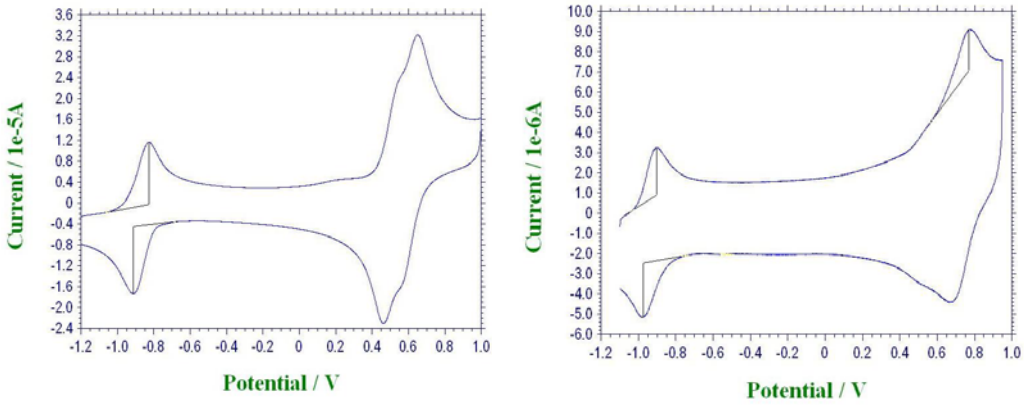

(51) **(65)**

Dye	E_{ox} (V)	E_{red} (V)	HOMO (eV)	LUMO (eV)
51	0.56	-0.87	-5.05	-3.62
65	0.72	-0.94	-5.20	-3.55

Figure 46. Cyclic Voltammogram and electrochemical parameters of compounds **51** and **55**

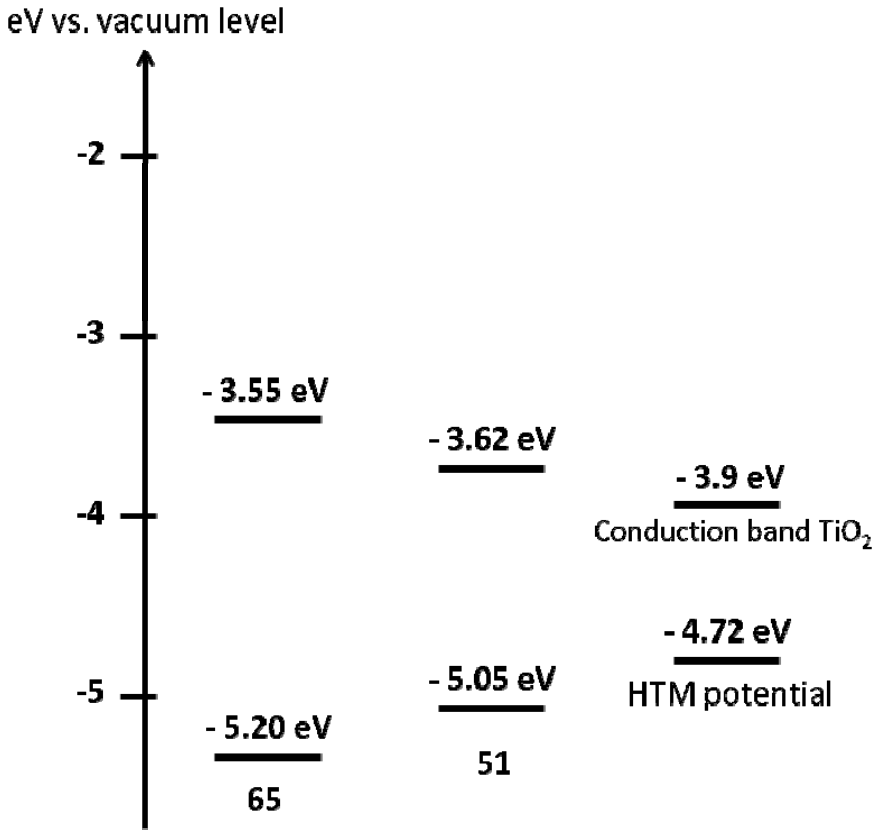

Figure 47. Energy level diagrams of **51** and **65** from electrochemical data

CHAPTER 4

CONCLUSION

In this study, we have synthesized six different sensitizers for dye sensitized solar cells. Two of these sensitizers were further studied in solid state DSSC. It was shown that Bodipy dyes with suitable modifications can be easily transformed into satisfactory sensitizers in the visible and near-IR region of the solar spectrum. IPCE obtained at longer wavelengths were impressive. The results showed that compound **49** was the most effective sensitizer with overall conversion efficiency of 2.46%. This is the highest efficiency ever reported for a liquid electrolyte based DSSC with Bodipy dyes. In solid state DSSC, efficiencies were diminished as expected.

Bodipy sensitizers with their high molar extinction coefficients absorb sun light effectively. The major problem is in electron transfer processes which yields low short circuit photocurrent density. Further structural optimization suppressing the aggregate formation of dyes on semiconductor and increasing the electron density in the excited state is very like to yield more efficient sensitizers.

We will continue in fine tuning Bodipy structure towards ever efficient dyes for dye sensitized solar cells through rational design.

REFERENCES

1. Service, R. F. *Science* **2005**, *309*, 548.

2. Van Zolingen, R. J. C.; Van de Sanden, M. C. M.; Janssen, R. A. J. *Solar Cells*, Technische Universiteit Eindhoven, **2010**.

3. Hagfeldt, A.; Gratzel, M.; *Acc. Chem. Res*. **2000**, *33*, 269.

4. Gratzel, M. *Nature* **2001**, *414*,338.

5. Waldau, A. J. *PV Status Report 2003* **2003**, *European Commission*, EUR 20850 EN.

6. O'Regan, B.; Gratzel, M. *Nature* **1991**, *353*, 737.

7. Hwang, S.; Lee, J. H.; Park, C.; Lee, H.; Kim, C.; Park, C.; Lee, M. H.; Lee, W.; Park, J.; Kim, K.; N. G.;Park, Kim, C. *Chem. Commun*. **2007**, 4887.

8. Boschloo, G.; Haggman, L.; Hagfeldt, A. *J. Phys. Chem. B* **2006**, *110*, 13144.

9. Hara, K.; Kurashige, M.; Ito, S.; Shinpo, A.; Suga, S.; Sayama, K.; Arakawa, H. *Chem. Commun*. **2003**, 252.

10. Wang, Z. S.; Cui, Y.; Hara, K.; Dan-oh, Y.; Kasada, C.; Shinpo, A. *Adv. Mater*. **2007**, *19*, 1138.

11. Kim, S.; Choi, H.; Baik, C.; Song, K.; Kang, S. O.; Ko, J. *Tetrahedron* **2007**, *63*, 11436.

12. Edvinsson, T.; Li, C.; Pschirer, N.; Sch_neboom, J.; Eickemeyer, F.; Sens, R.; Boschloo, G.; Herrmann, A.; M_llen, K.; Hagfeldt, A. J. *Phys. Chem. C* **2007**, *111*, 15137.

13. Kim, C.; Choi, H.; Kim, S.; Baik, C.; Song, K.; Kang, M. S.; Kang, S. O.; Ko, J. *J. Org. Chem*. **2008**, *73*, 7072.

14. Teng C.; Yang, X.;Yuan, C.; Li, C.; Chen, R.; Tian H.; Li, S.; Hagfeldt, A.; Sun, L. *OrgLett*. **2009**, *11* (23), 5542.

15. Mishra A.; Fischer, M. K. R.; Bauerle P. *Angew. Chem. Int. Ed*. **2009**, *48*, 2474.

16. Hagfeldt A.; Gratzel M. *Chem. Rev*. **1995**, *95*, 49.

17. Bach, U.; Lupo, D.; Comte, P.; Moser, J. E.; Weissörtel, F.; Salbeck, H.; Spreitzer, H.; Gratzel, M. *Nature* **1998**, *395*, 583.

18. Nazeeruddin, M. K.; Zakeeruddin, S. M.; Lagref,, J. J.; Liska, P.; Comte, P.; Barolo, C.; Viscardi, G.; Schenk, K.; Gratzel M. *Coord. Chem. Rev*. **2004**, *248*, 1317.

19. Gratzel, M. *Inorg. Chem*. **2005**, *44*, 6841.

20. Robertson, N.; *Angew. Chem. Int. Ed*. **2006**, *45*, 2338.

21. Ooyama, Y.; Harima, Y. *Eur. J. Org. Chem*. **2009**, 2903.

22. Tsubomura, H.; Matsumura, M.; Noyamura, Y.; Amamyiya, T. *Nature* **1976**, *261*, 402.

23. Bach, U.; Lupo, D.; Comte, P.; Moser, J. E.; Weissörtel, F.; Salbeck, J.; Spreitzer, H.; Gratzel, M. *Nature*, **1998**, *395*, 583.

24. O'Regan, B.; Schwartz, D. *J. Appl. Phys*. **1996**, *80*, 4749.

25. Sanadeera, R.; Fukuri, N.; Saito, Y.; Kitamura, T.; Wada, Y.; Yanagida, S. *Chem. Commun*. **2005**, 2259.

26. Murakoshi, K.; Kogure, R.; Yanagida, S. *Chem Lett*, **1997**, *5*, 471.

27. O'Regan, B.; Schwarz, D. T. *Chem. Mater*. **1998**, *10*, 1501.

28. Barbe, C. J.; Arendse, F.; Comte, P.; Jirousek, M.; Lenzmann, F.; Shklover, V.; Gratzel, M. *J. Am. Ceram. Soc*. **1997**, *80*, 3157.

29. Hagberg, D. P.; Yum, J. H.; Lee, H.; De Angelis, F.; Marinado, T.; Karlsson, M. K.; Humphry-Baker, R.; Sun, L.; Hagfeldt, A.; Gratzel, M.; Nazeeruddin, M. K. *J. Am. Chem. Soc*. **2008**, *130*, 6259.

30. Li, C.; Yum, J. H.; Moon, S. J.; Herrmann, A.; Eickemeyer, F.; Pschirer, N. G.; Erk, P.; Schöneboom, J.; Müllen, K.; Gratzel, M.; Nazeeruddin, M. K. *ChemSusChem* **2008**, *1*, 615.

31. Snaith, H. J.; Moule, A. J.; Klein, C.; Meerholz, K.; Friend, R. H.; Gratzel, M. *Nano Lett*. **2007**, *7*, 3372.

32. Karthikeyan, C. S.; Peter, K.; Wietasch, H.; Thelakkat, M. *Sol. Energy Mater. Sol. Cells* **2007**, *91*, 432.

33. Poplavskyy, D.; Nelson, J. *J. Appl. Phys*. **2003**, *93*, 341.

34. Günes, S.; Neugebauer, H.; Sariciftci, N. S. *Chem. Rev*. **2007**, *107*, 1324.

35. Wöhrle, D.; Meissner, D. *Adv. Mater*. **1991**, *3*, 129.

36. Qin H.; Wenger, S.; Xu, M.; Gao, F.; Jing, X.; Wang, P.; Zakeeruddin, S. M.; Gratzel M. *J. Am. Chem. Soc*. **2008**, *130*, 9202.

37. Halls, J. J. M.; Pichler, K.; Friend, R. H.; Moratti, S. C.; Holmes, A. B. *Appl. Phys. Lett*. **1996**, *68*, 3120.

38. Theander, M.; Yartsev, A.; Zigmantas, D.; Sundstro¨m, V.; Mammo, W.; Andersson, M. R.; Inganas, O. *Phys. Rev. B* **2000**, *61*, 12957.

39. Haugeneder, A.; Neges, M.; Kallinger, C.; Spirkl, W.; Lemmer, U.; Feldmann, J.; Scherf, U.; Harth, E.; Gügel, A.; Müllen, K. *Phys. Rev. B* **1999**, *59*, 15346.

40. Stübinger, T.; Brütting, W. *J. Appl. Phys*. **2001**, *90*, 3632.

41. Markov, D. E.; Amsterdam, E.; Blom, P. W. M.; Sieval, A. B.; Hummelen, J. C. *J. Phys. Chem. A* **2005**, *109*, 5266.

42. Jum, J. H.; Chen, P.; Gratzel, M.; Nazeeruddin, M. K. *ChemSusChem*, **2008**, *1*, 699.

43. Snaith, H.; Schmidt-Mende, L. *Adv.Mater*, **2007**, *19*, 3187.

44. Snaith, H. J.; Schmidt-Mende, L.; Gratzel, M.; Chiesa, M. *Phys. Rev. B* **2006**, *74*, 45306.

45. Schmidt-Mende, L.; Bach, U.; Humphry-Baker, R.; Horiuchi, T.; Miura, H.; Ito, S.; Uchida, S.; Gratzel, M. *Adv. Mater*. **2005**, *17*, 813.

46. Tachibana, Y.; Moser, J. E.; Gratzel, M.; Klug, D. R.; Durrant, J. D. *J. Phys. Chem*. **1996**, *100*, 20056.

47. Anderson, N. A.; Lian, T. *Coord. Chem. Rev*. **2004**, *248*, 1231.

48. Bach, U.; Tachibana, Y.; Moser, J.; Haque, S. A.; Durrant, J. D.; Gratzel, M.; Klug, D. R. J. *Am. Chem. Soc*. **1999**, *121*, 7445.

49. Nazeeruddin, M. K.; Kay, A.; Rodicio, R.; Humphry-Baker, R.; Muller, E.; Liska, P.; Vlachopoulos, N.; Gratzel, M. *J. Am. Chem. Soc*. **1993**, *115*, 6382.

50. Hara, K.; Kurashige, M.; Dan-oh, Y.; Kasada, C.; Shinpo, A.; Suga, S.; Sayama, K.; Arakawa, H. *New J. Chem*. **2003**, *27*, 783.

51. Hara, K.; Dan-oh, Y.; Kasada, C.; Ohga, Y.; Shinpo, A.; Suga, S.; Sayama, K.; Arakawa, H. *Langmuir* **2004**, *20*, 4205.

52. Hara, K.; Miyamoto, K.; Abe, Y. Yanagida, M. *J. Phys. Chem. B* **2005**, *109*, 23776.

53. Kitamura, T.; Ikeda, M.; Shigaki, K.; Inoue, T.; Anderson, N. A.; Ai, X.; Lian, T.; Yanagida, S. *Chem. Mater*. **2004**, *16*, 1806.

54. Chen, Y.; Li, C.; Zeng, Z.; Wang, W.; Wang, X.; Zhang, B. *Chem. Lett*. **2005**, *34*, 762.

55. Wang, X. F.; Koyama, Y.; Nagae, H.; Yamano, Y.; Ito, M.; Wada, Y. *Chem. Phys. Lett*. **2006**, *420*, 309.

56. Hwang, S.; Lee, J. H.; Park, C.; Lee, H.; Kim, C.; Park, C.; Lee, M. H.; Lee, W.; Park, J.; Kim, K.; Park, N. G.; Kim, C. *Chem. Commun*. **2007**, 4887.

57. Liang, M.; Xu, W.; Cai, F.; Chen, P.; Peng, B.; Chen, J.; Li, Z. *J. Phys. Chem. C* **2007**, *111*, 4465.

58. Ning, Z.; Zhang, Q.; Wu, W.; Pei, H.; Liu, B.; Tian, H. *J. Org. Chem*. **2008**, *73*, 3791.

59. Koumura, N.; Wang, Z. S.; Mori, S.; Miyashita, M.; Suzuki, E.; Hara, K. *J. Am. Chem. Soc*. **2006**, *128*, 14256.

60. Chen, Z.; Li, F.; Huang, C. *Curr. Org. Chem*. **2007**, *11*, 1241.

61. Future Generation Photovoltaic Technologies: Proceedings of the 1st NREL Conference (March 22–26, 1997; Denver, Colorado), American Institute of Physics Conference Proceedings No. 404 (Ed.: R. D. McConnell), AIP, Woodbury, NY, **1997**.

62. Gratzel, M. *J. Photochem. Photobiol. A* **2004**, *164*, 3.

63. Nazeeruddin, M. K; De Angelis, F.; Fantacci, S.; Selloni, A.; Viscardi, G.; Liska, P.; Ito, S.; Takeru, B.; Gratzel, M. *J. Am. Chem. Soc*. **2005**, *127*, 16835.

64. Nazeeruddin, M. K.; Splivallo, R.; Liska, P.; Comte, P.; Gratzel, M. *Chem. Commun*. **2003**, 1456.

65. Wang, P.; Zakeeruddin, S. M.; Exnar, I.; Gratzel, M. *Chem. Commun*. **2002**, 2972.

66. Wang, P.; Zakeeruddin, S. M.; Moser, J. E.; Nazeeruddin, M. K.; Sekiguchi, T.; Gratzel, M. *Nat. Mater*. **2003**, *2*, 402.

67. Wang, P.; Wenger, B.; Humphry-Baker, R.; Moser, J. E.; Teuscher, J.; Kantlehner, W.; Mezger, J.; Stoyanov, E. V.; Zakeeruddin, S. M.; Gratzel, M. *J. Am. Chem. Soc*. **2005**, *127*, 6850.

68. Nazeeruddin, M. K.; Pechy, P.; Renouard, T.; Zakeeruddin, S. M.; Humphry-Baker, R.; Comte, P.; Liska, P.; Cevey, L.; Costa, E.; Shklover, V.; Spiccia, L.; Deacon, G. B.; Bignozzi, C. A.; Gratzel, M. *J. Am. Chem. Soc*. **2001**, *123*, 1613.

69. Nazeeruddin, M. K.; Pechy, P.; Gratzel, M. *Chem. Commun*. **1997**, 1705.

70. Shankar, K.; Bandara, J.; Paulose, M.; Wietasch, H.; Varghese, O. K.; Mor, G. K.; LaTempa, T. J.; Thelakkat, M.; Grimes, C. A. *Nano. Lett*., **2008**, *8* (6), 1654.

71. Krüger, J.; Plass, R.; Cevey, L.; Piccirelli, M.; Gratzel, M.; Bach, U. *Appl. Phys. Lett*. **2001**, *79*, 2085.

72. Krüger, J.; Plass, R.; Gratzel, M. *Appl. Phys. Lett*. **2002**, *81*, 367.

73. Kuang, D.; Klein, C.; Snaith, H. J.; Moser, J. E.; Humphry-Baker, R.; Comte, P.; Zakeeruddin, S. M.; Gratzel, M. *Nano Lett*. **2006**, *6*, 769.

74. Kuang D.; Klein, C.; H. J.Snaith, R. Humphry-Baker, S. M. Zakeerudin, M. Gratzel, *Inorg. Chim. Acta* **2008**, *361*, 699.

75. Snaith, H. J.; Moule, A. J.; Klein, C.; Meerholz, K.; Friend, R. H.; Gratzel, M. *Nano Lett*. **2007**, *7*, 3372.

76. Hara, K.; Sato, T.; Katoh, R.; Furube, A.; Yoshihara, T.; Murai, M.; Kurashige, M.; Ito, S.; Shinpo, A.; Suga, S.; Arakawa, H. *Adv. Funct. Mater*. **2005**, *15*, 246.

77. Hara, K.; Sayama, K.; Ohga, Y.; Shinpo, A.; Suga, S.; Arakawa, H. *Chem. Commun*. **2001**, 569.

78. Wang, Z. S.; Cui, Y.; Dan-oh, Y.; Kasada, C.; Shinpo, A.; Hara, K. *J. Phys. Chem. C* **2007**, *111*, 7224.

79. Koumura, N.; Wang, Z. S.; Mori, S.; Miyashita, M.; Suzuki, E.; Hara, K. *J. Am. Chem. Soc*. **2006**, *128*, 14256.

80. Wang, Z. S.; Koumura, N.; Cui, Y.; Takahashi, M.; Sekiguchi, H.; Mori, A.; Kubo, T.; Furube, A.; Hara, K. *Chem. Mater*. **2008**, *20*, 3993.

81. Choi, H.; Baik, C.; Kang, S. O.; Ko, J.; Kang, M. S.; Nazeeruddin, M. K.; Gratzel, M. *Angew. Chem. Int. Ed*. **2008**, *47*, 327.

82. Li, S.-L.; Jiang, K.-J.; Shao, K.-F.; Yang, L.-M. *Chem. Commun*. **2006**, 2792.

83. Tian, H.; Yang, Y.; Chen, R.; Pan, Y.; Li, L.; Hagfeldt, A.; Sun, L. *Chem. Commun*. **2007**, 3741.

84. Ito, S.; Miura, H.; Uchida, S.; Takata, M.; Sumioka, K.; Liska, P.; Comte, P.; Pechy, P.; Gratzel, M. *Chem. Commun*. **2008**, 5194.

85. Burke, A.; Schmidt-Mende, L.; Ito, S.; Gratzel, M. *Chem. Commun*. **2007**, 234.

86. Treibs, A.; Kreuzer, F. H. *Justus Liebigs Ann. Chem*. **1968**, *718*, 208.

87. Karolin, J.; Johansson, L. B.-A.; Strandberg, L.; Ny, T. *J. Am. Chem. Soc.*, **1994**, *116*, 7801.

88. Haugland, R. P. *Handbook of Fluorescent Probes and Research Chemicals*, 6th ed.; Molecular Probes: Eugene, OR, **1996**.

89. Tan, K.; Jaquinod, L.; Paolesse, R.; Nardis, S.; Di Natale, C.; Di Carlo, A.; Prodi, L.; Montalti, M.; Zaccheroni, N.; Smith, K. M. *Tetrahedron*, **2004**, *60*, 1099.

90. Bozdemir, O. A.; Cakmak, Y.; Sozmen, F.; Ozdemir, T.; Siemiarczuk, A.; Akkaya, E. U. *Chem. Eur. J*. **2010**, *16*, 6346.

91. Erbas, S.; Gorgulu, A.; Kocakusakogullari, M.; Akkaya, E. U. *Chem. Commun.* **2009**, *33*, 4956.

92. Yuan, M.; Li, Y.; Li, J.; Li, C.; Liu, X.; Lv, J.; Xu, J.; Liu, H.; Wang, S. Zhu, D. *Org. Lett.*, **2007**, *9*, 2313.

93. Coskun, A.; Akkaya, E. U. *J. Am. Chem. Soc.*, **2005**, *127*, 10464.

94. Coskun, A.; Deniz, E.; Akkaya, E. U. *Org. Lett.*, **2005**, *7*, 5187.

95. Bozdemir, O. A.; Yılmaz, M. D.; Buyukcakir, O.; Siemiarczuk, A.; Tutas, M.; Akkaya, E. U. *New J. Chem.*, **2010**, *1*,151.

96. Forgie, J. C.; Skabara, P. J.; Stibor, I.; Vilela, F.; Vobecka Z. *Chem. Mater*. **2009**, *21*, 1784.

97. Hattori, S.; Ohkubo, K.; Urano, Y.; Sunahara, H.; Nagano, T.; Wada, Y.; Tkachenko, N. V.; Lemmetyinen, H.; Fukuzumi, S. *J. Phys. Chem. B* **2005**, *109*, 15368.

98. Erten-Ela, S.; Yilmaz, D.; Icli, B.; Dede, Y.; Icli, S.; Akkaya, E.U. *Org. Lett.* **2008**, 10, 3299.

99. Kumaresan, D.; Thummel, R. P.; Bura, T.; Ulrich, G.; Ziessel, R. *Chem. Eur. J.* **2009***, 15,* 6335.

100. Rousseau, T.; Cravino, A.; Bura, T.; Ulrich, G.; Ziessel, R.; Roncali, J. *Chem. Commun*, **2009**, 1673.

101. He, Z.; Wong, W.-Y.; Yu, X.; Kwok, H.-S.; Lin, Z. *Inorg. Chem*. **2006**, *45*, 10922.

102. Atılgan, S.; Ozdemir, T.; Akkaya, E.U. *Org. Lett*. **2008**, *10*, 4065.

103. Cakmak, Y.; Akkaya, E. U. *Org. Lett*. **2009**, *11*, 85.

APPENDIX A

NMR SPECTRA

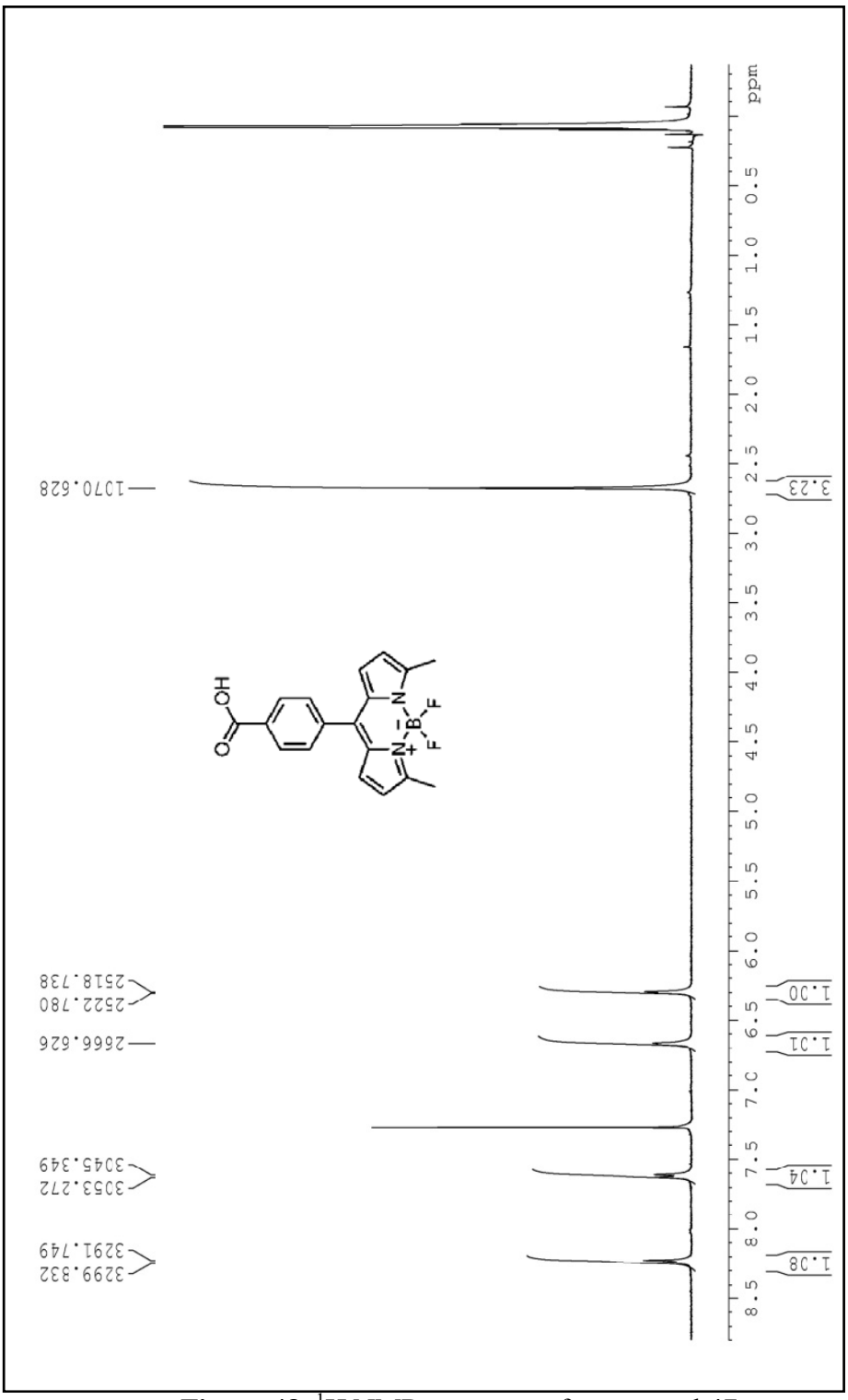

Figure 48. [1]H NMR spectrum of compound **47**

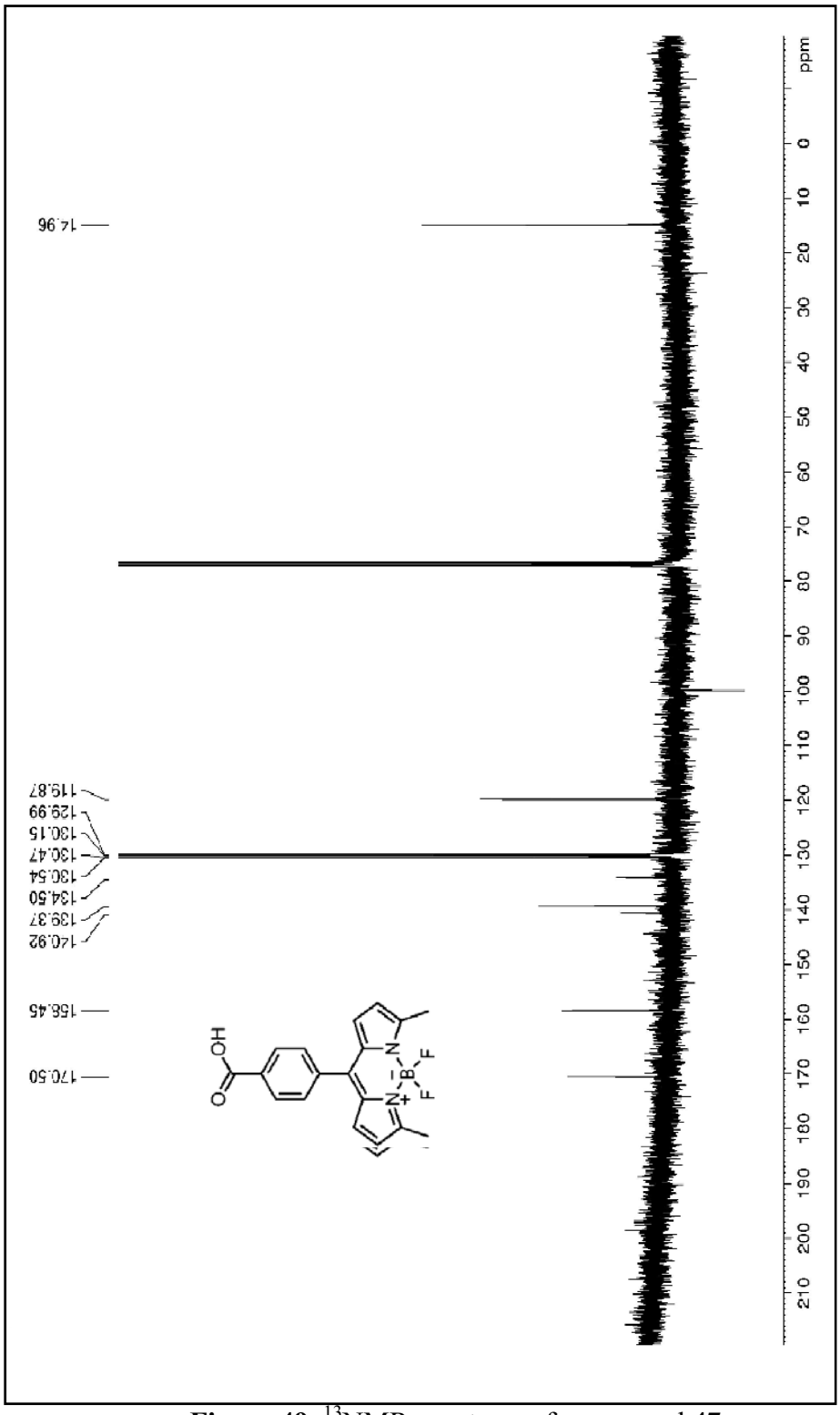

Figure 49. ^{13}NMR spectrum of compound **47**

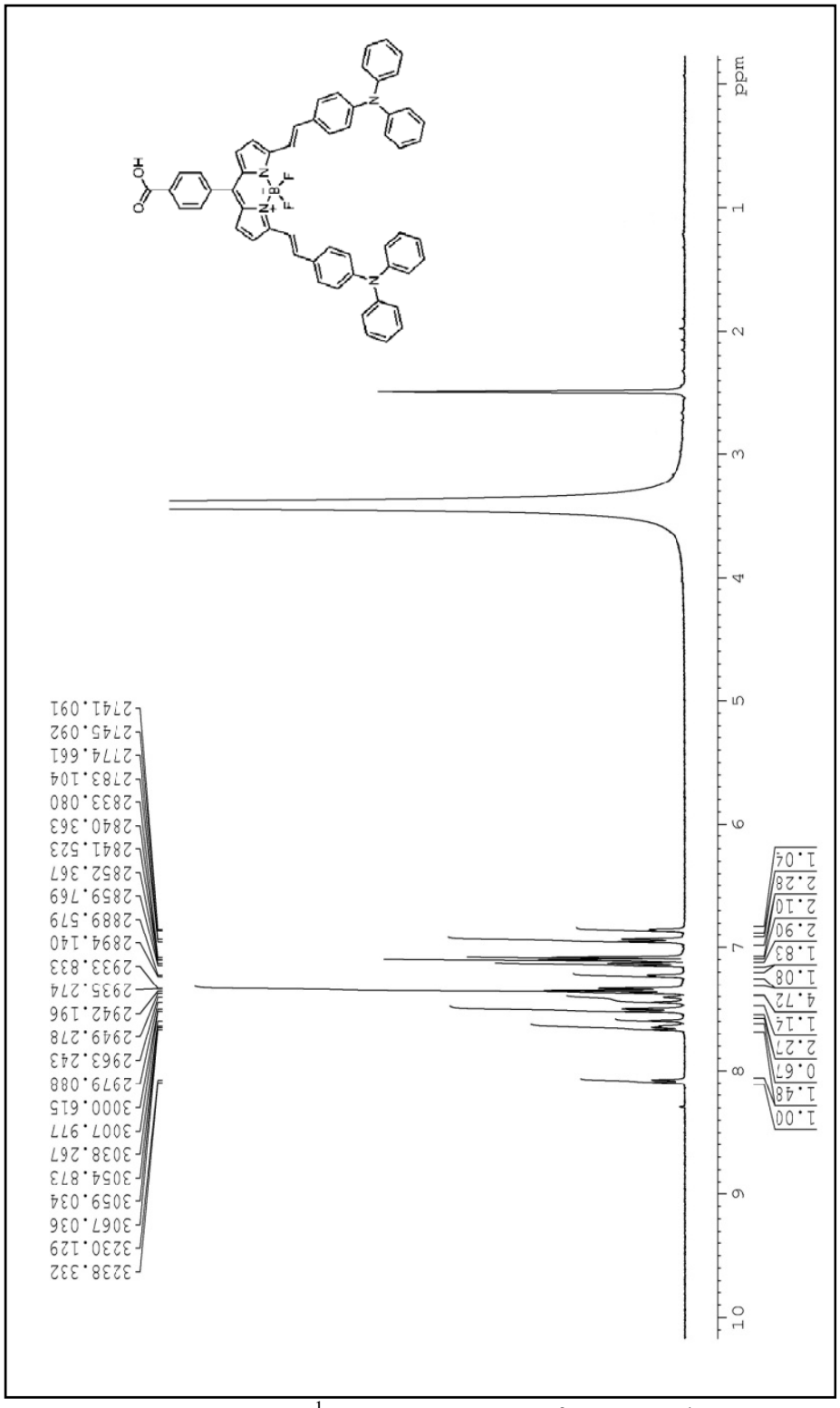

Figure 50. ^{1}H NMR spectrum of compound **49**

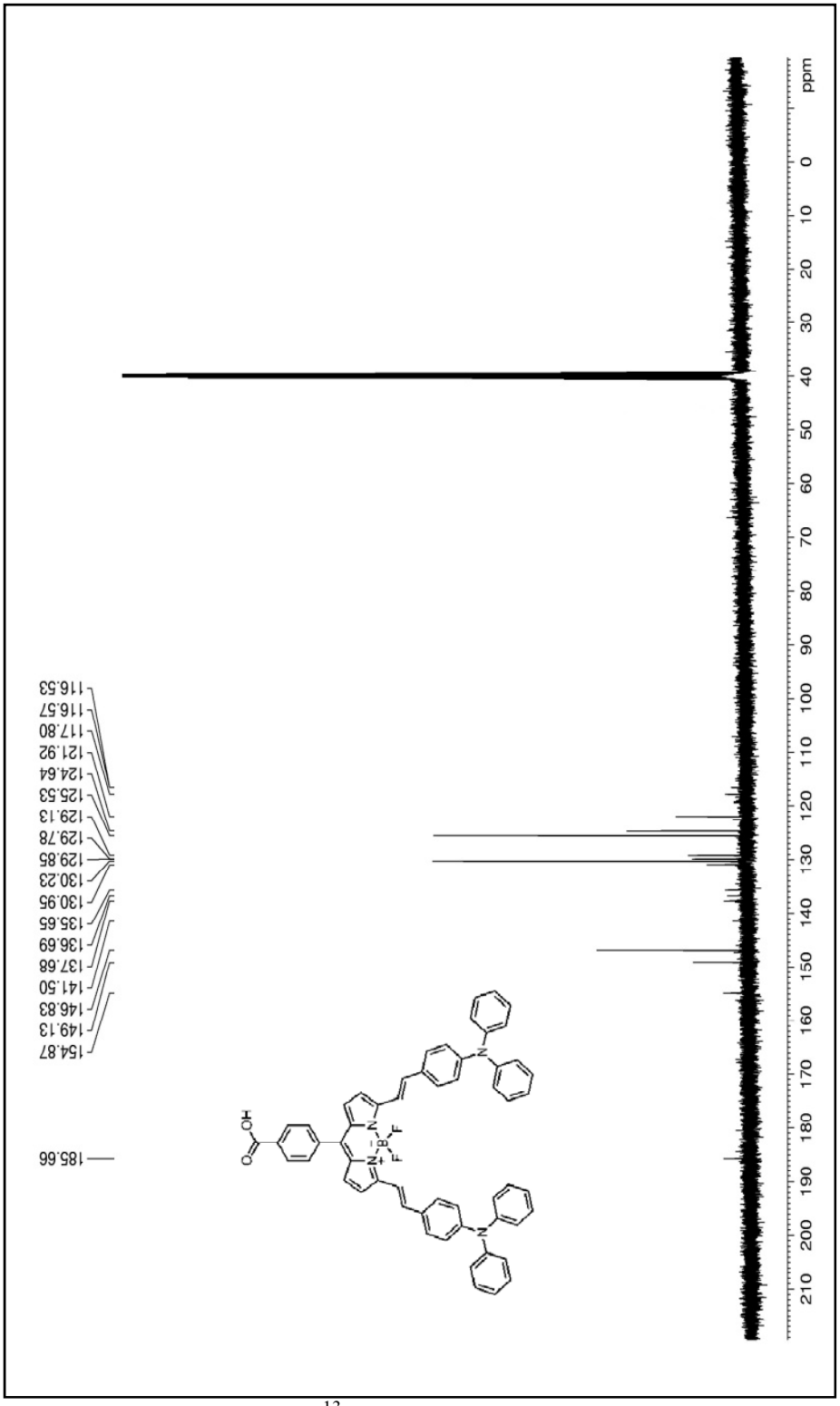

Figure 51. ^{13}NMR spectrum of compound **49**

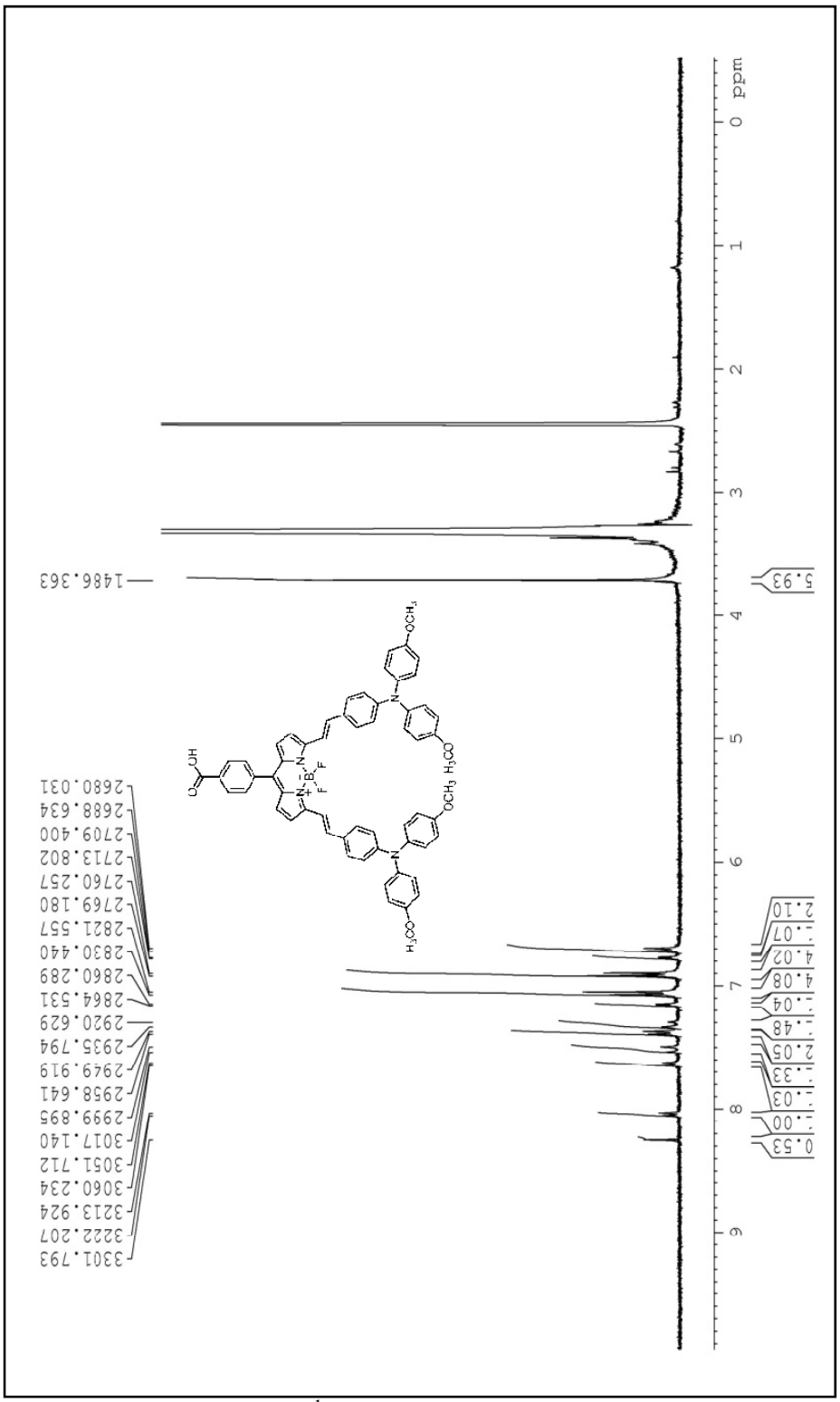

Figure 52. ^{1}H NMR spectrum of compound **51**

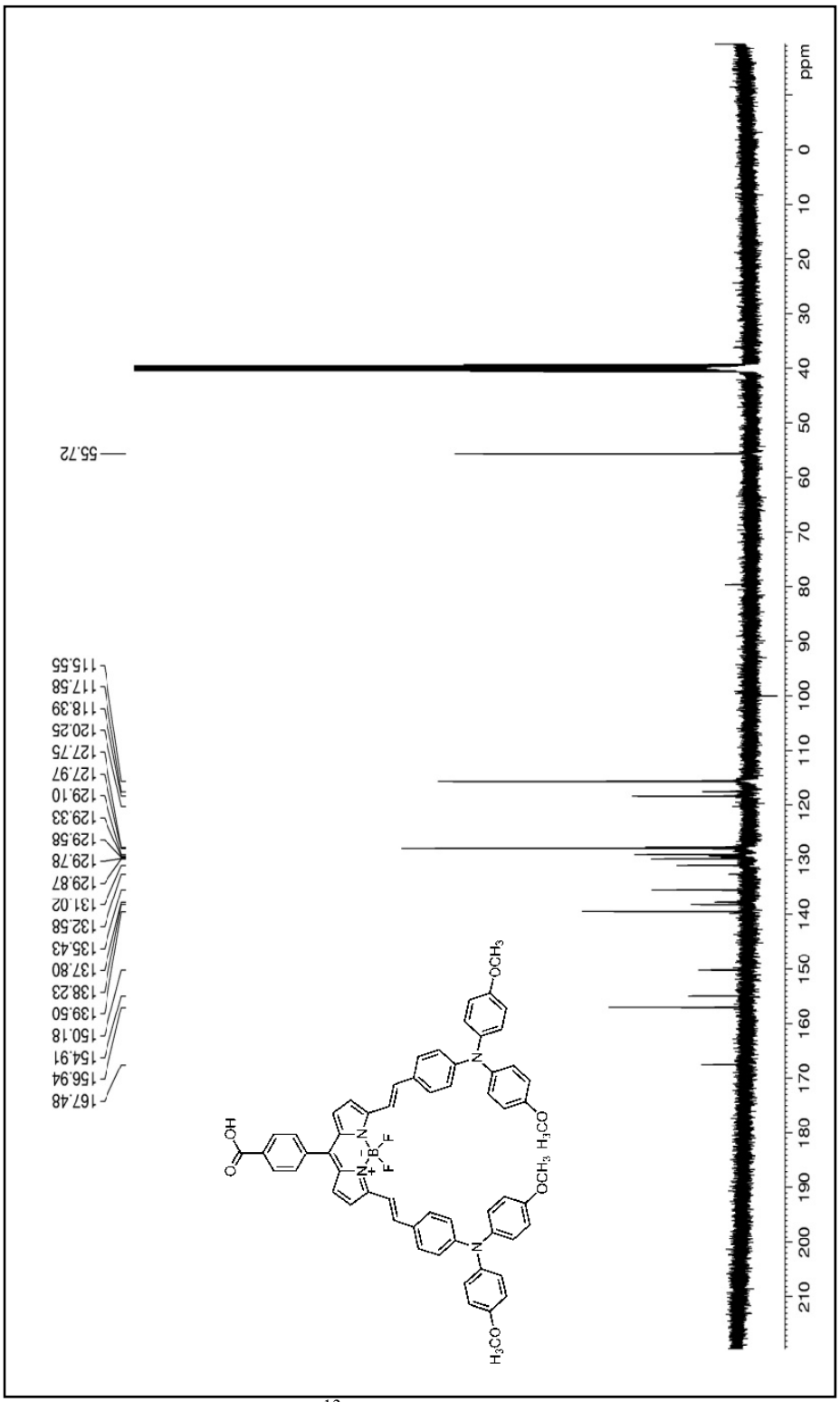

Figure 53. ^{13}NMR spectrum of compound **51**

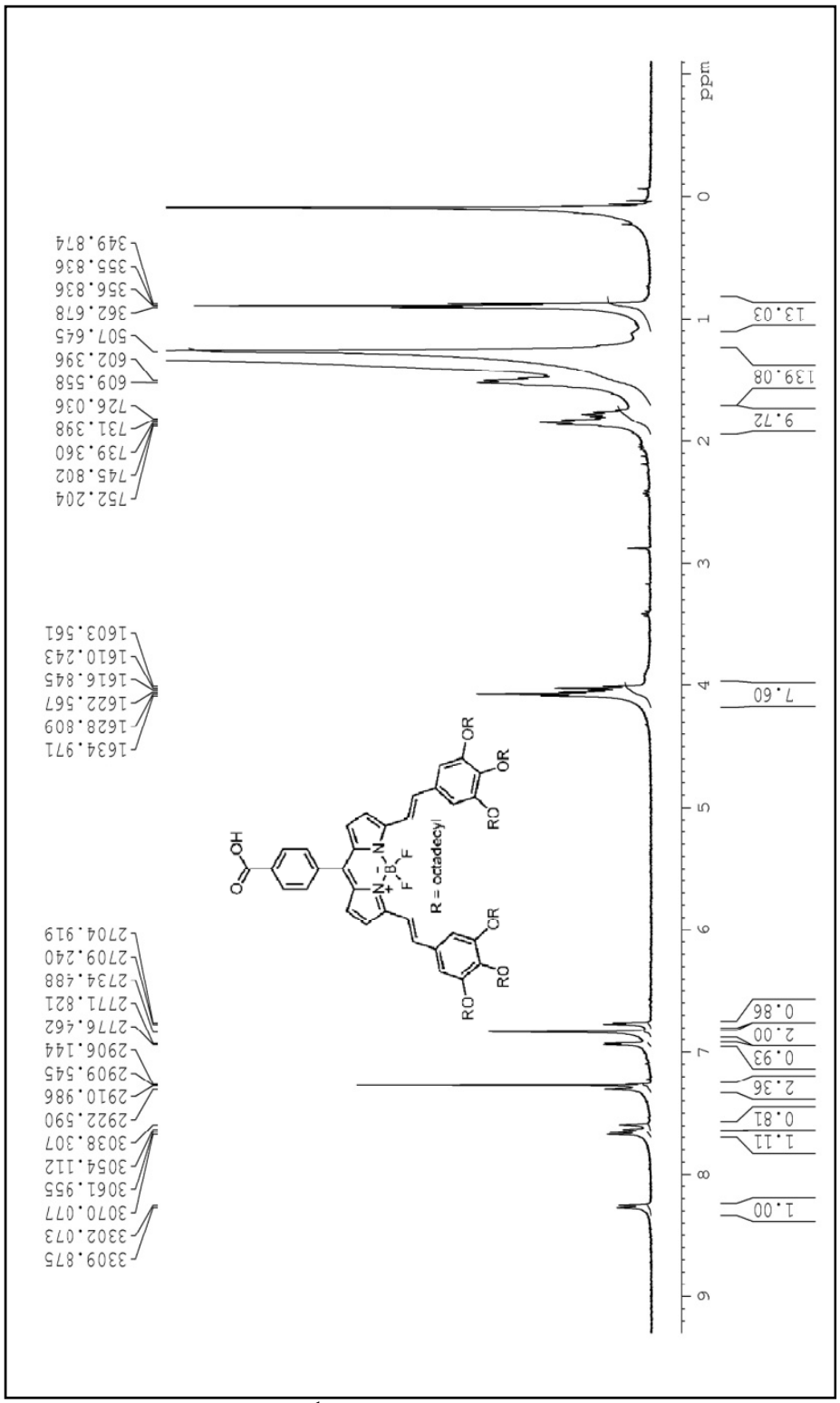

Figure 54. ^{1}H NMR spectrum of compound **53**

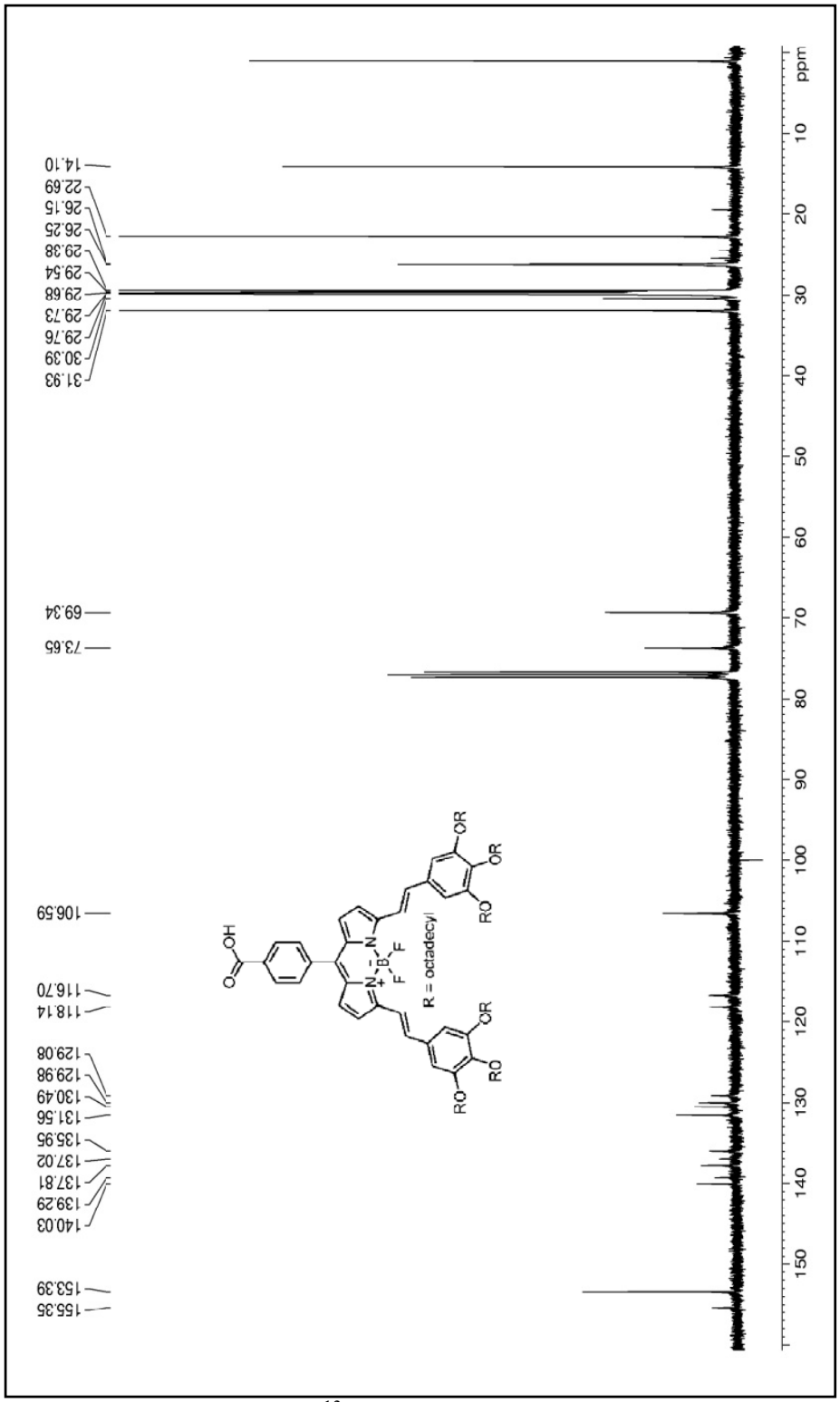

Figure 55. ^{13}NMR spectrum of compound **53**

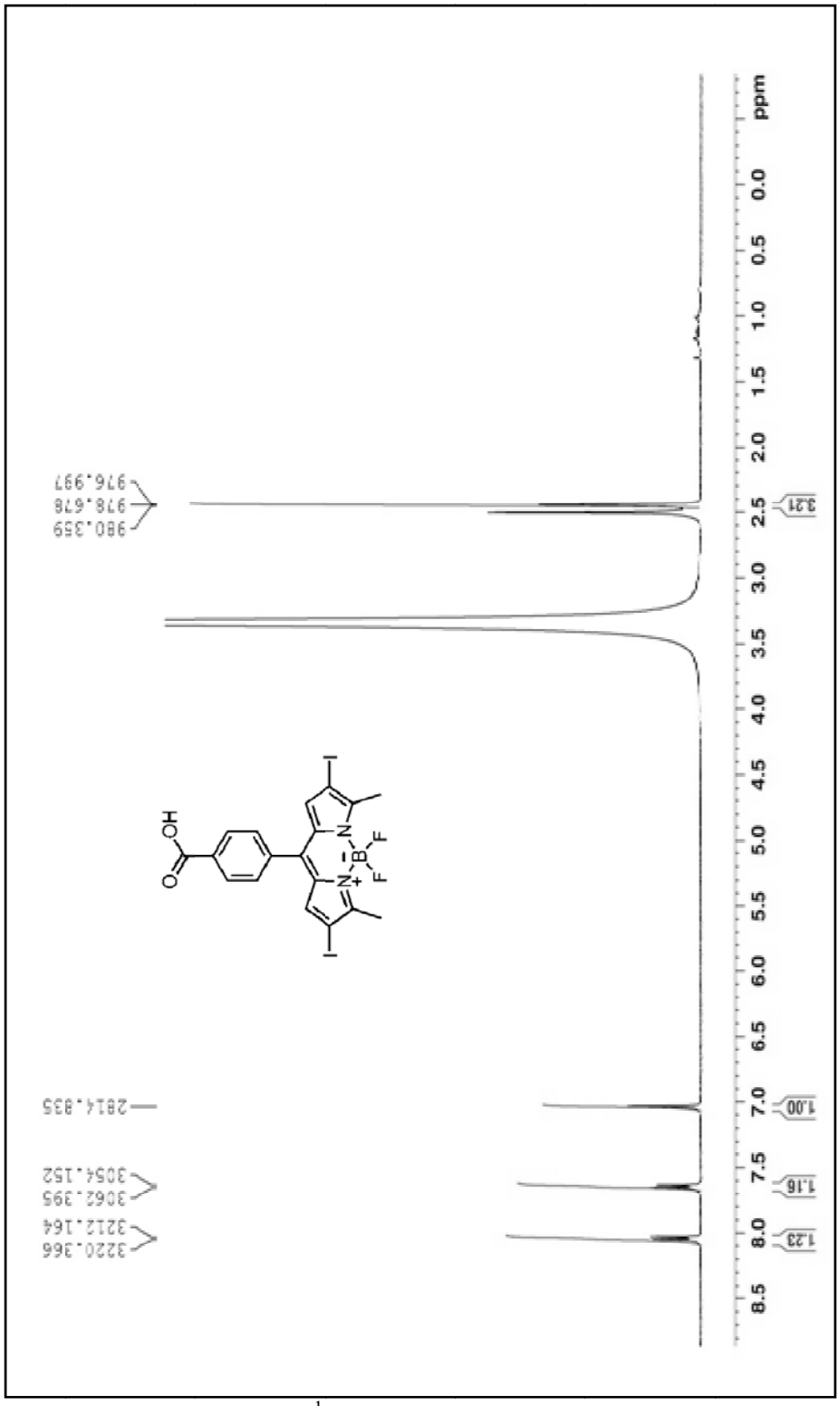

Figure 56. ^{1}H NMR spectrum of compound **54**

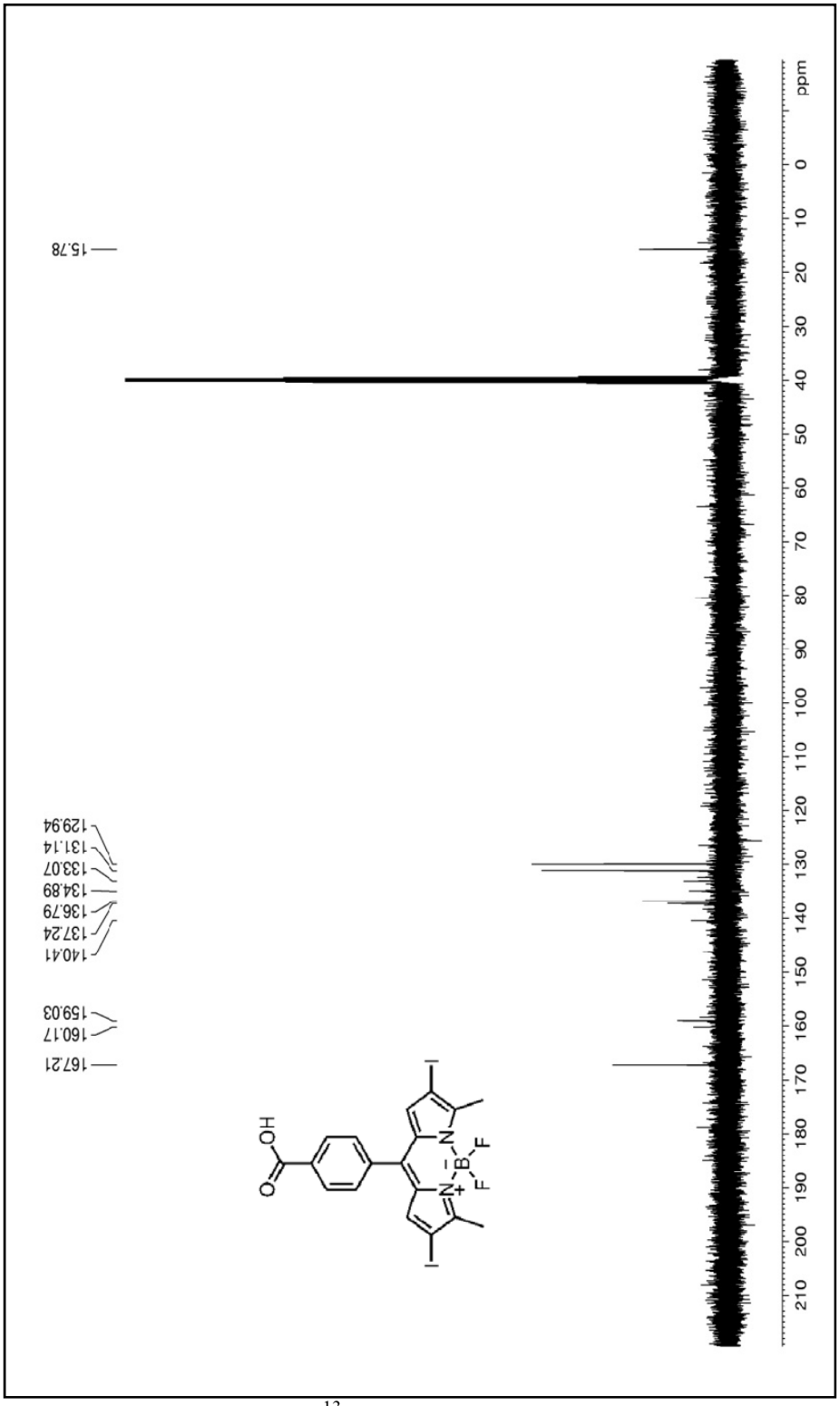

Figure 57. ^{13}NMR spectrum of compound **54**

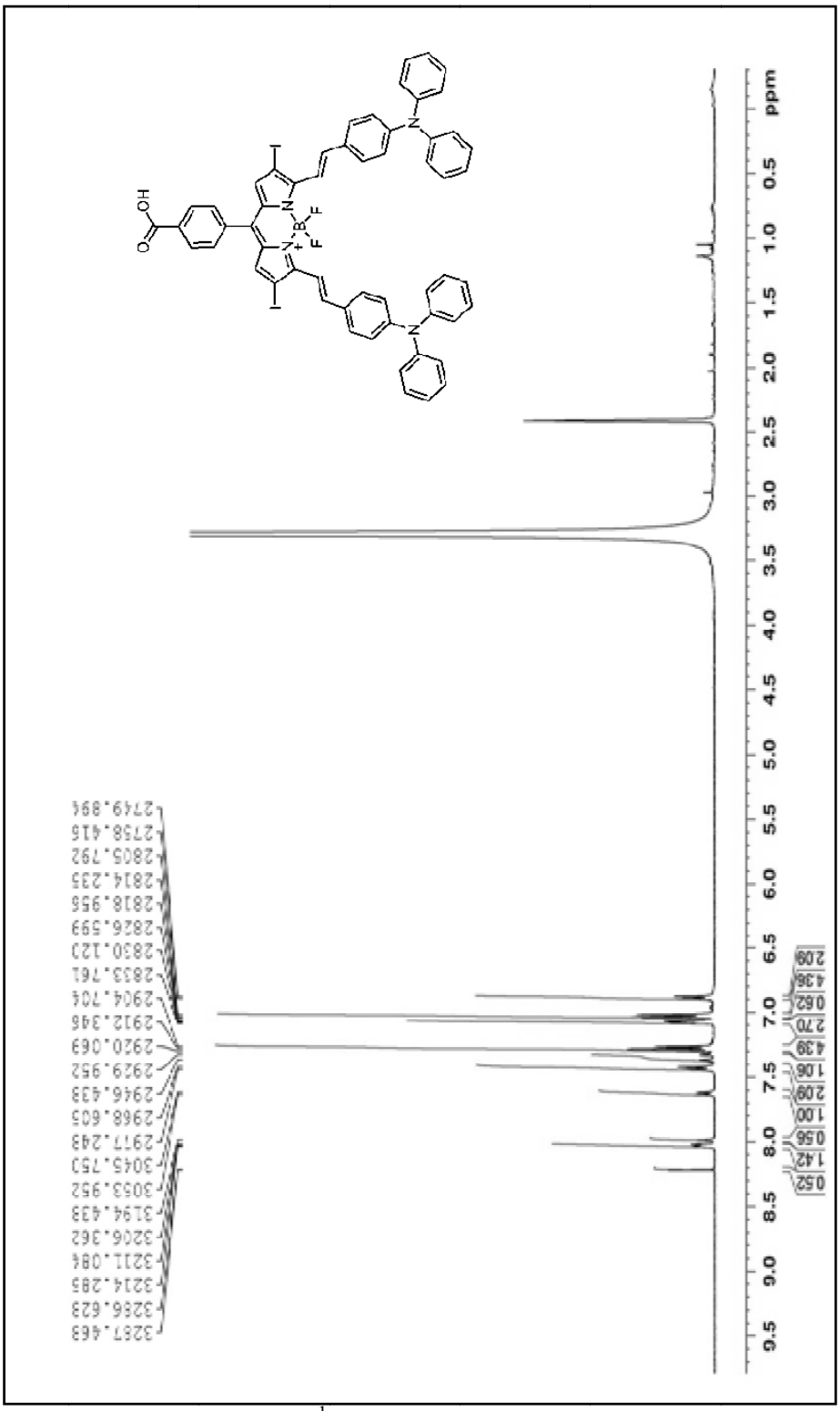

Figure 58. ^{1}H NMR spectrum of compound **55**

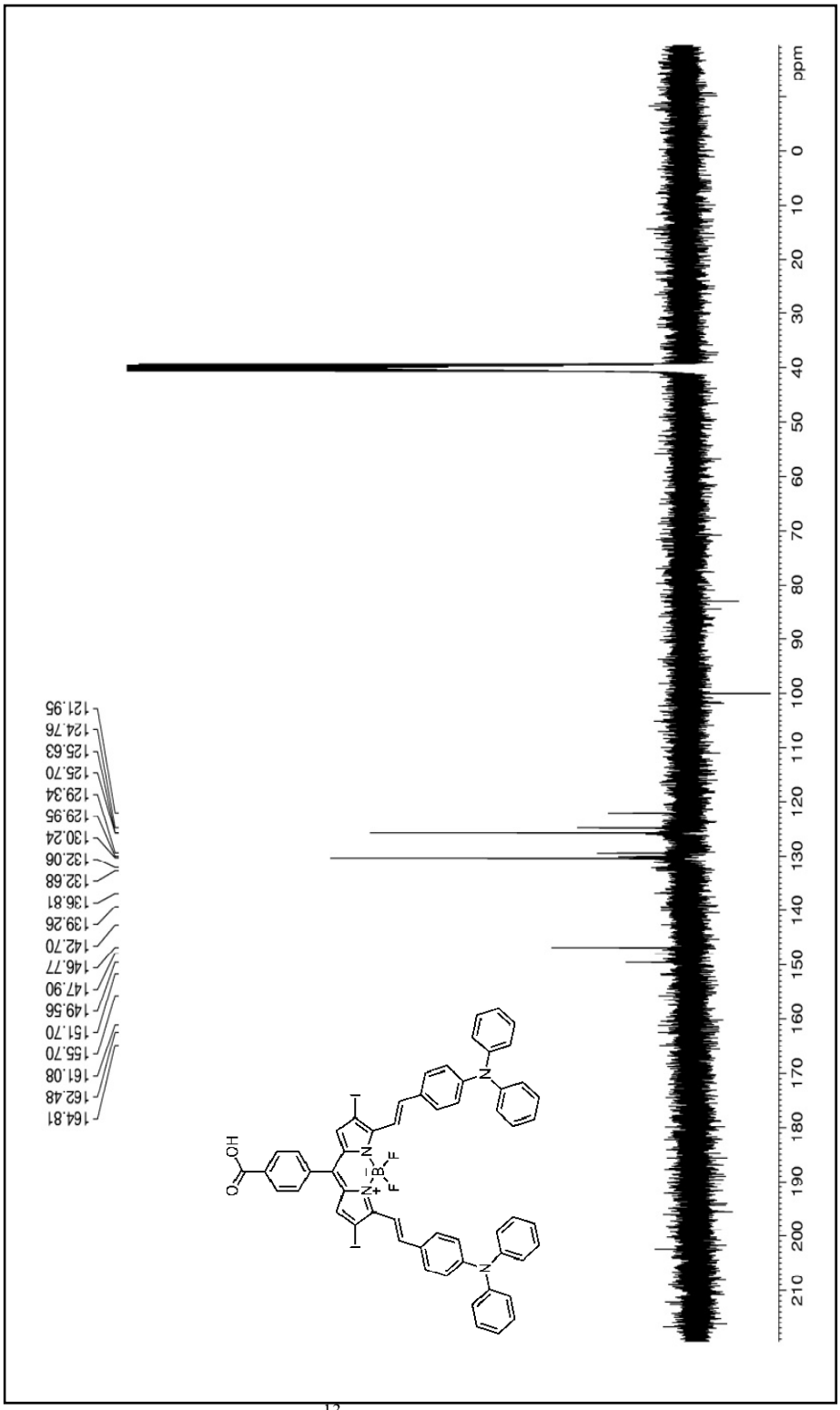

Figure 59. ^{13}NMR spectrum of compound **55**

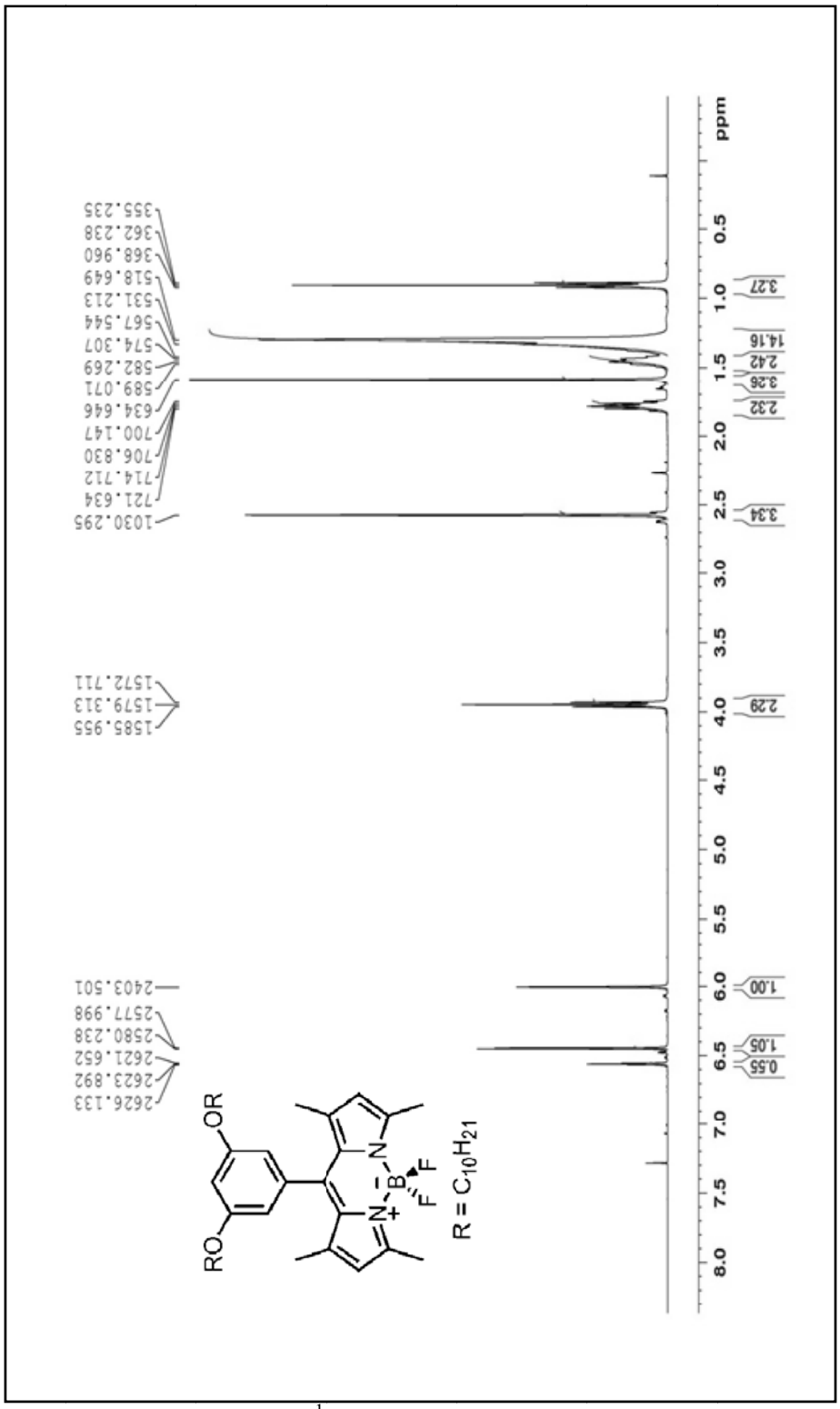

Figure 60. ^{1}H NMR spectrum of compound **58**

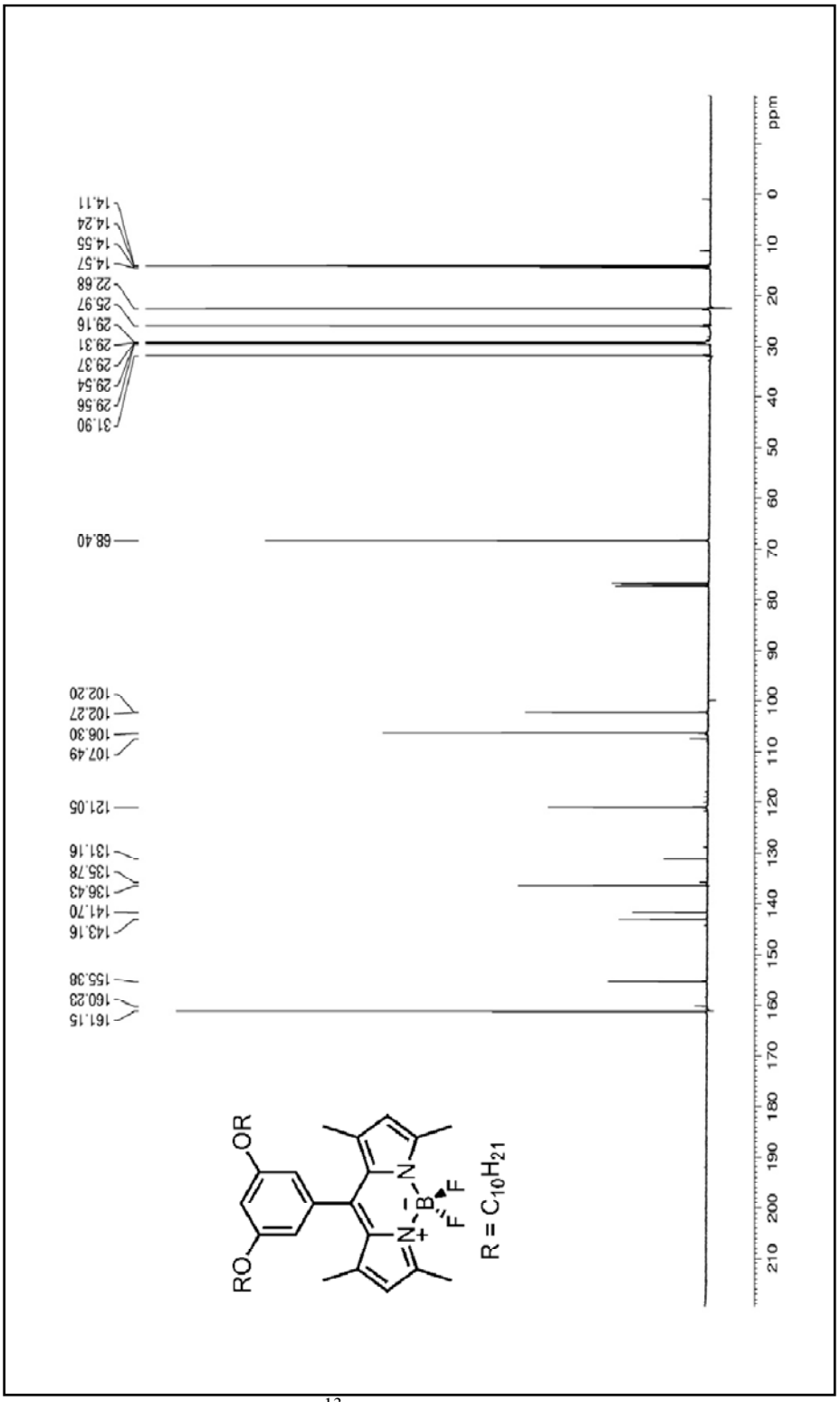

Figure 61. ^{13}NMR spectrum of compound **58**

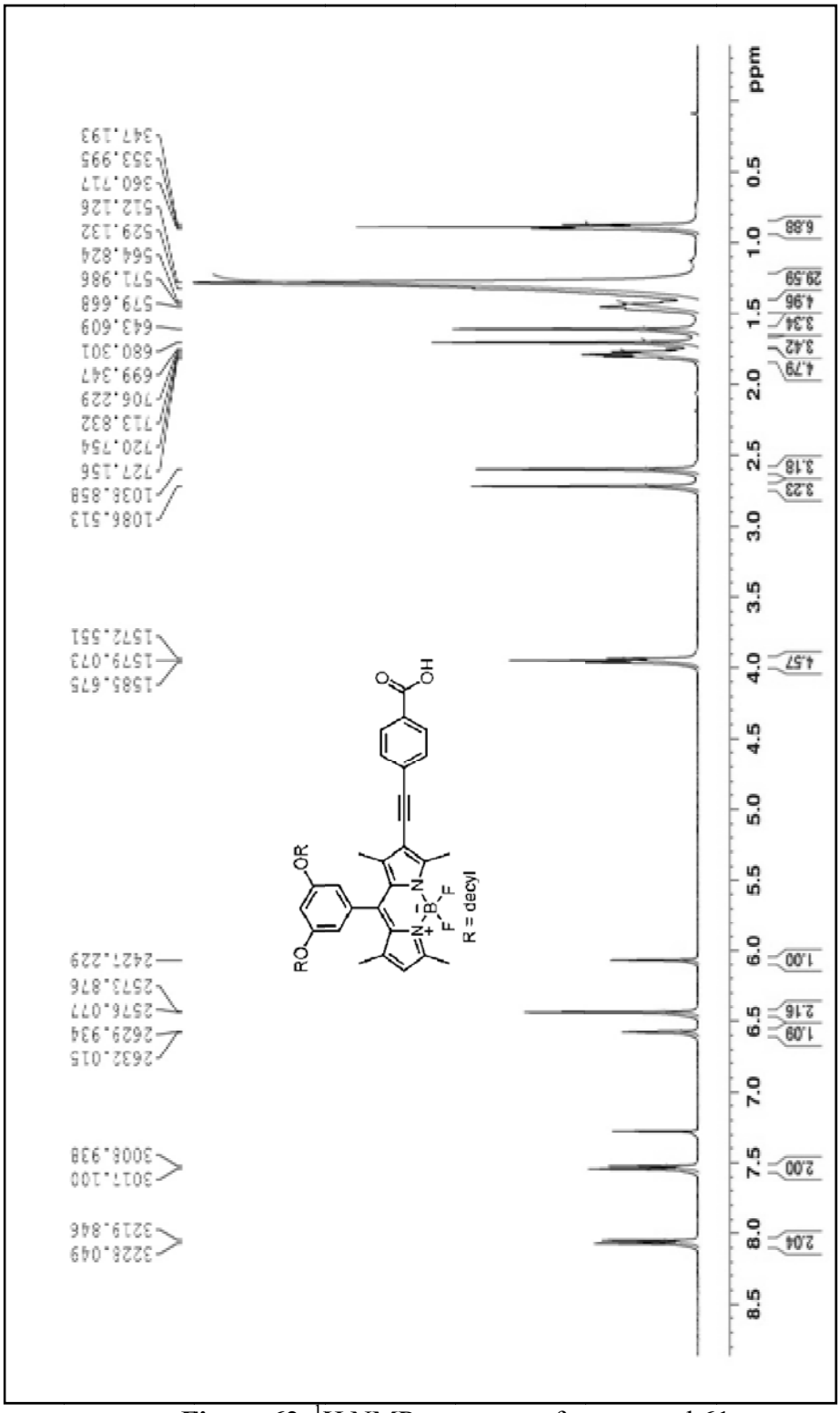

Figure 62. ^{1}H NMR spectrum of compound **61**

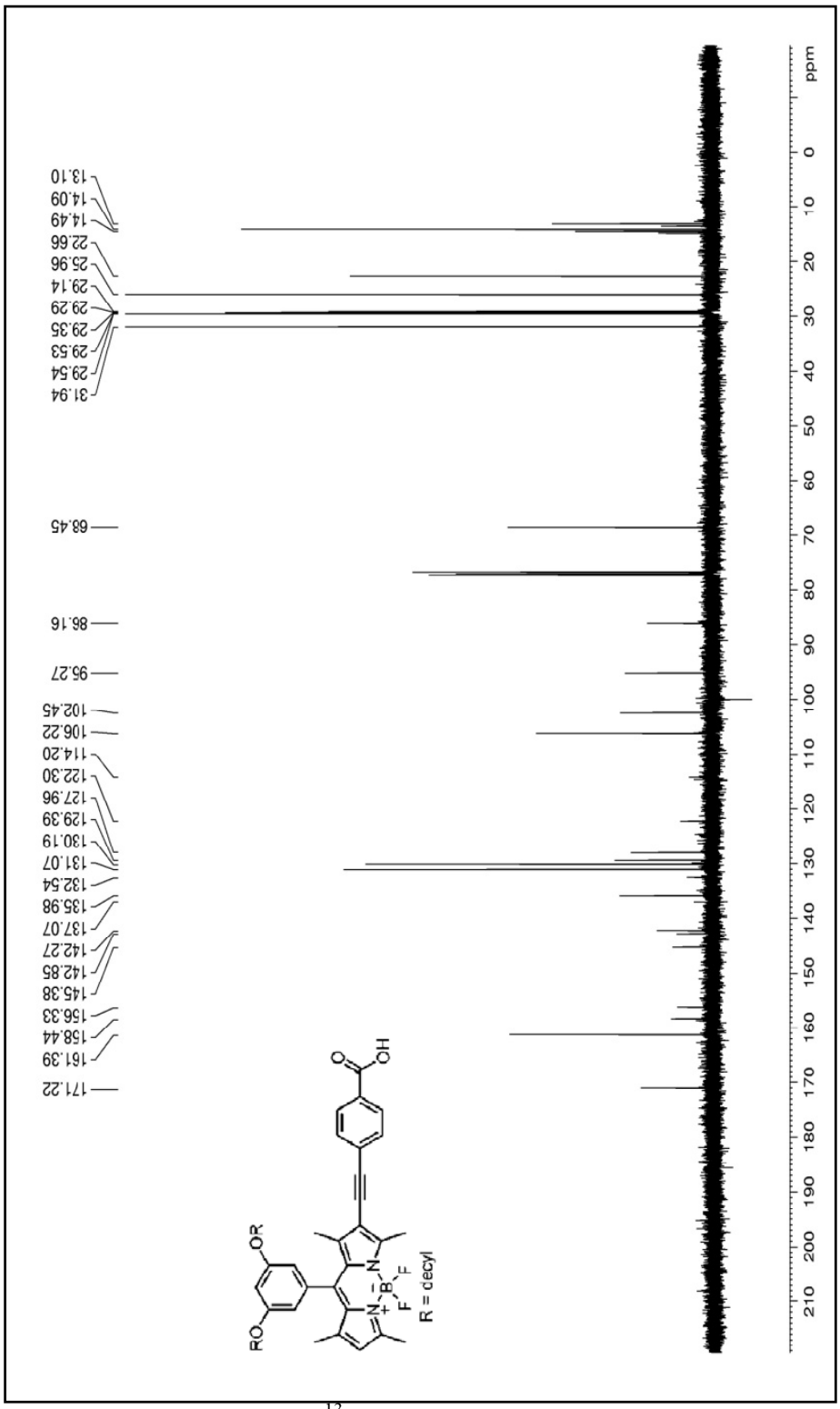

Figure 63. ^{13}NMR spectrum of compound **61**

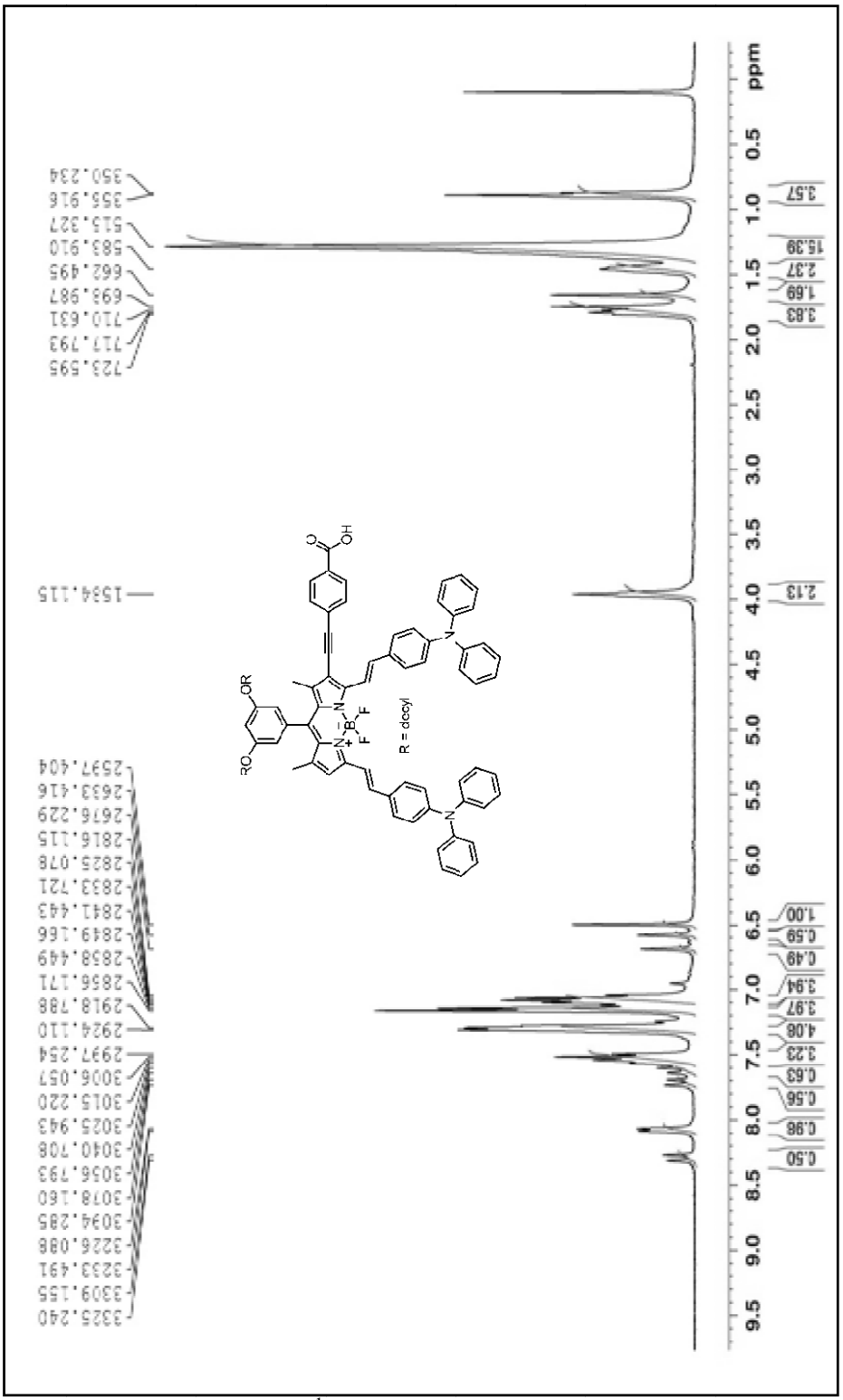

Figure 64. ^{1}H NMR spectrum of compound **62**

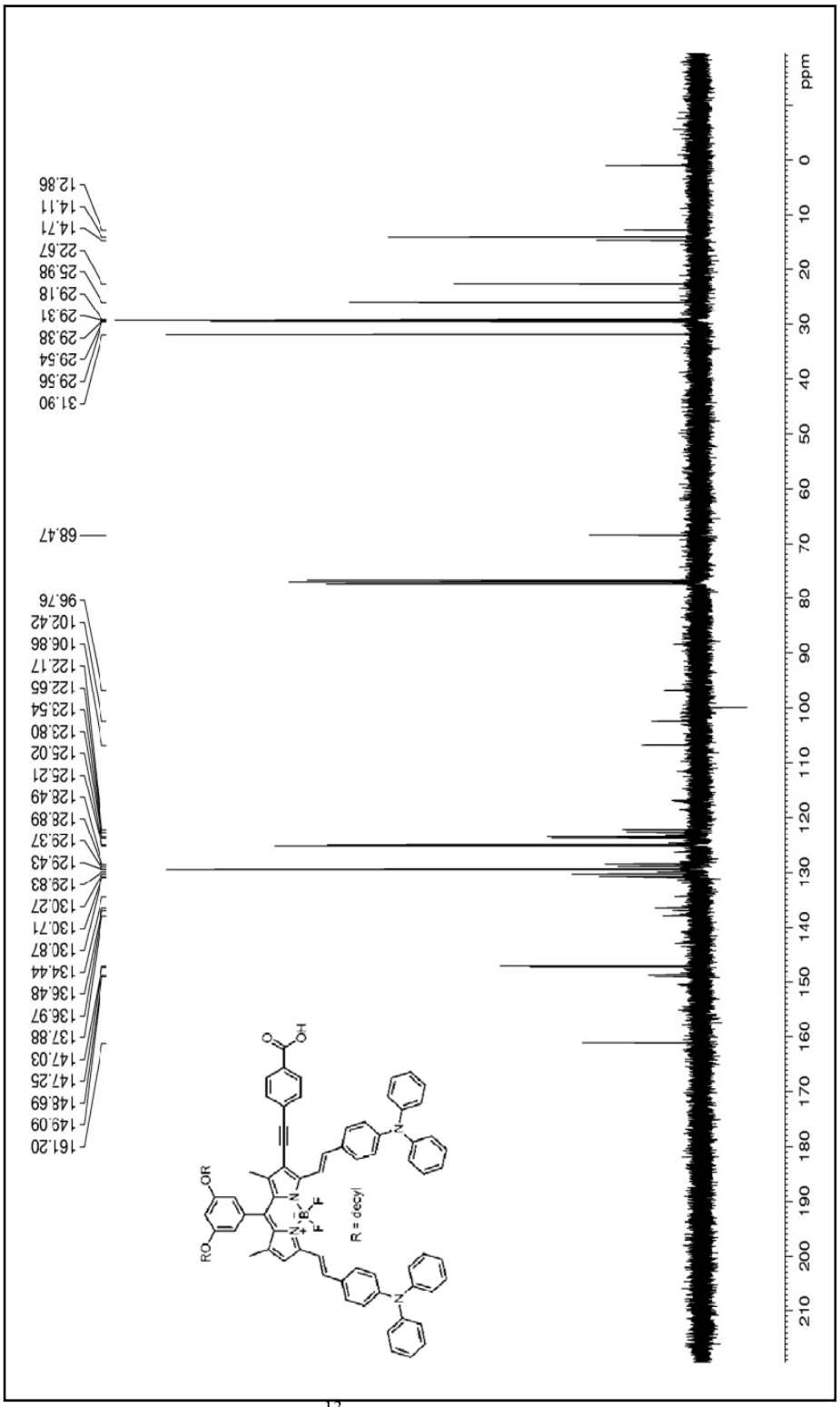

Figure 65. ^{13}NMR spectrum of compound **62**

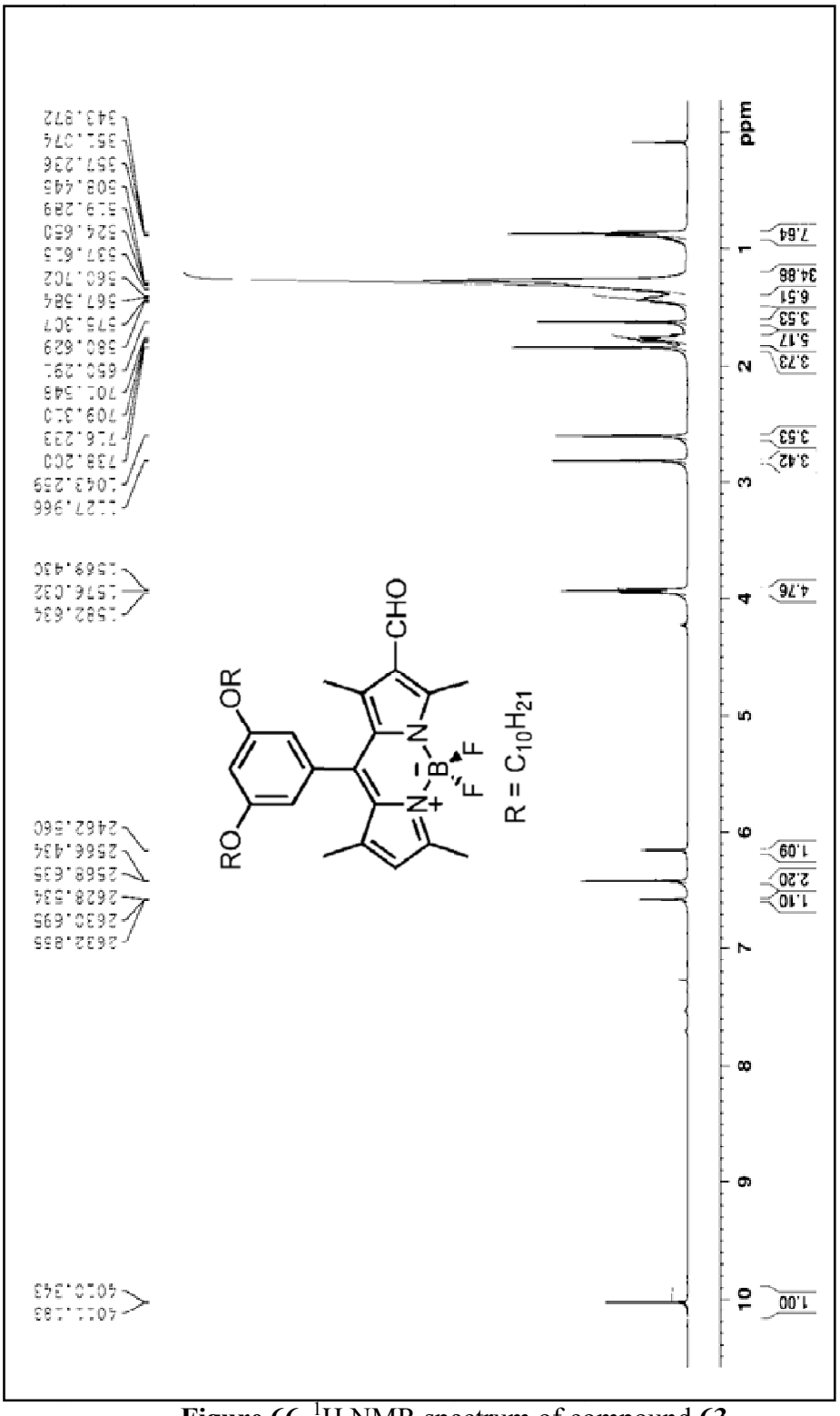

Figure 66. ^{1}H NMR spectrum of compound **63**

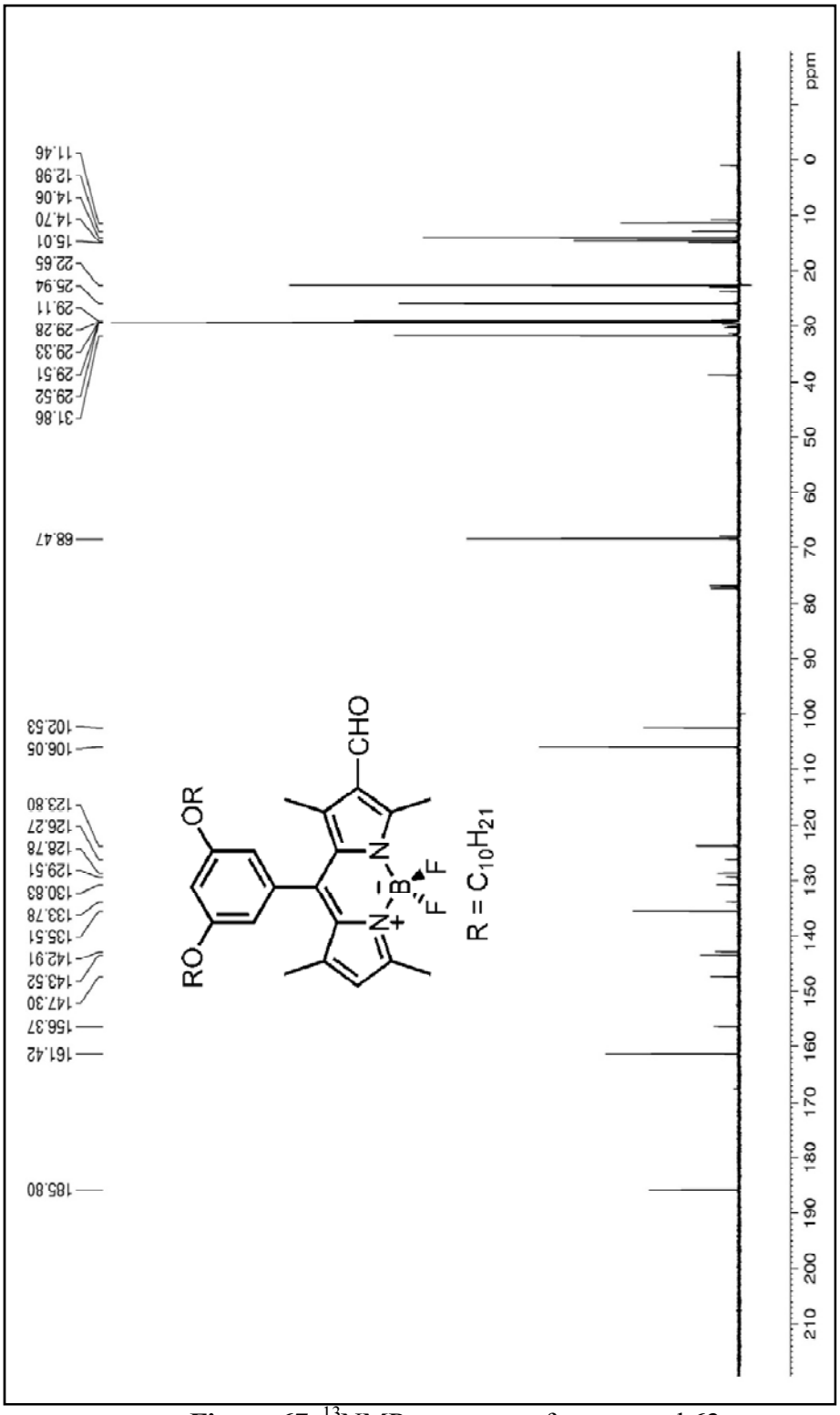

Figure 67. ^{13}NMR spectrum of compound **63**

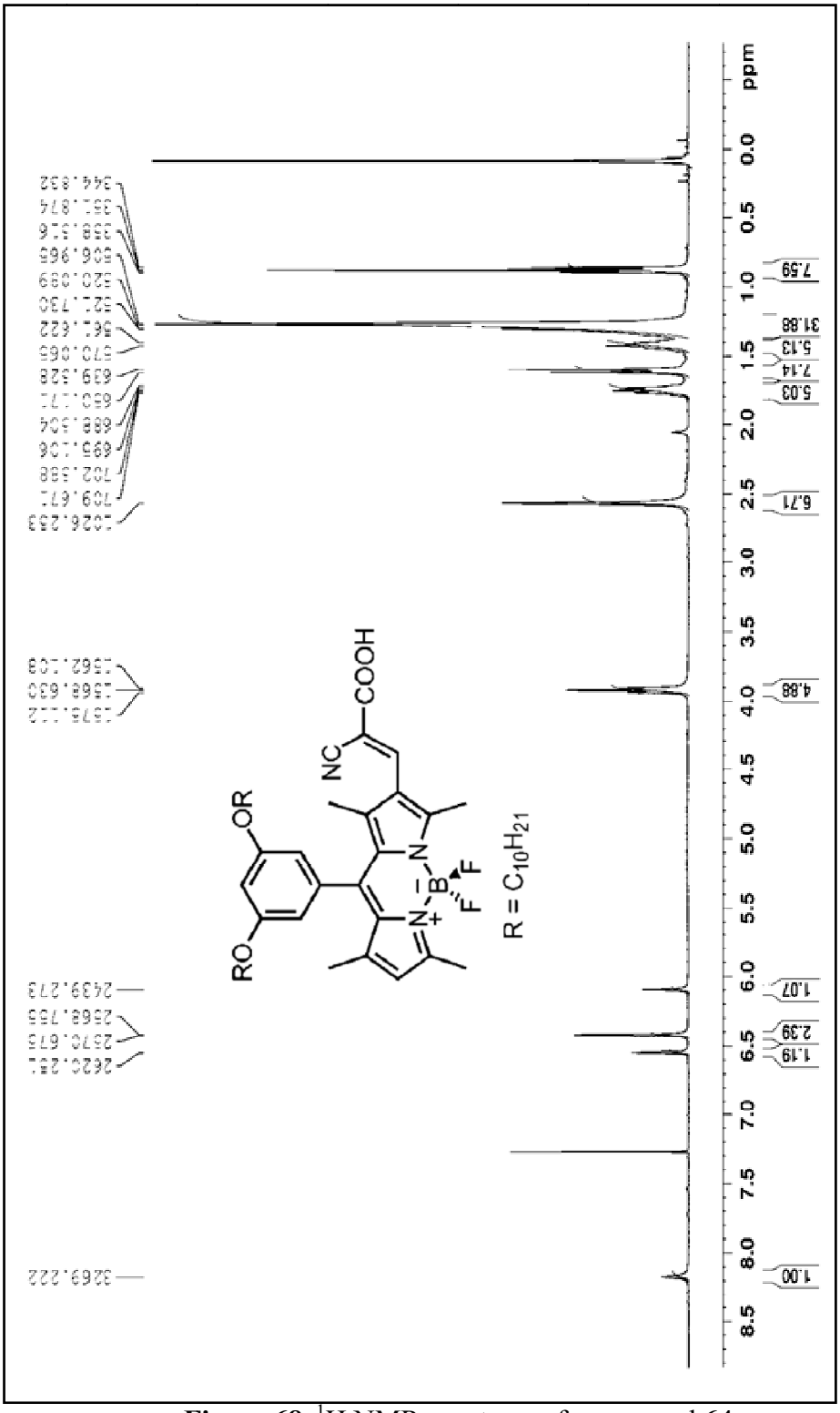

Figure 68. ^{1}H NMR spectrum of compound **64**

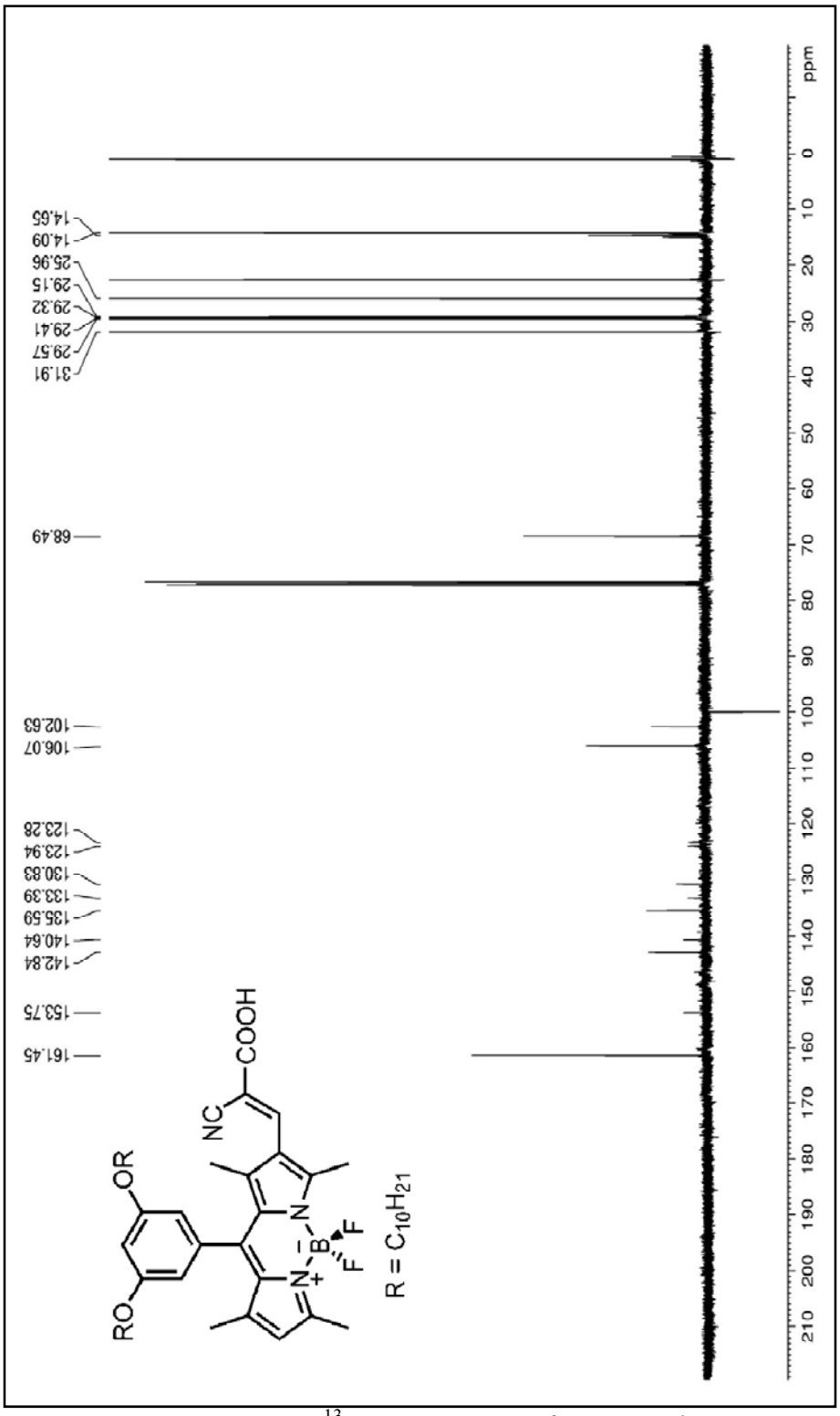

Figure 69. ^{13}NMR spectrum of compound **64**

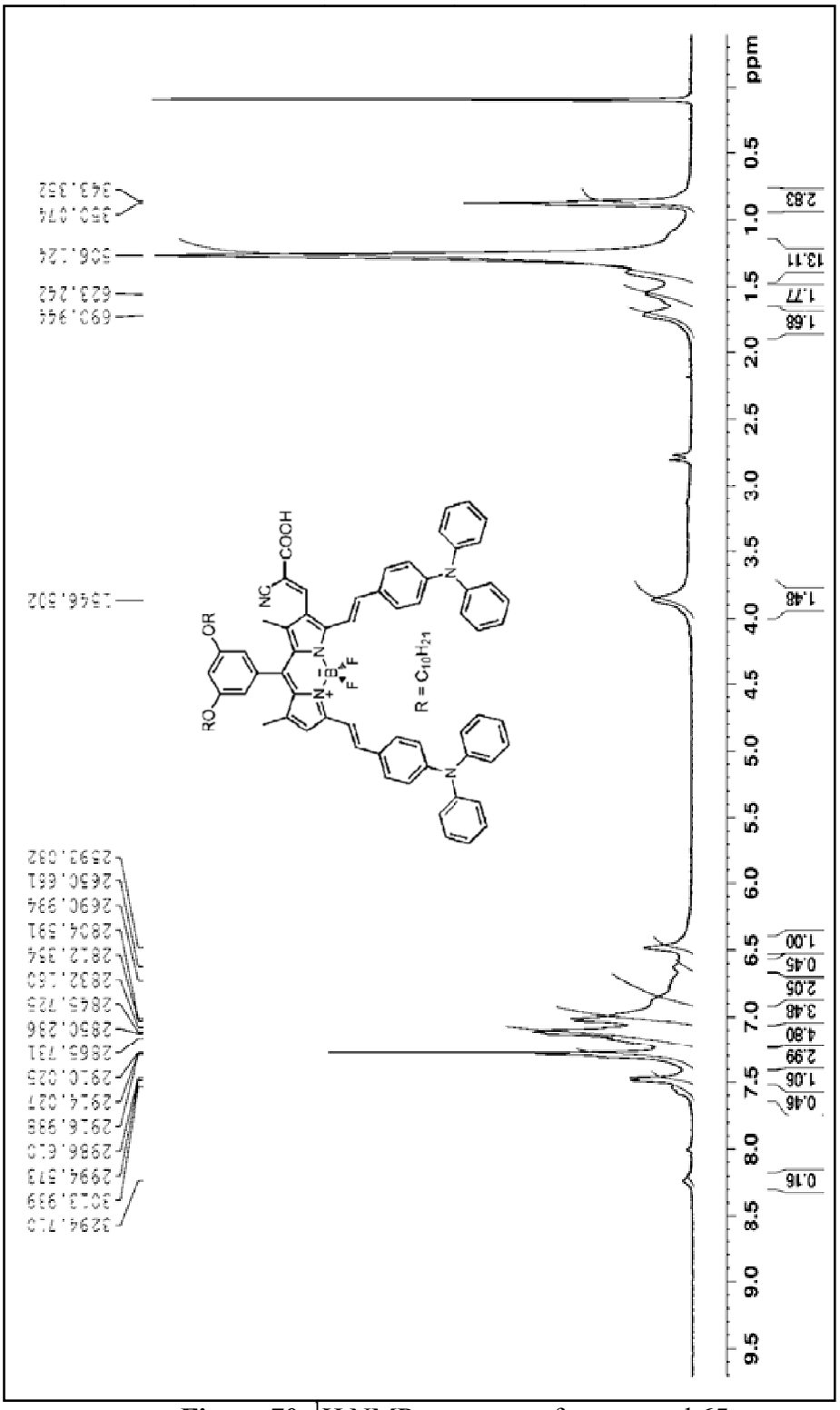

Figure 70. ^{1}H NMR spectrum of compound **65**

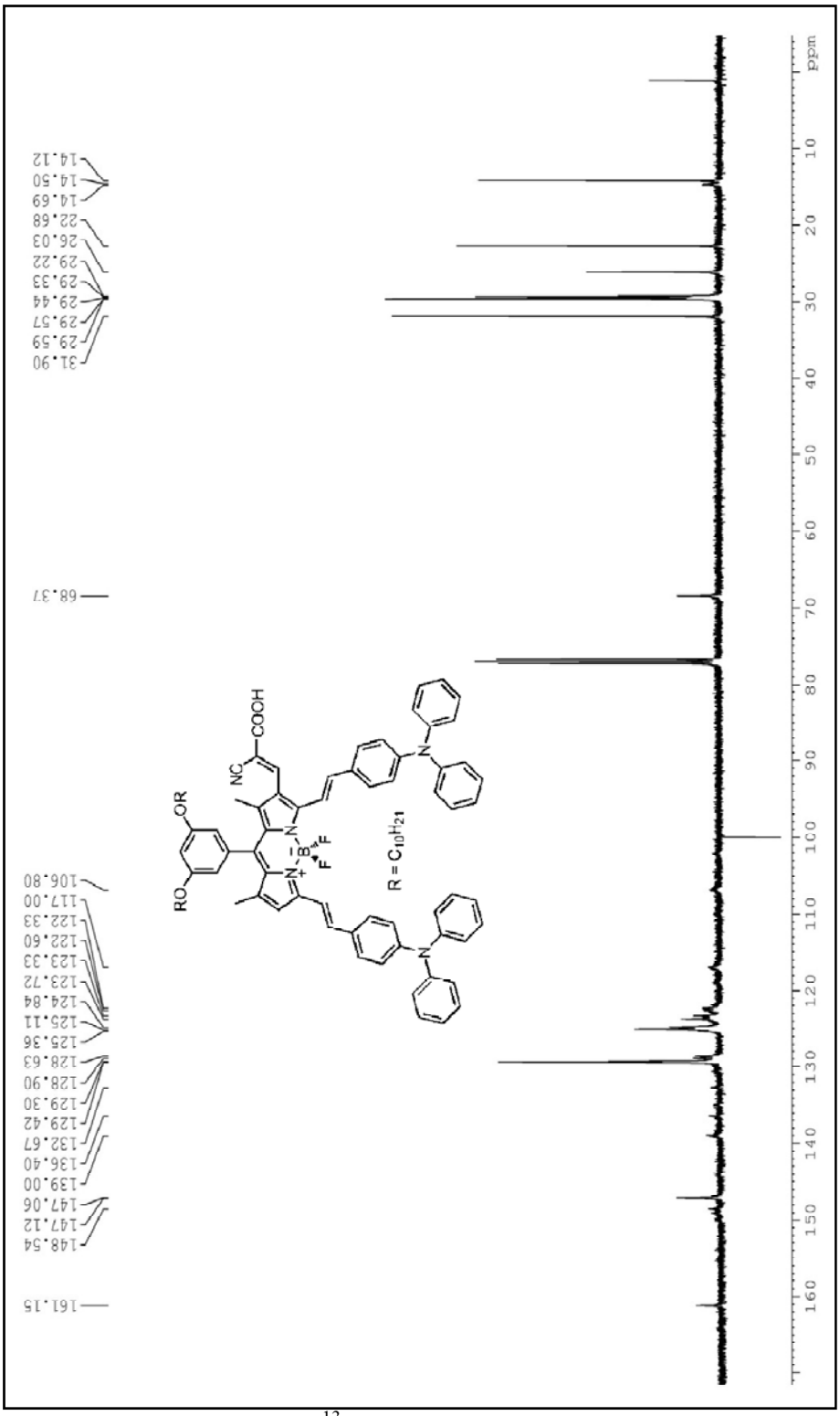

Figure 71. ^{13}NMR spectrum of compound **65**

APPENDIX B

MASS SPECTRA

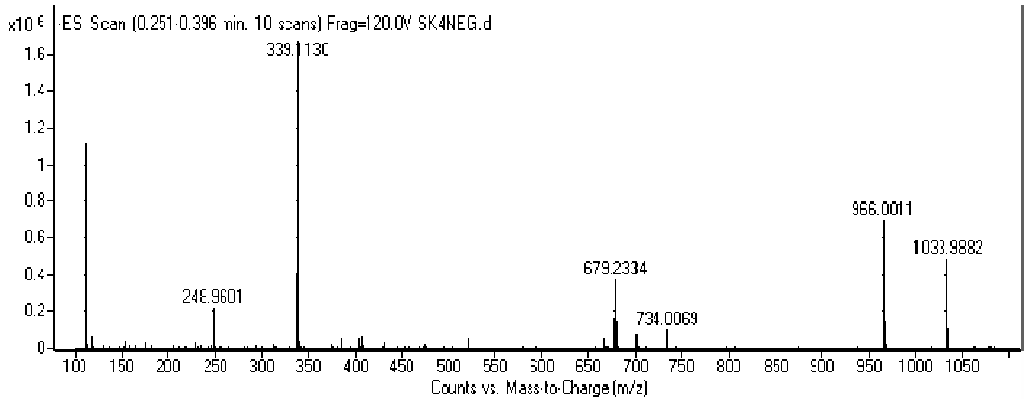

Figure 72. ESI-HRMS of compound **47**

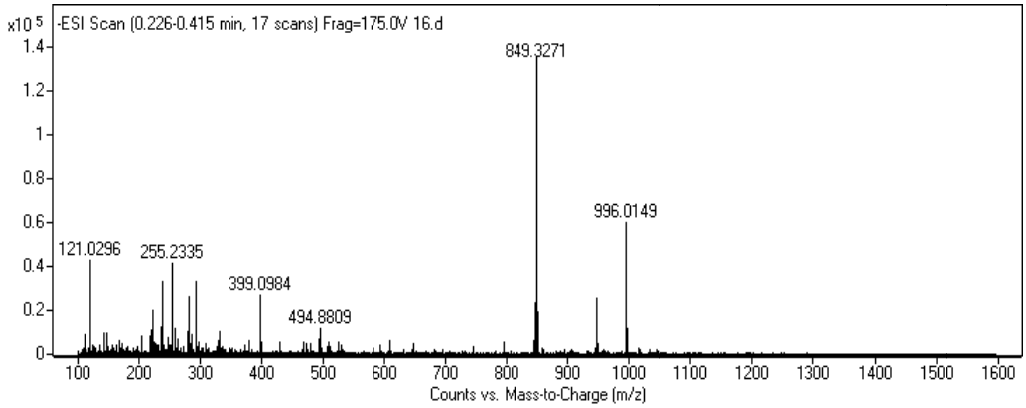

Figure 73. ESI-HRMS of compound **49**

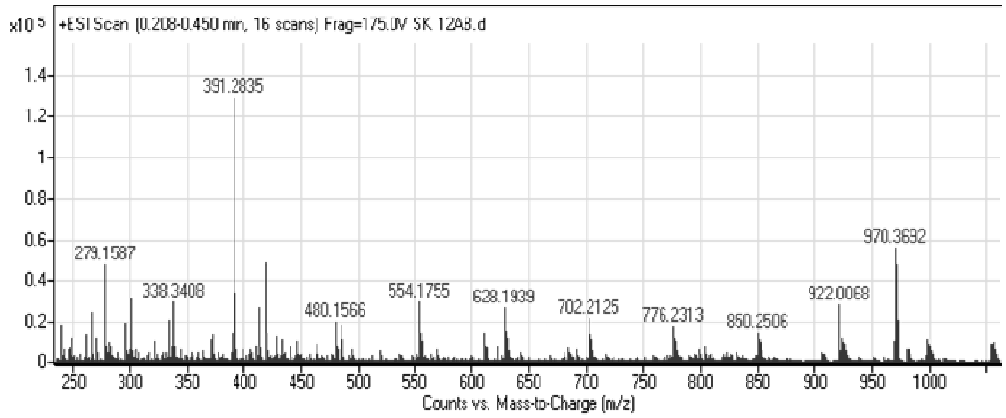

Figure 74. ESI-HRMS of compound **51**

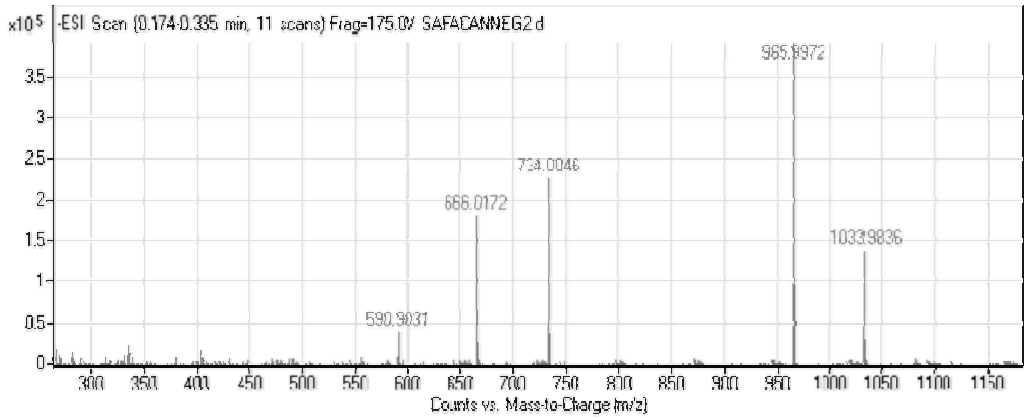

Figure 75. ESI-HRMS of compound **54**

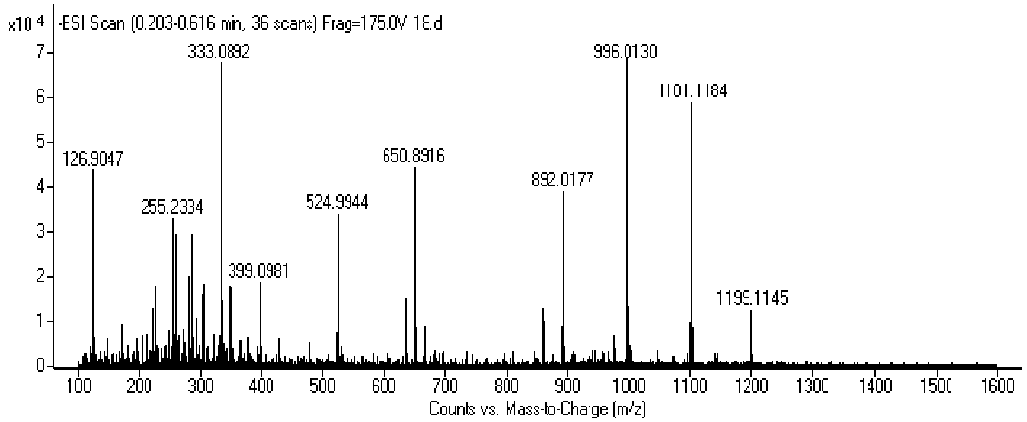

Figure 76. ESI-HRMS of compound **55**

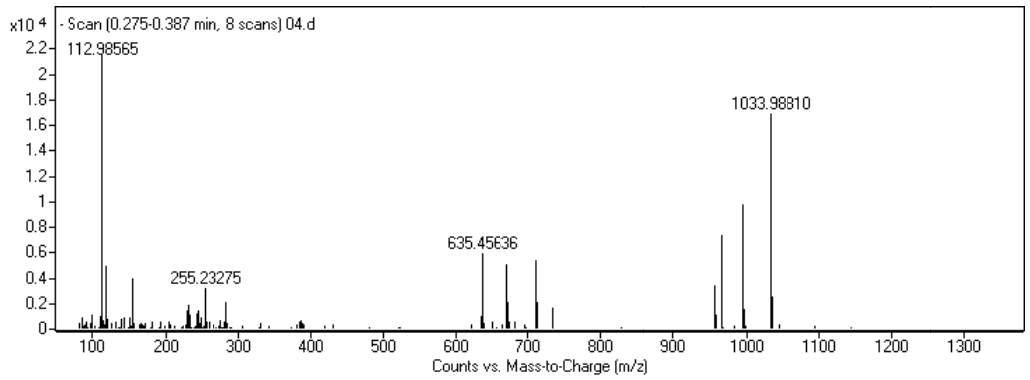

Figure 77. ESI-HRMS of compound **58**

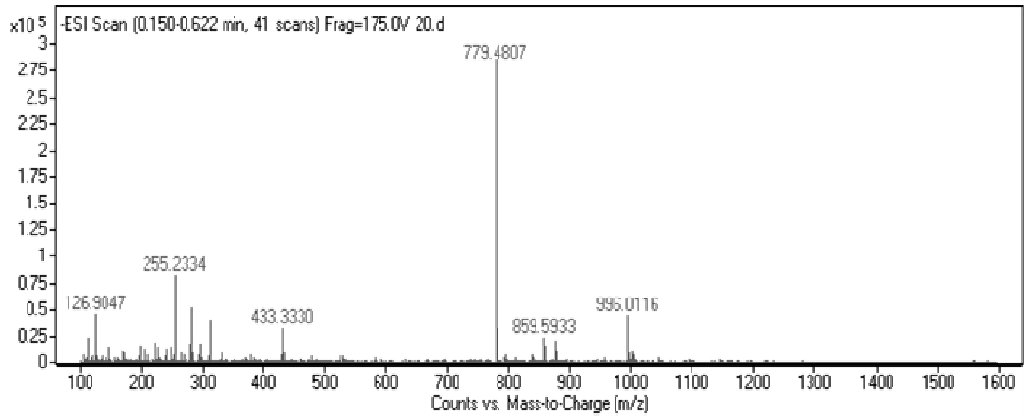

Figure 78. ESI-HRMS of compound **61**

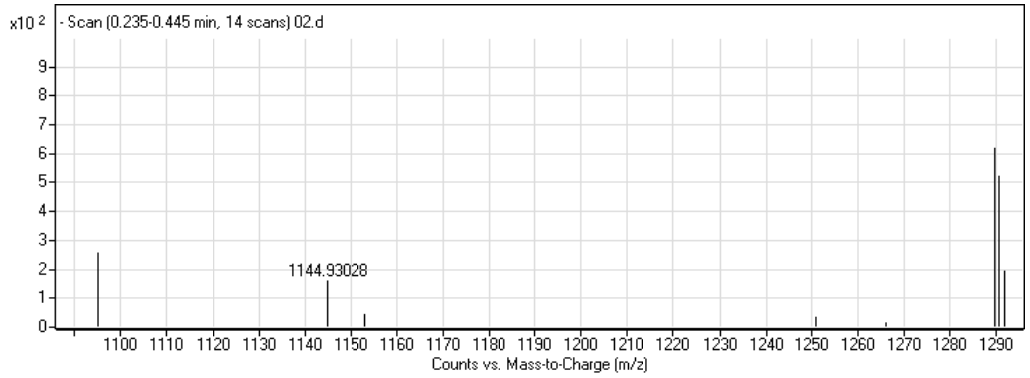

Figure 79. ESI-HRMS of compound **62**

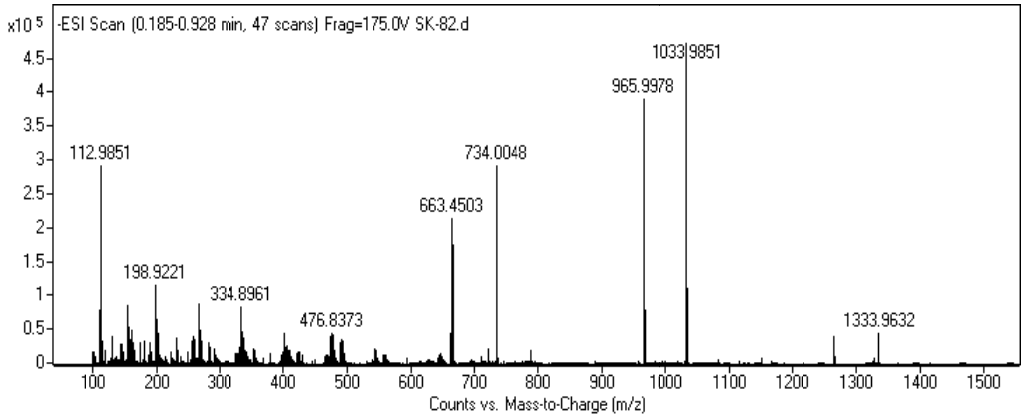

Figure 80. ESI-HRMS of compound **63**

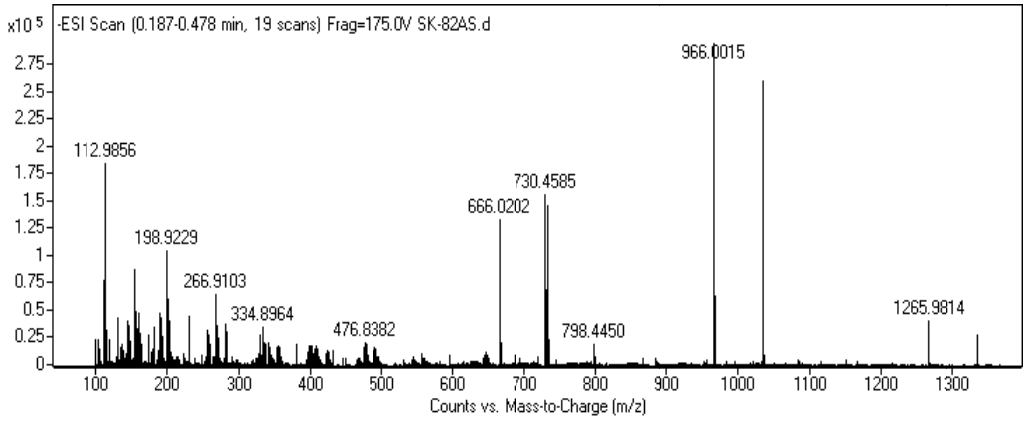

Figure 81. ESI-HRMS of compound **64**

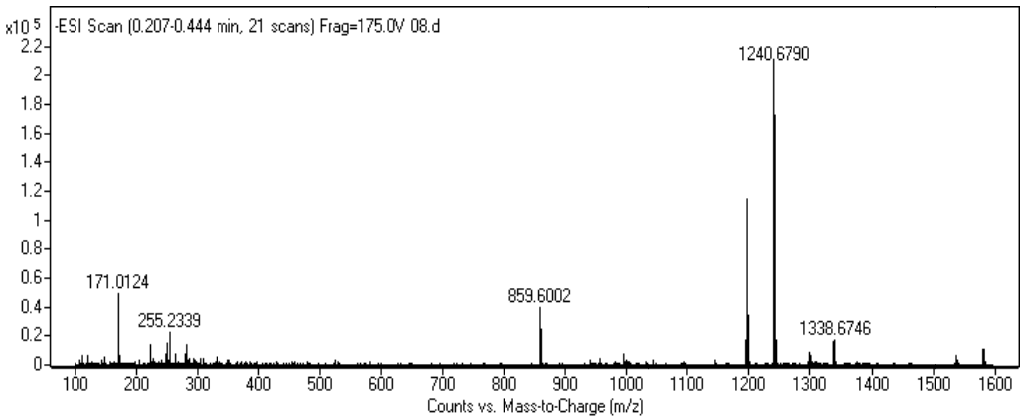

Figure 82. ESI-HRMS of compound **65**